Terminal Oxidation of Long Linear Alkanes in Liquid Phase

By

Edouard Huguet

Thesis submitted to Cardiff University for the degree of Doctor of Philosophy

April 2009

ProQuest LLC
789 East Eisenhower Parkway
P.O. Box 1346
Ann Arbor, MI 48106-1346

DECLARATION

This work has not previously been accepted in substance for any degree and is not concurrently submitted in candidature for any degree.

Signed ..... (candidate) Date 19/03/2010

STATEMENT 1

This thesis is being submitted in partial fulfillment of the requirements for the degree of .....PhD.....(insert MCh, MD, MPhil, PhD etc, as appropriate)

Signed ..... (candidate) Date 19/03/201

STATEMENT 2

This thesis is the result of my own independent work/investigation, except where otherwise stated.
Other sources are acknowledged by explicit references.

Signed ..... (candidate) Date 19/03/201

STATEMENT 3

I hereby give consent for my thesis, if accepted, to be available for photocopying and for inter-library loan, and for the title and summary to be made available to outside organisations.

Signed ..... (candidate) Date 19/03/2010

STATEMENT 4: PREVIOUSLY APPROVED BAR ON ACCESS

I hereby give consent for my thesis, if accepted, to be available for photocopying and for inter-library loans **after expiry of a bar on access previously approved by the Graduate Development Committee.**

Signed ..... (candidate) Date 19/03/201

ABSTRACT

The aim of this project is to investigate the terminal activation of long chain linear alkanes in the liquid phase using the selective oxidation of *n*-decane to 1-decanol as a model reaction.

Firstly the autoxidation of *n*-decane with oxygen was studied. The product distribution is a mixture of C_{10} ketones and alcohols with shorter chain carboxylic acids. The radical autoxidation mechanism promotes oxidation in the internal position and a very low terminal selectivity is found in the product profile.

A range of VMgO catalysts were tested for the oxidation of *n*-decane with oxygen. Leached vanadium from VMgO leads to an improvement to the conversion over the autoxidation while the same terminal selectivity was observed.

Cobalt substituted zeolites catalysts were also investigated. The porous structure of the different zeolites did not improve the terminal selectivity. No cobalt leaching was observed. The silanation of the external surface of the zeolites before ion exchange with cobalt reduces the conversion compared to the same cobalt zeolites without silanation, but does not improve the terminal selectivity.

Finally, a comparison of the best results published in the literature for the oxidation of *n*-hexane in the liquid phase has been carried out. Higher terminal selectivities for the autoxidation were observed than those reported. Autoxidation terminal selectivities match with the best catalysts reported in the literature.

ACKNOWLEDGEMENTS

Firstly thanks go to my academic supervisor Professor Graham Hutchings, who gave me the opportunity for this PhD and invaluable guidance throughout the period of this investigation. I would like to thank my second academic supervisor Dr. Jonathan Bartley, who has supervised my work and for his availability to correct this thesis. I would like also thank my industrial supervisors Mike Watson (Johnson Matthey), Xavier Baucherel (Johnson Matthey), Frans Prinsloo (Sasol) and Chris Nicolaides (Sasol) whose support and help has been greatly appreciated during all the teleconferences, face to face meeting and placement in the company;

I also thank Professor Donald Bethel, Dr. Carley and Dr. Willock for their cooperation and valuable support during the entire period. I would like to thank the help of Rob Jenkins and Alun Davies for fixing everything that went wrong.

Thanks to my group, especially Peter, Sivaram, Salem, Raja, Yuan, Nishlan, Kieran, Laura, Matt, Ferg, Jenny, Adrian, Tony, Nikos, Sankar, Nick and Dan.

Finally, I would like to thanks my family during the time of my PhD for their help and support.

I dedicate this thesis to my Grandfather Pierre.

Contents

CHAPTER 1

INTRODUCTION

1.1. Definition of catalyst and catalytic cycle.

Catalysts are substances that change the rate of a reaction without being used up during the reaction and without itself being one of the reactants or products (in other words, without being consumed) [1]. A catalyst does not change the thermodynamics of the reaction, but simply provides a new and easier pathway by lowering the activation energy. A simple catalytic cycle is described in **Figure 1.1.**

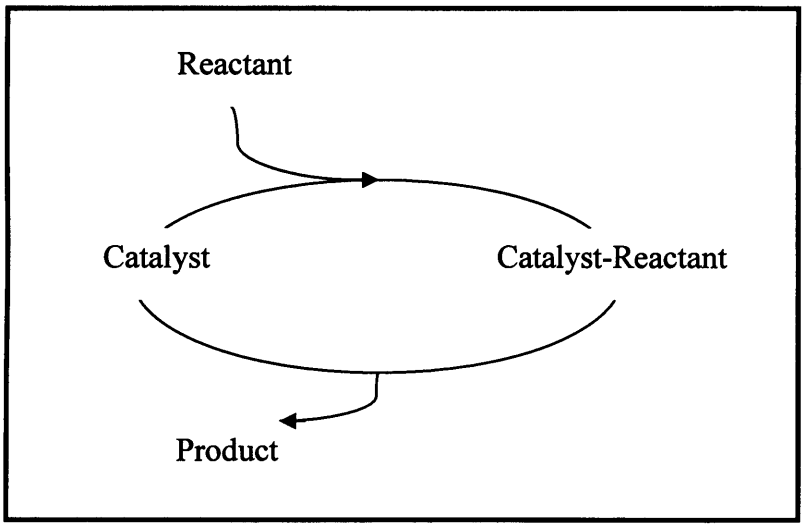

Figure 1.1 Simple catalytic cycle.

The reactants are bound to the catalyst during the reaction and the products are released, regenerating the initial state of the catalyst. In theory, an ideal catalyst would not be consumed. In practice the catalyst undergoes chemical changes and its activity becomes lower (catalyst deactivation). A good catalyst has three virtues: activity, selectivity and lifetime.

1.2. Categories of catalysis.

Catalysis can be classified into two large groups: homogeneous catalysis and heterogeneous catalysis. In homogeneous catalysis, the catalyst and reactants are in the same phase however in heterogeneous catalysis, the catalyst and reactants are in different phases. With respect to homogeneous catalysis, one advantage is that homogeneous catalysts exhibit a higher activity per unit mass of metal than heterogeneous catalysts [2]. The major disadvantage for homogeneous catalysis is that the catalyst and the product need to be separated after reaction. The separation often involves distillation and makes catalyst recovery difficult. For heterogeneous catalysis, the advantage is that there is little difficulty in separating and recycling the catalyst.

1.3. Aim of this thesis.

The aim of this project is a fundamental investigation of liquid phase long linear *n*-alkane terminal activation using the selective oxidation of *n*-decane to 1-decanol as a model reaction **(Figure 1.2)**. The terminal catalytic functionalisation of long chain linear alkanes like *n*-decane remains a challenging task because it is difficult to control the regioselectivity. This project was funded and supervised by two companies, Sasol and Johnson Matthey.

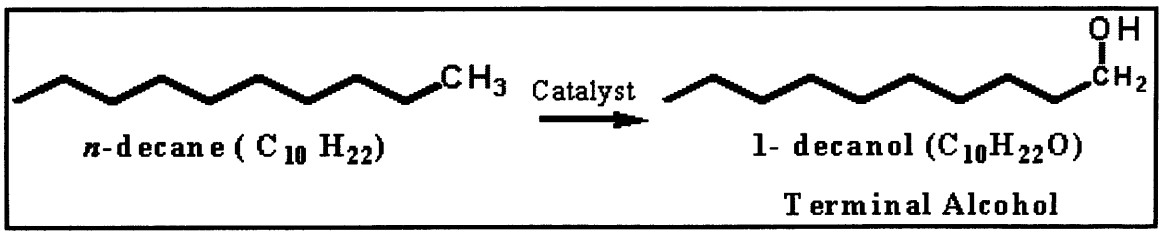

Figure 1.2 Objective of this thesis.

1.4. Motivation of this study.

The largest amount of saturated hydrocarbons is obtained from natural gas and petroleum [3]. Alkanes are a relatively cheap feedstock and are environmentally friendly. There is a large

production of alkanes in South Africa from Sasol's Fischer Tropsch process [4]. This abundance together with their low cost and low environmental impact makes them ideal feedstock for conversion, in the presence of an oxidant, to valuable products. Selective oxidation of hydrocarbons to produce oxygen-containing organic compounds, such as alcohols, aldehydes, ketones, epoxides and acids, is of key importance for modern chemistry processes, which is also a key goal of the work presented in this thesis. The oxygenated products can be used as a starting point for further chemical functionalisation and can also be used to produce many plasticizers and surfactants for detergents.

1.5. Reactivity of saturated hydrocarbons.

Alkanes are saturated and lack functional groups. There is no selective region of attack (regioselectivity) and there is no preferred reaction site. Hydrocarbons can only undergo reaction after cleavage of C-H or C-C bonds. The scope of primary reaction steps is essentially limited to oxidative dehydrogenation, dehydrogenation, substitution and chain cleavage. The terminal catalytic functionalisation of long chain linear alkanes like decane remains a challenging task because it is difficult to control the regioselectivity which is governed by the relative carbon hydrogen bond dissociation energies. The bond dissociation energies decrease from 104 kcal mol^{-1} to 94.6 kcal mol^{-1} for the primary and secondary carbon atoms respectively whereas the corresponding selectivities increase [5].

In *n*-decane, there are 8 CH_2 groups and 2 CH_3 groups meaning 16 secondary hydrogens and 6 primary hydrogens (**Figure 1.3**), with the carbon hydrogen bond dissociation for CH_3 9.6 kcal mol^{-1} stronger than the carbon hydrogen bond dissociation for CH_2. This difference explains the difficulty in selectively oxidising the terminal position of long linear alkanes.

Internal position will be oxygenated first along the chain resulting to a mixture of internal alcohols and ketones.

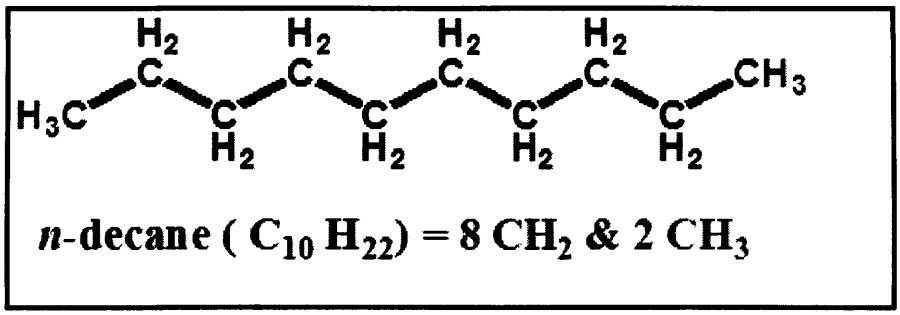

Figure 1.3 *n*-decane.

Another problem which makes this reaction difficult in liquid phase is autoxidation, which is the spontaneous reaction of oxygen with alkanes. The selectivity of the autoxidation is governed by the energy of the C-H bond dissociation and favours the oxidation in the internal positions of the linear alkanes. The autoxidation reaction will be detailed in **Chapter 3** of this thesis.

1.6. Oxidations of alkanes to more valuable products.

A large segment of the modern chemical industry is based on catalytic selective oxidation described in **Figure 1.4**. More than 60 % of the chemicals and intermediates synthesized via catalytic processes worldwide are products of oxidation [6].

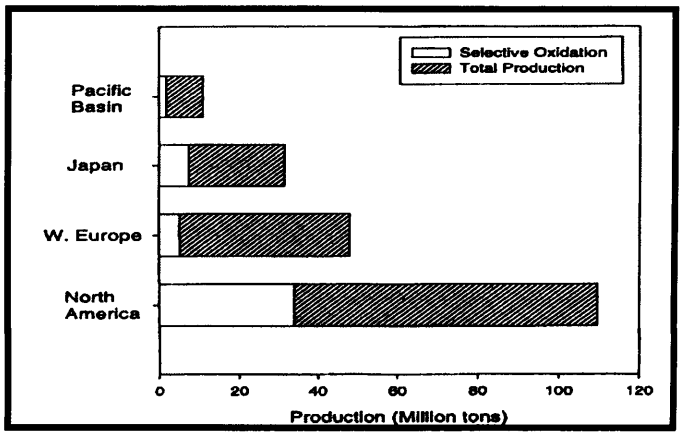

Figure 1.4 World organic chemical production in 1991 [6].

Figure 1.4 shows that the selective oxidation represents a large part in the market in 1991 over the world. 25% of the selective oxidation is performed by the use of heterogeneous catalysts and one of the most important applications is the functionalisation of hydrocarbons.

1.7. Production of long linear alcohols in industry.

The most important industrial routes to produce terminal linear alcohols are the Ziegler chemistry and the "oxo" process [7-8]. The Ziegler chemistry (**Figure 1.5**) is a five step process: hydrogenation, ethylation, growth reaction, oxidation and hydrolysis. The starting material is ethylene.

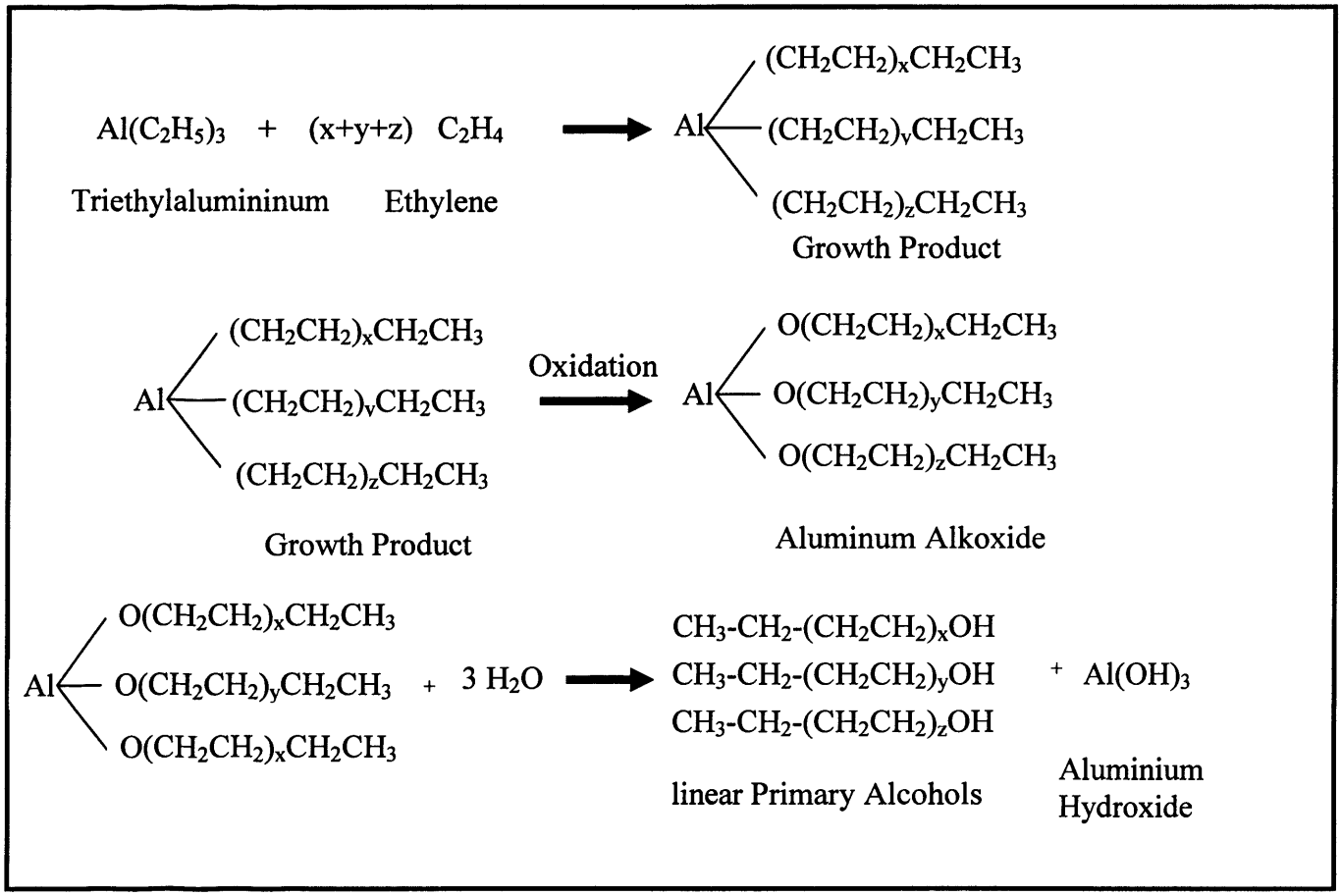

Figure 1.5 The basis of this Ziegler technology.

Al_2O_3 is not recycled during the reaction so it is not a catalytic process.

The second industrial route is the hydroformylation or the so called "oxo" process (**Figure 1.6**). It is a heterogeneous catalytic process. A terminal olefin reacts with carbon monoxide and hydrogen to produce the linear terminal alcohols [8-11].

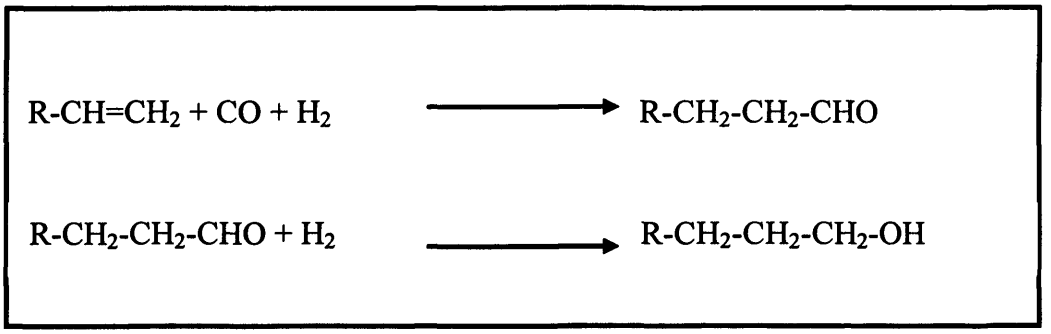

Figure 1.6 The oxo-process.

The Ziegler process and the "oxo" process are multi step reactions and do not use linear alkanes as feed, so to find a way to execute the hydroxylation at the end of the long linear hydrocarbons heterogeneously with oxygen or air as oxidant will be more economic and a cleaner process for industry.

1.8. Chemical properties long linear alcohols.

The industrial importance of long linear alcohols is based on the large number of reactions the hydroxyl group may undergo (**Figure 1.7 [8]**).

Terminal Linear alcohol	+ Oxygen	→	Aldehyde + carboxylic acid
	+ Alakali Melt	→	carboxylic acid
	+ Alkali	→	Dimeric Alcohol
	+ Proton	→	Ether, Olefin
	+ Alkyne	→	Vinyl Ether
	+ Carboxylic acid	→	Ester
	+ Hydrogen Halide	→	Alkyl Halide
	+ Ammonia/ Amine	→	Amine
	+ Aldehyde/ Ketone	→	Acetal
	+ Sulfide	→	Thiol
	+ Alcoholate/H_2S	→	Xanthate
	+ Metal	→	Metal alkoxide
	+ Ethylenoxide	→	Ethoxilates/Ethersulfates

Figure 1.7 Lists of some typical examples of reactions can undergo terminal alcohol [8].

Many of the resulting derivatives are intermediates of commercial importance.

1.9. Use of terminal long linear alcohols.

Linear primary alcohols are used in the composition of plastics and cement, where they increase the fluidity of the material. They are also widely used in the composition of detergents [12-13]. Linear primary alcohols are amphiphiles, one part is polar (hydroxyl group) and one part is apolar (alkane chain). The amphiphiles molecules can be used as surfactants. These molecules have limited solubility in any solvent and will aggregate at the interface between two phases to form micelles. Micelle can dissolved an organic compound like grease in water, which would normally be insoluble. This property is the mechanism of all the detergents.

1.10. Catalysts used in this research.

1.10.1. Testing in Liquid phase.

All the catalysts presented in this work have been tested in the liquid phase. Three phase reactions between gaseous (oxygen) and liquid (*n*-decane) and solid catalysts are often encountered in industrial chemistry [15].

Advantages of the liquid phase process:

- Lower reaction temperatures than gas phases processes.
- Liquid-phase reactions generally give higher time –yields than gas phase process.

Disadvantages of the liquid-phase processes are:

- Separation and purification of the products is laborious.
- The intensive mixing of the compounds requires mechanically stable catalysts.

1.10.2. Different Catalysts investigated.

1.10.2.1. Supported vanadium oxide catalysts in heterogeneous catalysis.

The current level of the annual production of vanadium in the world is 38,000 tonnes. About 80%, of the vanadium produced is used as steel additive, as it makes steel shock and vibration resistant [16]. The most dominant non-metallurgical use of vanadium is in catalysis, which represents about 5% of the annual production of vanadium. It is the most widely used metal oxide catalyst [17-20]. Some of the reactions catalyzed by vanadium oxides with alkanes are shown in **Table 1.1**.

Table 1.1 Reaction of alkanes with vanadium based catalyst.

Catalytic reaction with alkanes	References.
Selective oxidation of alkanes and alkenes	[21-22]
Selective oxidation of alkanes with peroxides	[24]
Oxidative dehydrogenation of alkanes	[25]
Partial oxidation of methane to formaldehyde	[26-27]
Direct conversion of methane to aromatics	[28]

There is no literature reported on the heterogeneous oxidation of long linear alkanes over VMgO catalyst in liquid phase. **Chapter 4** discusses the results of *n*-decane oxidation using O_2 over different VMgO catalysts in the liquid phase.

1.10.2.2. Zeolites.

1.10.2.2.1. Composition and structure.

Zeolites are microporous solid catalysts (**Figure 1.8 [29]**). They contain silicon, aluminium, oxygen and cations in their framework. Silicon atoms and aluminium atoms are linked to four

oxygens atoms to form a tetrahedral (SiO_4 and AlO^-_4). These tetrahedres are linked together by their corners to form the negative frameworks of the zeolites. The negative charges are balanced with a mobile cation (NH_4^+ or Na^+) to keep the framework neutral. These cations can be exchanged by oxidation centre as Co^{2+} or Mn^{2+}. 133 different frameworks of zeolites with different size of pores and different shape of channels are listed in the Atlas of zeolites [30].

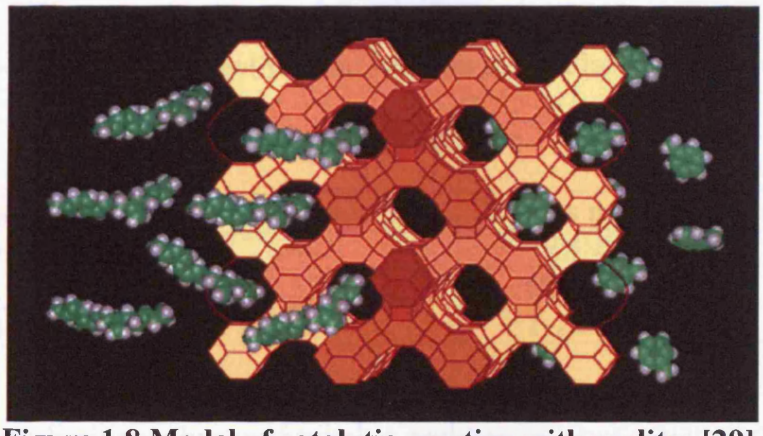

Figure 1.8 Model of catalytic reaction with zeolites [29].

1.10.2.2.2. Shape selectivity.

The structure of channels of the zeolites is predetermined by the composition and type of the zeolites. The accessibility of the pores for molecules is subject to definite geometric restrictions. The shape selectivity of the zeolites is based on the interaction of reactants with the pore system. Only starting materials of a certain size and shape can penetrate into the interior of the zeolites pores and undergoes reaction with the catalytic actives sites present in the channel [31-32]. For the geometrics constraints, three variants can overlap.

- Reactant selectivity occurs when some of the molecules in a reactant mixture are too large to diffuse through the catalyst pores.
- Product selectivity. Bulky products can not diffuse out of the pores.

- Restricted transition state selectivity. When there are multiple pathways in a reaction, but one or more are suppressed because the transition state would require more space than is available in the cavities or pores.

Table 1.2 compares the pore apertures of the zeolites used in this work with the kinetic molecular diameters of some starting materials. Molecules are not rigid and the kinetic diameter gives only a rough estimation of the molecular size.

Table 1.2 Pores apertures of zeolites and kinetics molecular diameter of *n*-hexane, xylene and cyclohexane.

Molecule	Kinetic diameter (nm)	Zeolites pores size (nm)
n-hexane	0.49	ZSM-5 (0.54)
Xylene	0.57	Mordenite (0.67)
Cyclohexane	0.62	Y-Zeolites (0.74)

With these data, a preliminary choice of suitable zeolites for a particular starting material can be made. Mordenite, Y-zeolites and ZSM-5 were investigated for the oxidation of *n*-decane in liquid phase. The results are in **Chapter 5**.

1.11. Literature review for the terminal functionalisation of linear alkanes.

Most of the literature on alkane activation focuses on short chain linear alkanes ranging from methane to butane or cyclic hydrocarbons (cyclohexane). Different catalytic approaches for terminal functionalisation of long linear alkanes are presented in the following sections.

1.11.1. Biochemical oxidation process.

An enzyme is a protein, which has catalytic activity and is specific for its substrate. Enzymes can oxidise the terminal group of linear alkane with oxygen [33]. These enzymes are the mono-oxygenase class. The catalytic active metal centre of the mono-oxygenase (Fe) is surrounded by a large protein structure, which controls the approach of the substrate to the

oxidation centre. These enzymes are very selective and they oxidise only at the terminal position is observed. The problems associated with these biological oxidation processes are the low rates of reactions, the high dilution of the feed, which will give the product recovery difficult, the use of a co-oxidant (NADH), which is essential for the catalatityc activity of the enzyme and storage. All these constraints limit their use for the industrial production of terminal hydroxylated alkanes.

1.11.2. Homogeneous catalysis.

Homogeneous catalysts can hydroxylate the terminal position in alkanes. The first example of a homogeneous catalyst is the metallophophyrin class of compounds [34]. They were modelled on enzymatic mono-oxygenase with the metal centrally located in the porphyrin macrocycle. Ligands around the active metal provide a selective route for the alkane to access to oxidation centre, which is responsible for the selectivity. The metallophophyrin complex use sacrificial oxidants such as iodosylbenzene. The primary selectivity using the metallophophyrins for the activation of hydrocarbons is generally low, for example with *n*-decane, 82% of the yield is mostly internal alcohols with only 18% of terminal selectivity.

n-Octane can be efficiently oxidized by hydrogen peroxide in acetonitrile using tetra-*n*-butylammonium salts of vanadium-containing polyphosphomolybdates $[PMo_{11}VO_{40}]^{4-}$ and $[PMo_6V_5O_{39}]^{12-}$ as catalysts. The terminal selectivity is 8.2 % and 92% of the product distribution is internal alcohols and ketones [35].

The disadvantages of these homogeneous catalysts are the difficult separation of the products, the poor selectivity to a single oxygenated product (side reactions), organic ligands are often unstable under oxidation conditions and very expensive, the use of sacrificial oxidant and the

use of a solvent. These homogeneous catalysts are also very difficult to recycle (quick deactivation after catalytic cycles) and have a very low turnover. All these process are still far from industrial utilization.

1.11.3. Indirect methods for the selective oxidation: Two steps processes.

Long chain alkanes can be converted to functionalised compounds via a two-step process. A two step process can be a disadvantage as it will be more expensive but it can be more regioselective than the direct oxidation and so will pay off the extra cost of this process. Different strategies have been identified:

Terminal Dehydrogenation: This produces a terminal alkene and subsequent hydration of this alkene gives the terminal alcohol.

VMgO has been reported as heterogeneous catalysts for the dehydrogenation of *n*-hexane in gas phase [36]. The conversion is 5% with less than 2 % of terminal selectivity. Then a hydroxylaton of *n*-terminal alkene is needed. The most widely used methodology is a two steps organic process. To obtain a terminal alcohol the first step is a regioselective hydroboration with sodium perborate followed by oxidation over H_2O_2/ NaOH. Addition of water with one equivalent of sulphuric acid obeys Markovnikov's rule and will gives a secondary alcohol (undesired product).

The major problems of this multi steps process are the low conversion, low selectivity to the terminal alkene and also the high cracking for the first step.

Boronation [37]: Terminal functionalisation of linear alkanes with boron and deprotection of this terminal organoboron compound by H_2O_2 to obtain the terminal alcohol. This is a homogeneous process which leads to the formation of a single, terminal functionalization product from linear alkanes using a transition metal-catalyst.

Bis(pinacolato)-diborane (B_2pin_2) or pinacolborane (HBpin) react with *n*-octane on Rh complexes $Cp^*Rh(\eta^4\text{-}C_6Me_6)$ ($Cp^* = C_5Me_5$; Me = methyl) to give high-yields (65%) of linear alkylboranes under thermal conditions (150°C). These reactions allow regiospecific functionalization of alkanes under thermal conditions. The organoborane products (R-Bpin) are intermediates that can serve as precursors to terminal alcohols. The boron at the end of the alkane can be deprotected by hydrogen peroxide and be easily converted to a terminal alcohol with a yield greater than 85 %.

This method is very selective with very good yield for each step but B_2pin_2 is very expensive (£ 38.00 per g) and a large excess of catalyst would be needed to obtain a good yield and selectivity so this is a very expensive process. Moreover this method is very slow 110 h to obtain a yield of 64 % with 100 % selectivity to terminally activated alkanes.

Ammoxidation [38]: This process is particularly attractive and as it leads to a terminal functionalisation of the alkane. Once the terminal functionalisation has been achieved the nitrile group can be oxidised to give the primary alcohol.

The ammoxidation of alkanes is a good way to obtain terminal selectivity. The only way to create a triple bond with an alkane is at the terminal position. The catalyst used is antimony-vanadium phosphorous oxide/alumina ($Sb\text{-}VPO/Al_2O_3$). For *n*-hexane (425°C), the conversion is 15% with the selectivity of 30 % to the monosubstitued (hexanenitirle) and 40% to the disubstitued (adiponitrile). Takahashi [39] have shown a catalytic method for the reduction of the nitrile to the corresponding alcohol in one step. They report the reduction of nitriles with 2-propanol over hydrous zirconium oxide at 300°C in the vapour phase. The reaction was carried out in a glass flow reactor with a fixed-bed catalyst and a flow of

nitrogen. The reduction of aliphatic nitriles proceeded efficiently to give the corresponding alcohols (**Table 1.3**).

Table 1.3 The reduction of nitriles with 2-propanol over hydrous zirconium at 300°C.

Nitrile	Conversion (%)	Selectivity (%) Terminal alcohol.
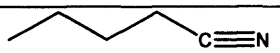	98	73%
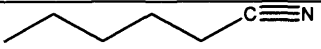	89	78%
	58	52%

The conversion and the yield were lowered by increasing carbon chain lengths but 58 % of conversion with 52 % of selectivity was obtained for the undecane.

This multi step process is very interesting; the two steps are carried out by heterogeneous catalysts and very high selectivity for each step. The only disadvantage can be the cracking of the products and the use of ammonia for the first step (ammoxidation).

1.11.4. Heterogeneous catalysis in liquid phase.

Heterogeneous catalysts will be the most simple and economic methods for making terminal linear alcohols directly from hydrocarbons with air or oxygen as oxidant. The heterogeneous system was favoured by the industrial sponsor of this project.

Oxidation of *n*-octane in liquid phase was carried out by Singh [40]. The oxidation of *n*-octane are catalysed by chromium silicate-1 (CrS-1) using *tert*-butyl hydroperoxide (alkane /TBHP mole ratio 3) as oxidant.

Table 1.4 Results for *n*-octane oxidation over CrS-1 and VS-1.

Catalyst	Conversion (%)	Total Terminal Selectivity (%)
CrS-1	7.7	9.4
VS-1	8.7	7.3

The terminal selectivity is low and the ratio of alkane/TBHP used in this process is not economic.

Liquid phase oxidation of *n*-decane using alkyl hydroperoxide as the oxygen donor in presence of supported palladium catalysts [41] is also reported. The ratio of *n*-decane/TBHP is 0.6 in this process for 13.6% conversion with 56.6% and 12.9% selectivity to decanones and decanols, respectively. No detailed data for the terminal selectivity are shown.

Thomas [42-48] has reported best results of the literature for the heterogeneous terminal oxidation of *n*-hexane in liquid phase. His results are presented in (**Table 1.5**). The terminal selectivity is extremely high compared to the previous work [40] with air as oxidant, which is a very economically favourable process.

Table 1.5 Thomas's results for the oxidation of *n*-hexane with AlPO catalyst.

Catalyst	Conversion (%)	Total Terminal Selectivity (%)
Co-AlPO-5	2.4	8.6
Co-AlPO-5	7.2	61.3
Co-AlPO-18	8.7	65.5

A very high terminal selectivity of 65.5 % is obtained with a majority of terminal acid in the product distribution. No autoxidation results are presented in this study. These results are unprecedented. Iglesia [48] tried to reproduce Thomas's data with the same catalyst for the

oxidation of *n*-hexane using very close experimental conditions. The data is reported in **Table 1.6**.

Table 1.6 Iglesia's results for oxidation of *n*-hexane with AlPO catalysts.

Catalyst	Conversion (%)	Total Terminal Selectivity(%)
Mn-AlPO-5 Mn-AlPO-18	0.02-0.05	7

Very low conversion with very low terminal selectivity was found. The main conclusion of Iglesia is that Mn-AlPO-18 did not lead to any preference for terminal oxidation of *n*-hexane in contradiction with Thomas's results. After this difference between the results of Thomas and Iglesia, it is difficult to believe in Thomas's results, but maybe Iglesia can not prepare the right catalyst and some difference in experimental conditions use by Iglesia are present. These differences are well detailed in **Chapter 6**.

The second best results for the terminal oxidation of *n*-hexane in liquid phase has been published by Iglesia [50]. These results are presented in **Table 1.7**.

Table 1.7 Iglesia's results for oxidation of *n*-hexane with Mn-ZSM-5 catalysts

Time (hours)	Conversion (%)	Terminal selectivity (%) with Mn-ZSM-5	Terminal selectivity (%) Autoxidation
0.5	0.007	24	7
2.5	0.013	18	8
4	0.047	15	8
7	0.1	10	7

Fisrtly compared to Thomas's results with AlPO catalysts, there is a huge difference between the conversion and terminal selectivity with the same substrate (*n*-hexane) in liquid phase. Iglesia is showing data for the autoxidation reaction and demonstrate a clear difference in terminal selectivity with a catalyst present, while conversion is unaffected. In the case of a catalyst (Mn-ZSM-5) being present, the terminal selectivity is initially high (>20 %), but this declines as the conversion increases (~10% terminal selectivity when conversion is 0.1 %). In contrast the autoxidation has a steady terminal selectivity of around 8 % throughout the conversion range tested. Two points are also not clear in these results, the autoxidation and the reaction with Mn-ZSM-5 have the conversion for the same time and the stable terminal selectivity of the autoxidation compared to the terminal selectivity for the catalyst, which decrease versus conversion. A detailed comparative study will be presented in **Chapter 6**.

1.12. References.

[1] The Basis and Application of Heterogeneous Catalysis, M. Bowker, Oxford Chemistry, Primers, Oxford Science Publications, (1998).

[2] Industrial Catalysis, J. Hagen, Wiley-VCH, (2006).

[3] Selective Oxidation by Heterogeneous Catalysis, G. Centi, F. Cavani, F. Trifiro, Academic, Plenum, (2001).

[4] M.E. Dry, Catalysis Today 71, (2002), 227.

[5] J.A. Kerr, Bond Dissociation Energies by Kinetic Methods, Chemical Reviews 66, (1966), 465.

[6] S.T. Oyama, A.N. Desikan, J.W. Hightower, Catalytic Selective Oxidation, Symposium Series 523, ACS, Washington DC, Chapter 1, (1993), 1.

[7] T. Mole, E.A. Jeffery, Organoaluminium Compounds, Elsevier, Amsterdam (1972).

[8] All about the Fatty Alcohols, Condea, (2000).

[9] Several New Surfactants, R. B. S. Georgeville, Quebec, Canada, (2004).

[10] Produkte aus der Oxosynthese, Ruhrchemie AG, Frankfurt (1969).

[11] J. Falbe, Synthesen mit Kohlenmonoxid, Springer-Verlag, Berlin (1967).

[12] H.J. Richter, J. Knaut, Journal of the American Oil Chemists' Society, 61, (1984), 160.

[13] J. Knaut, H.J. Richtler, Journal of the American Oil Chemists' Society, 62, (1985), 317.

[14] Introduction to Modern Colloid Science, R.J. Hunter, Oxford Science Publications, (1993).

[15] Industrial Catalysis, J. Hagen, Willey-VCH, (2005).

[16] B.M. Weckhuysen, D.E. Keller, Catalysis Today, 78, (2003), 25.

[17] F. Trifiro, B. Grzybowska, Applied Catalysis A: General, 157, (1997).

[18] G.C. Bond, S.F. Tahir, Applied Catalysis A: General, 71, (1991), 1.

[19] G. Deo, I.E. Wachs, J. Haber, Critical Reviews in Surface Chemistry, 4, (1994), 141.

[20] G. Ertl, H. Knozinger, J. Weitkamp, Handbook of Heterogeneous Catalysis, Wiley–VCH, Weinheim, (1997).

[21] J.M. Lopez Nieto, P. Concepcion, A. Dejoz, H. Knozinger, F. Melo, M.I. Vazquez, Journal of Catalysis, 189, (2000), 147.

[22] K. Wada, H. Yamada, E. Watanabe, T. Mitsudo, Journal of the Chemistry Society, Faraday Transactions 94, (1998), 1771.

[23] P. Rao, A.V. Ramaswamy, Journal Chemistry Society, Chemistry of the Communication, (1992), 1245.

[24] A. Khodakov, B. Olthof, A.T. Bell, E. Iglesia, Journal of Catalysis, 181, (1999), 205.

[25] K. Chen, A. Khodakov, J. Yang, A.T. Bell, E. Iglesia, Journal of Catalysis 186, (1999), 325.

[26] M.A. Banares, L.J. Alemany, M.L. Granados, M. Faraldos, J.L.G. Fierro, Catalysis Today 33, (1997), 73.

[27] A. Parmaliana, F. Fursteri, A. Mezzapica, M.S. Scurrell, N.Giordano, Journal of the Chemistry Society 9, (1993), 751.

[28] B.M. Weckhuysen, D. Wang, M.P. Rosynek, J.H. Lunsford, Journal of Catalysis, 175, (1998), 347.

[29] Web: database of zeolites.

[30] C. Baerlocher, W.M. Meier, D. Holson, Atlas of Zeolite Framework Types. Amsterdam: Elsevier, (2001).

[31] J. Dwyer, Chemistry and Industry 7, (1984), 258.

[32] S.M. Csicsery, Zeolites 4, (1984), 202.

[33] M. Baik, M. Newcomb, R.A. Friesner, S.J. Lippard, Chemical Reviews 6, 103, (2003), 2385.

[34] G. Süss-Fink, L. Gonzalez, G.B. Shul'pin, Applied Catalysis A: General, 217, (2001), 111.

[35] B.R. Cook, T.J. Reinert, K.S. Suslick, Journal of the American Chemical Society, 108, (1986), 7281.

[36] H.B. Friedrich, N. Govender, M.R. Mathebula, Applied Catalysis A: General 297, (2006), 81.

[37] H.Y. Chen, S. Schlecht, T.C. Semple, J.F. Hartwig, Science 287, (2000), 1995.

[38] B.M. Reddy, B. Manohar, Journal of Chemical Society 3, (1993), 330.

[39] K. Takahashi, M. Shibagaki, H. Matsushita, Chemical Letters 1, (1990), 311.

[40] A.P. Singh, T. Selvam, Journal of Molecular Catalysis A: Chemical, 113, (1996), 489.

[41] Deshpande, R. Madhukar, Rane, V. Hari, R. Vitthal, U.S. Patent No. 976737, (2006).

[42] J.M.Thomas, R. Raja, G. Sankar, R.G. Bell, Nature, (1999), 227.

[43] R. Raja, J.M. Thomas, Chemistry Communication, 17, (1998), 1841.

[44] R. Raja, G. Sankar, J.M. Thomas, Journal of the American Chemistry Society, 121, (1999), 119.

[45] J.M. Thomas, R. Raja, G. Sankar, R.G. Bell, Studies in Surface Science and Catalysis, 130, (2000), 887.

[46] R. Raja, G. Sankar, J.M. Thomas, Angewandte Chemistry International Edition, 39, (2000), 231.

[47] J.M.Thomas, R. Raja, G. Sankar, R.G. Bell, Accounts Chemical Research, 34, (2001), 191.

[48] R. Raja, J.M. Thomas, Journal of Molecular Catalysis A, 3, (2002), 181.

[49] B. Modén, B. Zhan, J. Dakka, J.G. Santiesteban, E. Iglesia, Journal of Physical Chemistry C, 111, (2007), 1402.

[50] B. Zhan, B. Modén, J. Dakka, J.G. Santiesteban, E. Iglesia, Journal of Catalysis 2, 245, (2007), 316.

Chapter two

Experimental Techniques

2.1. Introduction.

This chapter describes in detail the catalyst preparation, the basic principles of characterisation techniques used to examine the catalyst, the experimental conditions used for catalysts testing with a description of the reactor and finally the methods to analyse and quantify the products after reaction.

2.2. Catalyst preparation.

2.2.1. Preparation of vanadium magnesium oxide catalyst.

Various VMgO catalysts were prepared via an impregnation method [1-2] with varying vanadium loadings.

Table 2.1 Reagents for the preparation of a VMgO catalyst.

Reagent	Molar mass ($g.mol^{-1}$)	Supplier	Purity
MgO	40.29	Fisher scientific	98 %
NH_4VO_3	116.98	Aldrich	99 %
NH_4OH	35.05	Aldrich	25% (in solution)

MgO forms $MgCO_3$ when exposed to CO_2 in the atmosphere so it was calcined at 350°C for 12h in air to remove any carbonates and thus obtain only MgO. 10 ml of 25% (v/v) NH_4OH solution was added to 850 ml of deionised water (pH=12). VMgO catalysts were prepared by

dissolving appropriate amounts of NH_4VO_3 (**Table 2.2**) in this aqueous solution and were heated to 70°C until all the NH_4VO_3 dissolved. MgO (6.7g) was added to the solution while stirring and the suspension that was obtained was evaporated until it formed slurry. The slurry was placed in an oven set at 110 °C for 2 h. The resulting solid was crushed and calcined for 6 h at 550 °C in air. Nine different vanadium-loaded VMgO catalysts were prepared with this method (**Table 2.2**)

Table 2.2 Summary of the VMgO catalysts prepared by impregnation.

Catalyst name	Theoretical mass percentage loadings. (wt % V_2O_5)	Amounts of NH_4VO_3 (g)
VMgO-0 (blank)	0	0.00
VMgO-1	1	0.09
VMgO-5	5	0.45
VMgO-10	10	0.95
VMgO-20	20	2.14
VMgO-33	33	4.31
VMgO-50	50	8.56
VMgO-60	60	12.84
VMgO-70	70	19.97

2.2.2. Preparation of zeolites catalysts.

2.2.2.1. Method of calculation used for loading of metal by solid state ion exchange (SSIE).

The following detailed calculation [3] before preparation allows the incorporate different amount of Co^{2+} in the zeolites. The zeolites used in this work were manufactured by the company Zeolyst International [4]. Each zeolite is given with (SiO_2/Al_2O_3) mole ratio. An example of calculation is detailed below:

H-ZSM-5 with a ratio (SiO_2/Al_2O_3)= 30

(30 SiO_2/ Al_2O_3) * (Al_2O_3 /2Al) * (Si/ SiO_2) = (30 Si / 2Al) =30.

Si / Al =15

The framework unit of the zeolites is [$SiAlO^-_4$]. It is assumed to be in SiO_2/AlO_2^- for the calculation.

SiO_2/AlO_2^-=15

15 mol SiO_2 + 1 mol AlO_2^-

M SiO_2 = 60 g. mol^{-1}

M AlO_2^- = 59 $g.mol^{-1}$

1 mol of zeolites= 15*60 + 59 = 959 $g.mol^{-1}$

Weight (%) AlO_2^-=59/959 * 100 = 6.152

10g of zeolites was exchanged.

10g * 0.06152= 0.6152 g of AlO_2^-

0.6152 g of AlO_2^- * {27g (Al)/ (59g of AlO_2^-)} =0.28 g Al

M Al=27 $g.mol^{-1}$

0.28 / 27=0.0103 mol Al for 10g of zeolites.

1 mol Al = ½ mol Co^{2+} (charge balance for framework)

1 mol Co^{2+} for 1 mol Al => (use for the solid state ion exchange)

M $CoCl_2.6H_2O$= 237.93 $g.mol^{-1}$

1 mol $CoCl_2.6H_2O$ → 1 mol Co^{2+} + 2 mol Cl^- + 6 mol H_2O.

So need 0.0103 mol of Co^{2+}

0.0103 mol * 237.93 = 2.45 g of $CoCl_2.6H_2O$

Table 2.3 shows the mass of $CoCl_2.6H_2O$ used at the beginning of the preparation for the different Cobalt-zeolites prepared by solid state ion exchanged using the calculation above.

Table 2.3 Mass of $CoCl_2.6H_2O$ used for each catalyst.

Zeolites	SiO_2/Al_2O_3 Mole ratio	Cobalt loading for 1 Al	Mass of $CoCl_2.6H_2O$ (g)
Modernite	20	1	3.61
Y-zeolites	80	1	0.97
ZSM-5	280	1	0.281
ZSM-5	80	1	0.97
ZSM-5	30	0.1	0.245
ZSM-5	30	0.2	0.49
ZSM-5	30	1	2.45
ZSM-5	30	2	4.9
ZSM-5	23	0.1	0.318
ZSM-5	23	0.2	0.636
ZSM-5	23	1	3.18
ZSM-5	23	2	6.36

2.2.2.2. Preparation of cobalt ion exchange zeolites.

The zeolites was initially heated to 500°C for 3 h in air to remove organic templates used during the synthesis of the zeolites and to obtain the proton form of the zeolites.The Solid State Ion Exchange (SSIE) [5] was carried out by grinding the zeolites (10g) together with different mass of $CoCl_2.6H_2O$ (**Table 2.3**) for 5 minutes to obtain a pink homogeneous physical mixture.

Table 2.4 Reagents for the preparation of a Co-zeolites.

Reagent	Molar mass ($g.mol^{-1}$)	Supplier	Purity
Zeolites	-	Zeolyst International	
Cobalt(II) chloride hexahydrate $CoCl_2.6H_2O$	237.93	Aldrich	≥99%

A quartz tube was used to pack the crude Cobalt-zeolites mixture as described in **Figure 2.1.**

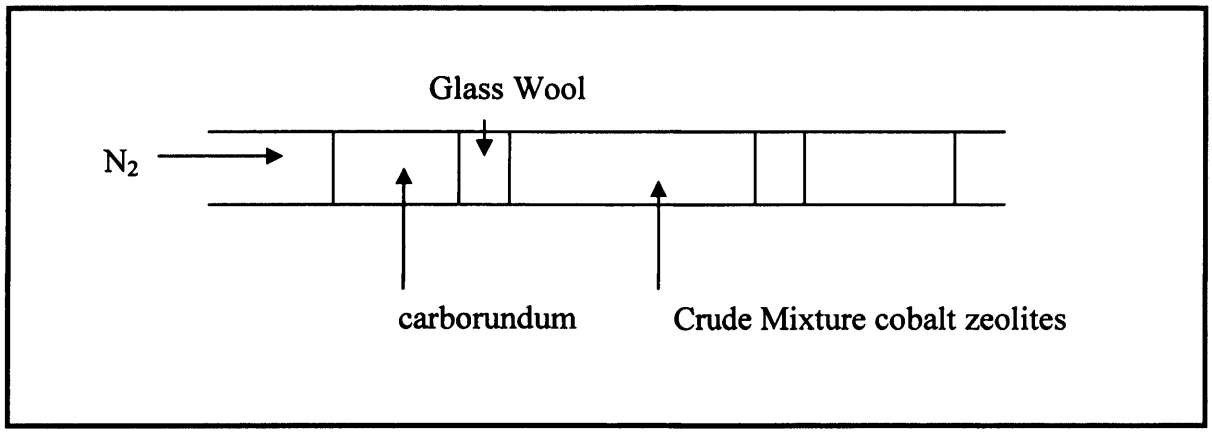

Figure 2.1 Packing of cobalt-zeolites mixture in quartz tube.

Before heating the mixture was flushed with a stream of nitrogen for 3 hours and then heated in inert gas stream nitrogen to remove volatile products such HCl for 3 hours at 500°C and left to cool down slowly at room temperature. A blue powder was obtained. The blue colour is the proof that Co^{2+} is bonded to Al otherwise a grey colour is observed [3].The catalyst was washed slowly (**Figure 2.2**) with deionised water without vacuum to remove unreacted cobalt and remove chloride ions.

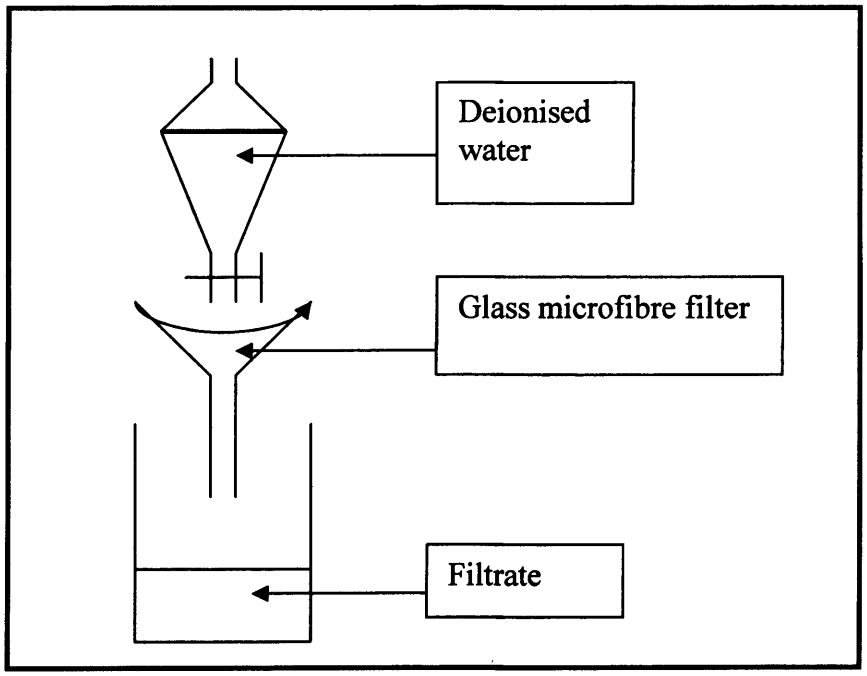

Figure 2.2 Set up for the washing process.

At the start of the washing a slightly pink colour was obtained and a test with silver nitrate ($AgNO_3$) has showed a cloudiness as a white precipitate (AgCl) is formed. This test was repeated until no precipitate was observed. Up to 15 days washing was required to remove all the chloride and prevent the leaching of cobalt during the testing of the catalyst in liquid phase. After the intense washing, zeolites were dried in air at room temperature.

2.2.2.3. Preparation of silanated zeolites.

Silanated zeolites were prepared following the method described by Iglesia and co-workers [6]. The modified zeolites were prepared by immersing zeolites (9.6 g) into an ethanol solution (100ml) containing 3-aminopropyl triethoxylsilane ($H_2N(CH_2)_3Si(OC_2H_5)_3$) (1.46 g) and subsequently evaporating the ethanol solvent at 333–393K. The sample was then treated at 823 K for 16 h in dry air in order to decompose the organosilane precursors and to form the silanated H–ZSM5.

Table 2.5 Reagents for the preparation of a Co-zeolites.

Reagent	Molar mass ($g.mol^{-1}$)	Supplier	Purity
Zeolites	-	Zeolyst International	
3-aminopropyl triethoxylsilane	221.37	Aldrich	99%

2.3. Catalysts characterisation.

2.3.1. X-ray powder diffraction (XRD).

X-ray powder diffraction (XRD) is a common method of determining the structure of a material. To produce a powder XRD pattern, the sample must be crystalline and have long range order. Bombarding a suitable target with electrons produces the X-rays. When the electrons hit the target, they excite electrons which return to their normal state shell with a consequent emission of X-rays [7]. The three-dimensional structure of crystalline materials can be defined as regular repeating planes of atoms that form a crystal lattice (**Figure 2.3**).

When a focused X-ray beam interacts with these planes of atoms, part of it will be diffracted. The diffracted X-rays will interfere constructively with and give a diffraction line for a particular angle of incidence if the Bragg's law is satisfied. The wavelengths of the X-rays produced by the powdered sample and diffracted by the analyzer crystal obey the Bragg equation. The Bragg Law links the d-spacings on the powdered sample to the angle of incident of the X-rays on the sample (**Figure 2.3**).

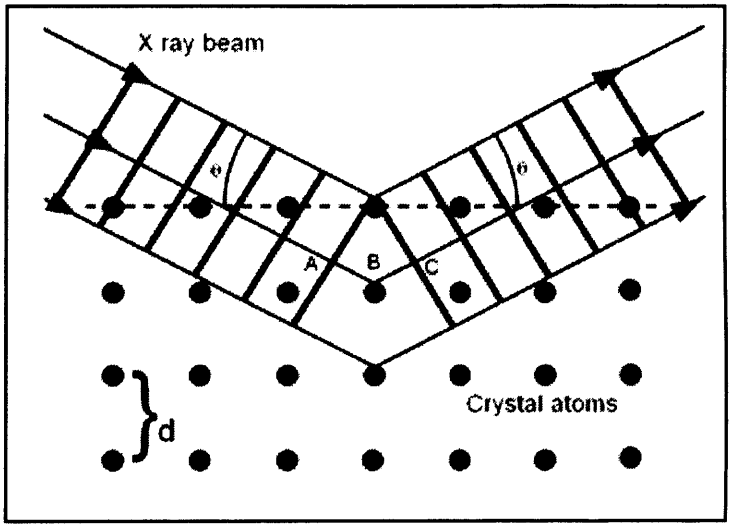

$$n\lambda = 2d\sin\theta$$

θ = angle between the crystal plane and the diffracted beam.

λ = wavelength of incident X-rays beam.

d = spacings between atomic layers in the powdered sample.

n = integer.

Figure 2.3 Bragg's Law of diffraction.

The data obtained shows a series of lines of varying intensities at different 2θ values, obtained as the analyser crystal turns. A qualitative analysis of the sample is thus carried out.

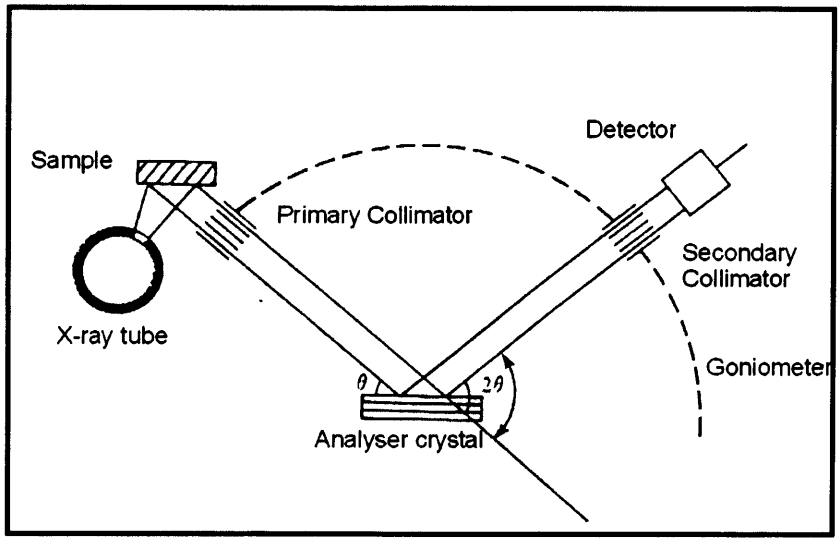

Figure 2.4 Schematic of an X-ray diffractometer.

The catalyst was ground up into a fine powder and then was placed on to a metal disc. It was placed on to the rotating stage. XRD analysis was performed using a PW 3040/60 Pananalytical Xpert Pro diffraction system with a monochromatic Cu $K_{\alpha 1}$ source operated at 40 keV and 30 mA.

2.3.2. Surface area method (BET) and micropore volume.

Surface area measurement is widely used to characterize porous materials. Surface area frequently plays a significant role in the reactivity of catalysts [8]. For example, for a catalyst, the greater the amount of surface available to the reacting gas or liquid the better is the conversion to products. BET is a rule to calculate the number of adsorbed gas molecules to form a monolayer on the surface. This rule is used to determine the surface area of a material at cryogenic temperatures (liquid nitrogen -196°C). The concept of BET theory is based on the following hypotheses: gas molecules physically adsorb on a solid in layers infinitely; there is no interaction between each adsorption layer and the Langmuir theory can be used for each layer. The Langmuir theory relates the coverage or adsorption of molecules on a solid surface

to a gas pressure at a fixed temperature. Based on the BET method, the specific surface area of a solid was calculated electronically using the BET equation [9].

$$P/[V(P_0-P)] = 1/(V_mC) + (C-1)/(V_mC) * P/P_0$$

where P= pressure

P_0= saturation pressure of the gas

V= adsorbed gas quantify

V_m=volume of gas to form a monolayer adsorbed gas.

C=constant

The volumes of pores were determined using the BJH method, which depends on an increase in pressure causing an increase of the thickness of the layer adsorbed on the pore walls [10].

Powder samples were analysed using the Quantachrome Autosorb-1. It is a fully automated analyzer for surface area and pore size measurements. Before performing a surface area analysis or pore size measurement, solid surfaces must be free from contaminants such as water. Surface cleaning (degassing) is carried out by placing the catalyst (0.1g) in a glass cell (12 mm diameter) and heating it under helium overnight at 300°C. Once clean, the sample inside the glass cell is brought to a constant temperature using a dewar containing liquid nitrogen. Then, small amounts of a gas (N_2) are admitted in steps into the evacuated sample chamber.

2.3.3. Inductively coupled plasma mass spectroscopy (ICP-MS).

The analysis by ICP-MS of a sample can be decomposed in four steps: Aerosol formation, ionisation, mass discrimination and detection with analysis. Liquid samples are mixed with argon to form a fine mist and then is vaporised in the plasma torch (6000°C) where the

sample is dried to a solid and then to a gas. The atoms in the plasma release one electron to form a singly charged ion. The singly charged ions exit the plasma and enter the discrimination region. A mass filter is made up of four metal rods aligned in a parallel diamond pattern. When the voltages are set to certain values only one particular ion is able to continue on a path between the rods and the others are forced out of this path. Many combinations of voltages are chosen which allows an array of different m/z ratio ions to be detected. The detector system will count the numbers of selected ions by the quadrupole. The detection limit for vanadium, cobalt and aluminium is 1-10 parts per trillion.

ICP-MS was used to detect the leaching of vanadium of VMgO catalyst in *n*-decane after run and also to determine the amount of Co/Al incorporated in the zeolites after solid state ion exchange. Samples were analysed By Dr. Iain McDonald [11] using a JY Horiba Ultima system.

2.3.4. Thermogravimetric analysis (TGA).

TGA can directly record the weight change with time or temperature due to dehydratation or decomposition in an atmosphere of nitrogen, helium, air, other gas, or in vacuum. For TGA the sample is continuously weighed as it is heated to elevated temperatures. Changes in weight are a result of the rupture or the formation of various physical and chemical bonds at elevated temperatures. All of the TGA analysis in the current work was carried out in a SETARAM Labsys thermogravimetric analyzer. A typical procedure for obtaining a TGA pattern is as follows. 50 mg of a sample of catalyst was placed into an aluminium oxide crucible for analysis. The analysis was performed in air. The temperature programme that was used was to have an isothermal time period at 25°C for 30 minutes, then a temperature ramp to 300°C at a ramp rate of 5°C/min.

2.3.5. X-ray Photoelectron Spectroscopy (XPS).

X-ray Photoelectron Spectroscopy (XPS) is used to determine the composition, the oxidation state of the elements that exist on the surface of the catalyst. This technique is highly surface specific with a depth 5 nm to 20 nm. When an atom absorbs a photon of energy hν, a core or valence electron with binding energy E_b is ejected with kinetic energy E_k:

$$E_k = h\nu - E_b - \varphi$$

hν is the X-ray energy

E_b is the binding energy of the photoelectron

Φ is the work function of the spectrometer (often ignored)

In this technique, the catalyst surface is irradiated with X-rays and the emitted photoelectrons are measured. The energy of core electrons is very specific for each element, the spectrum is able to provide information on the electronic state, elemental composition and chemical species that exist on the surface of samples. XPS analysis was carried out with an ESCALAB 220 spectrometer using an achromatic AlKα source and an analyser pass energy of 100eV.

2.4. Reactors used in the present work.

The Parr Series 5000 Multiple Reactor System (**Figure 2.5**) has been used to for the liquid phase oxidation of *n*-decane and *n*-hexane with oxygen. Six reactions at different pressures and temperatures can be run simultaneously, which allow catalytic data to be obtained quickly.

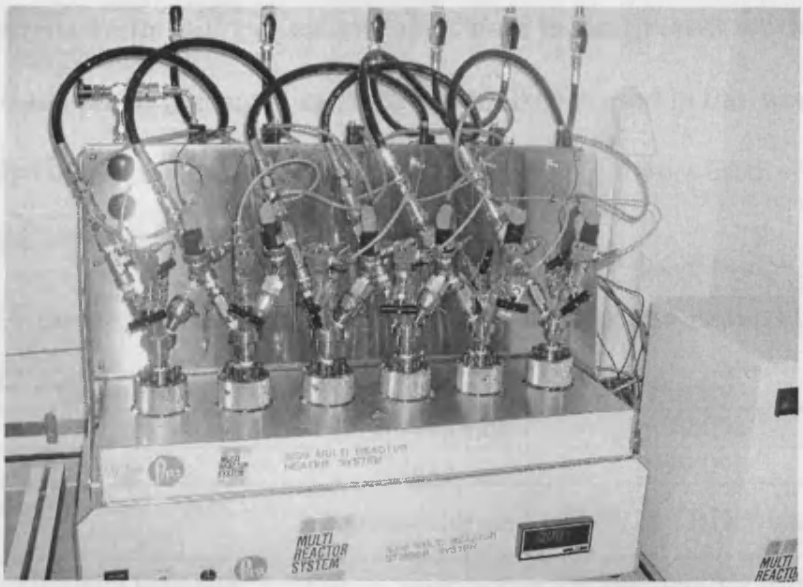

Figure 2.5 Multi reactor system and control box.

The principle features of the instrument include [12]:

- A system with 45 mL vessels.
- Six reactors with internal stirring.
- Operating pressures to 3000 psi.
- Operating temperatures to 275 °C.
- Individual temperature control.
- No autosample line.

All six vessels are stirred with a single magnetic stirrer and have the same stirring speed during a single run. The activities of the catalysts were tested with *n*-decane (10g) or *n*-hexane (10g). All the catalysts (0.05g) were tested with a stirring speed of 600 rpm. The reaction unit was flushed once with O_2, after which the pressure was increased to 5 bar or 15 bar of oxygen at room temperature, then the reactor was heated at desired temperature (80°C, 100°C, 110°C, 120°C or 130°C) for different runtimes. A small bucket of ice was used to cool down the reactor at the end of the reaction.

2.5. Purity of the reactants and radical initiators used in the present work.

Table 2.6 reports the purity and supplier of the linear alkanes used in this work (*n*-decane and *n*-hexane) and also the purity and supplier of the two radical initiators used.

Table 2.6 Purity and supplier of *n*-decane , *n*-hexane and radical initiator.

Compound	Supplier	Purity
n-decane	Sigma-Aldrich	≥ 99.0%
n-hexane	Fluka	≥ 99.0%
Tert-butylhydroperoxide (TBHP)	Sigma-Aldrich	~ 80% in TBHP/ water
Benzoyl peroxide (BPO)	Sigma-Aldrich	75% remainder water

2.6. Analysis of reactions solutions.

2.6.1. Gas Chromatography (GC).

The reaction solutions after reaction were analysed by gas chromathography (GC). The sample is injected into a heating block (Injection Port) where it is immediately vaporized and swept by the carrier gas into the column inlet. Each solute will travel at its own rate through the column and enter to a detector attached to the column exit [7]. Analysis was carried out using a Varian Star 3800 equipped with a Chrompack CP Wax 52CB, 25m, 0.53 mm, 2.0 microns capillary column. Stationary phases (**Figure 2.6**) with "wax" in their name are polyethylene glycol.

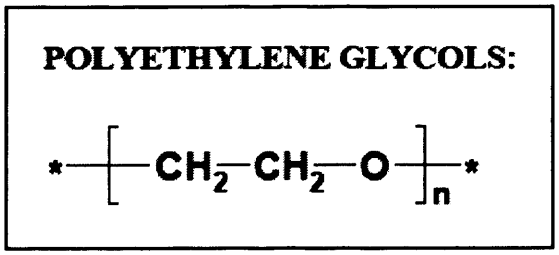

Figure 2.6 Stationary Phase.

The oxygen group in the polymer backbone is capable of hydrogen bonding. Compounds with the smallest hydrogen bond interaction with the column will elute from the column first (lowest boiling point) and compounds with higher hydrogen bonding interaction with the column (e.g. carboxylic acids) will elute last (highest boiling point). The higher the boiling point of the compound, the higher the retention time on the column. (**Table 2.7-2.8**).

Table 2.7 Order of elution and retention for each product for *n*-decane reaction.

Order on the GC trace	Compounds	Retention Time (min)
1	*n*-decane	3.44
2	5/4-decanone (5/4 one)	11.81
3	3-decanone (3 one)	12.54
4	2-decanone (2 one)	13.45
5	5/4-decanol (5/4 ol)	16.26
6	3-decanol (3 ol)	16.94
7	2-decanol (2 ol)	18.02
8	internal standard	20.44
9	pentanoic acid (C_5OOH)	25.25
10	1-decanol (1 ol)	25.65
11	hexanoic acid (C_6OOH)	29.30
12	heptanoic acid (C_7OOH)	32.69
13	octanoic acid (C_8OOH)	35.66
14	nonanoic acid (C_9OOH)	38.38
15	decanoic acid ($C_{10}OOH$)	40.85

The column did not allow separation of 2-decanone and decanal and only one peak was observed.

Table 2.8 Order of elution and retention for each product for *n*-hexane reaction.

Order on the GC trace	Compounds	Retention Time (min)
1	*n*-hexane	0.84
2	3-hexanone (3 one)	8.30
3	2-hexanone (2 one)	9.54
4	hexanal	9.54
5	3-hexanol (3 ol)	13.24
6	2-hexanol (2 ol)	13.85
7	1-hexanol (1 ol)	16.78
8	internal standard	22.19
9	hexanoic acid (C_6OOH)	25.12

The column did not allow separation of 2-hexanone and hexanal and only one peak was observed.

The GC was fitted with a flame ionisation detector (FID). The detection principle is based on the change in the electric conductivity of a hydrogen flame in an electric field when feeding organic compounds [13]. The organic compounds escaping from the separation column are burning for 99.97 % and 0.03% is fragmented. During subsequent oxidation by oxygen, which is fed into the flame from outside, ions are formed according the following reaction:

$$CH^* + O \rightarrow CHO^+ + e^-$$

The flow of ions is recorded as a voltage drop across a collecting electrode.

The programmed-temperature chromatography is the procedure in which the temperature of the column is changed systematically during a part or the whole of the separation. The oven programme is a little complicated but allows for a good separation for the analysis after *n*-decane reaction.

Start at 60°C hold for 7 min.

Ramp at 35°C/min to 115°C hold for 12 min.

Ramp at 4°C/min to 220°C hold for 1 min.

Ramp at 50°C/min to 240°C hold for 2 min.

The oven programme for the analysis and the separation after reaction with *n*-hexane reaction is:

Start at 35°C hold for 7 min.

Ramp at 35°C/min to 220°C hold for 3 min.

Injection parameters used was a split ratio on the GC was 10:1 suitable for quantitative and qualitative analysis (narrow peaks of analyte). 0.2 µl of sample was injected onto the column using a 1µl syringe.

2.6.2. Internal standard.

An internal standard was added to the reactions studied. The analyte chosen for the internal standard has a predictable retention time and area, allowing it to be used to determine if abnormalities have occurred. The standard chosen was 1,2,4-trichlorobenzene as that did not interfere with the reaction and eluted from the column at different retention time to the compounds studied (**Table 2.7- 2.8**). 0.15 ml of internal standard for *n*-hexane solutions and 0.3 ml of *n*-decane solutions were added to the crude mixture at the end of the reaction.

2.6.3. Calculations of internal response factors of each compound and quantification of the products after reaction.

The internal response factor (K) of each product was calculated by finding the ratio of a known amount of product over a constant amount of 1,2,4-trichlorobenzene (internal standard). Four different solutions were made up with internal standards and all the different

products. For example, the first calibrated solution for *n*-decane calibration was containing *n*-decane (10g), each products (10 mg) and 1,2,4- trichlorobenzene (0.15 ml). The second solution was containing the same mixture but with 30mg of each products. K was the average found by 4 different calibration solutions (10 mg, , 30 mg, 70 mg and 90 mg of each product) using this equation.

$$K = [(\text{Area IS}) * (\text{Amount SC})] / [(\text{Amount IS} * \text{area SC})]$$

K = Internal Response Factor.
IS = Internal Standard.
SC = Specific compound of interest.

Before to prepare the etalons solutions, calculations have been carried out to be in the range of masses of products made during the reaction. An example is detailed below for the 3-decanone.

Conversion= 3%

Selectivity= 10%

Mass of 3-decanone produced= 33 mg

Table 2.9 describe an example of K (internal response factor) for 3-decanone for each solution etalon.

Table 2.9 Internal reponse factor for each solution etalon

Solution etalon	Masse of 3-decanone	K
1	10 mg	0.64
2	30 mg	0.62
3	70 mg	0.63
4	90 mg	0.66
Average		0.64

A fresh known solution including standard and all the compounds in **Table 2.7** and **Table 2.8** were tested in this way on a regular basis to ensure results reported are accurate. The amount

of specific compound of interest added at the beginning to the fresh solution and the amount calculated from the GC trace were checked by this formula.

$$\text{Amount SC} = (\text{Amount IS} * \text{Area SC} * \text{K}) / (\text{Area IS})$$

K = Internal Response Factor.
IS = Internal Standard.
SC = Specific Compound of interest.

Calculations of conversion, selectivity and yield have been made with these formulas:

$$\text{Yield of each product (\%)} = \frac{\text{K (Area of Product / Area I.S.) * mass I.S}}{\text{(Mass of } n\text{-decane (10g)/ molar mass of decane * molar mass of product)}} * 100$$

Conversion (%)= Total Yield (%) = Sum Yield of each product.

Product Selectivity (%) = (Yield of each product / Total Yield)

The calcul of conversion has been ccarried out for the desired products (**Table 2.7**) but other products are present in the mixture after reaction. An example of GC trace for *n*-decane is shown in **Figure 2.7**.

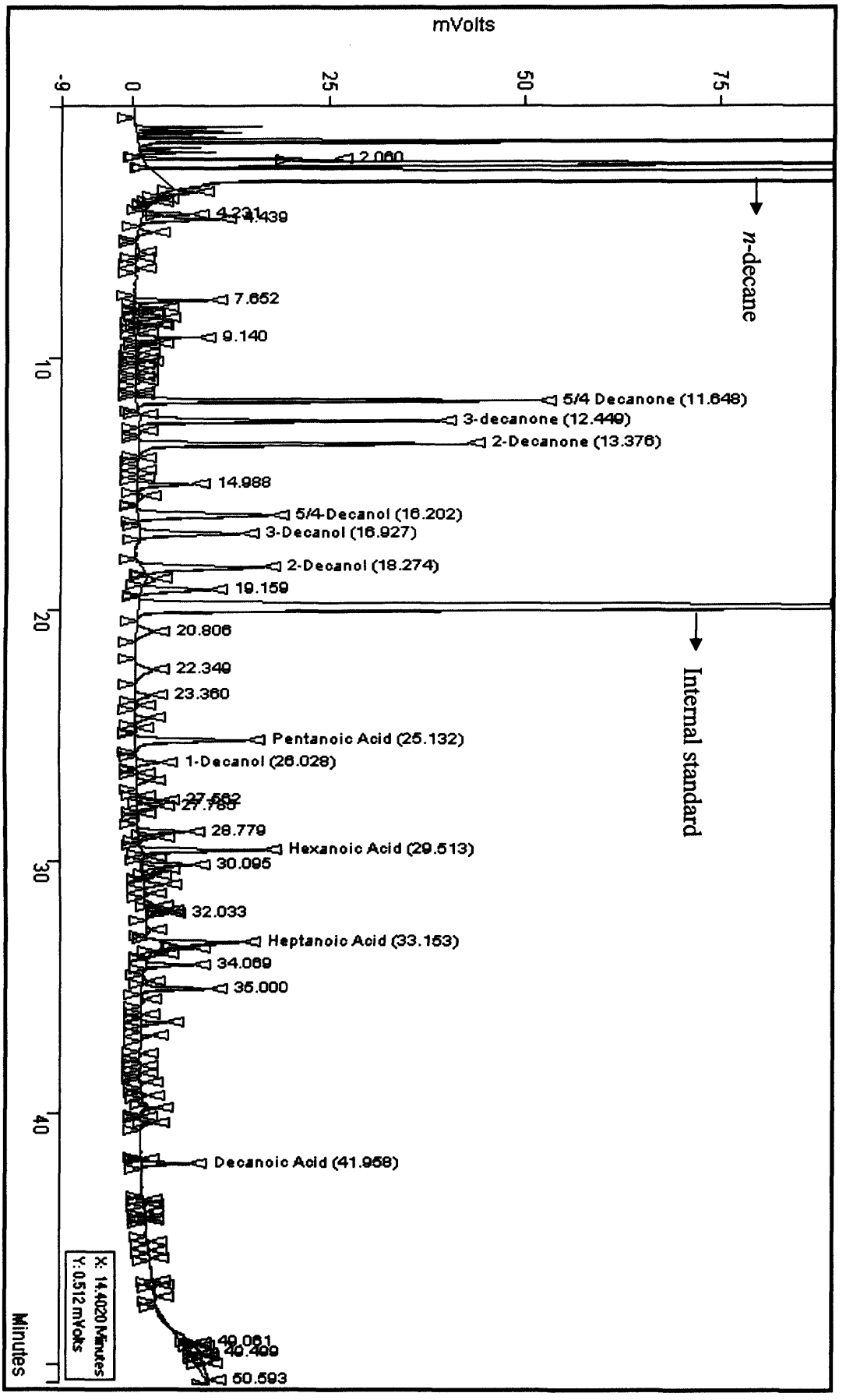

Figure 2.7 GC tace for the autoxidation (130°C, 24 hours)

2.7. Risk assessment

The experiments involve the three factors required for explosion: oxygen, fuel (*n*-decane) and potential ignition sources (heat). Auto-ignition of organic solvents under air / oxygen is a well known phenomena. The auto-ignition temperatures of *n*-decane and *n*-hexane under air at ambient pressure are given as 205 – 250°C. The lower temperature of 205°C was used for risk assessments. Increasing pressure and moving from an air to oxygen atmosphere are known to reduce the auto-ignition temperature and to account for this a 60°C margin was allowed to estimate the safe operating temperatures under the experimental conditions. This resulted in a modified safe operating temperature of approximately 140°C being assumed. The experiment was set up at ambient conditions, pressurised (the oxygen supply was closed once the rig had reached pressure) and then heated up to temperature using the automated control system. The autoclave was placed in a cabinet with safety doors and no personnel would open the cabinet doors during the heat up stage. The status of the vessels was checked via the PC controller system.

2.7. References.

[1] H.B. Friedrich, N. Govender, M.R. Mathebula, Applied Catalysis A: General 297, (2006), 81.

[2] P.M. Michalakos, M.C. Kung, I. Jahan, H.H. Kung, Journal of Catalysis 140, (1993), 227.

[3] C. Nicolaides, Chief Scientist- Hydrocarbon transformation group- Sasol.

[4] Zeolyst International http://www.zeolyst.com/

[5] H.G. Karge, Studies in Surface Science and Catalysis 105, (1997), 1901.

[6] W. Ding, G.D. Meitzner, E. Iglesia, Journal of Catalysis 206, (2002), 14.

[7] Instrumental methods of analysis, L.L. Meritt, J.A. Dean, New York, (1974).

[8] J.M. Thomas, W.J. Thomas, Principles and Practice of Heterogeneous Catalysis, Wiley, (1997).

[9] S. Brunauer, P. Emmet, E. Teller, Journal of American Chemistry Society, 60, (1938), 309.

[10] G. Leofanti, M. Padovan, G. Tozzola and B. Venturelli, Catalysis Today, 41, (1998), 207.

[11] Dr. Iain McDonald, School of Earth, Ocean and Planetary Sciences, Cardiff University.

[12] Par website http://www.parrinst.com.

[13] Analytical Chemistry, A Modern Approach to Analytical Science. Second Edition. R. Kellner, J.M. Mermet, M. Otto, M. Valcarcel, H.M. Widmer, Springer Berlin, (2006).

Chapter 3

Autoxidation of *n*-decane

3.1. Introduction.

Autoxidation or noncatalytic oxidation is the spontaneous reaction of oxygen with alkanes without the intervention of a flame. **Figure 3.1** shows the autoxidation reaction of *n*-decane.

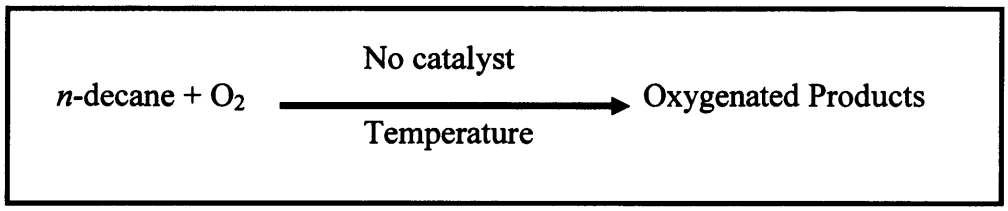

Figure 3.1 Autoxidation of *n*-decane.

The major products of the autoxidation are a mixture of alcohols, ketones and cracked acids. The liquid-phase autoxidation of hydrocarbons is an important process in the petrochemical value chain [1]. One of the major examples is the autoxidation of cyclohexane [1-2], which is converted to cyclohexanol and cyclohexanone widely used as feedstock for nylon production. Other industrially important autoxidation processes are the conversion of ethylbenzene to ethylbenzene hydroperoxide, the conversion of p-xylene to terephatalic acid [3] and the autoxidation of cumene which serves as feedstock for the production of phenol and acetone. The autoxidation mechanism of alkanes proceeds by a radical mechanism as described by reaction **Figure 3.2** given in eq.1-5. In this mechanism [4] I represents Initiator, RH the straight chain alkane, R* alkyl radical, ROO* the peroxyl radical or peroxide radical and ROOH the hydroperoxide. Different sources (I) can initiate the autoxidation. It can be radical

initiator such as benzoyl peroxide (BPO) or *tert*-butylhydroperoxide (TBHP) added voluntary at the beginning of the reaction or it can be impurities from the feed (ROOH, olefin), traces of metal in the stainless steel autoclave or heat. [3-5]. It should be noted that the propagation cycle is repeated many times before the termination reaction [6].

Initiation:	$I \rightarrow R^*$	eq.1
Propagation:	$R^* + O_2 \rightarrow RO_2^*$	eq.2
	$RO_2^* + HR \rightarrow RO_2H + R^*$	eq.3
Termination:	$RO_2^* + RO_2^* \rightarrow$ non radical products	eq.4
	$R^* + R^* \rightarrow R_2$	eq.5

Figure 3.2 Autoxidation mechanism [4].

A disadvantage of autoxidation chemistry is that the radical mechanism is not as selective as desired [6].

3.2. Experimental.

The liquid phase experiments were carried out in a high-pressure autoclave with a nominal volume of 45ml. *n*-decane (10g) (anhydrous, ≥99% from Sigma Aldrich) was tested at temperatures ranging from 80°C to 140°C for the desired time. The stirring speed was set to 600 rpm and the pot was flushed once with oxygen before charging with oxygen to a pressure of 15 bar at room temperature. In addition, some reactions were performed with a small amount of radical initiator added at the beginning of the reaction. Tert-butylhydroperoxide (TBHP 70% in water from Aldrich) and benzoyl peroxide (75%, remainder water from Aldrich) were used. At the end of the run, 150 µl of internal standard (1,2,4-trichlorobenzene) was added to the crude mixture of products before analysis was performed using a gas chromatograph (Varian Star 3800) fitted with a DB-WAX column and a flame ionization

detector (FID).

3.3. Results.

3.3.1. Effect of the temperature on the autoxidation of *n*-decane.

In the liquid phase autoxidation of alkanes, temperature is an important factor. If the temperature is too low there is no conversion however a high temperature will give a high conversion. The effect of the temperature on the conversion of *n*-decane for a run of 24 hours is shown in **Table 3.1.**

Table 3.1 Effect of the temperature on the conversion (%).

Temperature	Conversion (%)
80°C	0
100°C	0.1< conversion (%) <0.4
110°C	1.58
120°C	6.1< conversion (%) <10.70
130°C	21

Reactions conditions: 80°C to 130°C, stirring speed 600 rpm, 15 bar O_2, decane (10g) and runtime (24 hours).

For a run of 24 hours, a minimum temperature of 100°C is needed to promote the autoxidation of *n*-decane. Increasing the temperature provides a major increase in the conversion and greatly increases the number of products (e.g. 140 products for a reaction of 24 hours at 130°C) which makes the identification and analysis of all the products difficult. The primary major products made by the radical autoxidation mechanism are more reactive towards oxidation (oxidation of alcohols to ketones) [7]. The formation of ketone products will weaken the carbon-carbon bond in the α-position along the *n*-decane chain which can result in cleavage of the C-C bond to form two cracked products. It has to be considered as

well that *n*-decane is a long linear chain alkane with 10 carbons and can be functionalised in more than one position by the radical autoxidation mechanism and after can undergo many carbon-carbon bond cleavages. All these different reactions can explain the complexity of the GC trace even at low conversion.

3.3.2. Product profile at different temperature.

The products of the autoxidation of *n*-decane at different temperature are listed in **Table 3.2**.

Table 3.2 Product distribution at different temperature.

Temp.	Conv (%)	5/4 one	3 One	2 one	5/4 ol	3 ol	2 ol	1 ol	C_5 acid	C_6 acid	C_7 acid	C_8 acid	C_9 acid	C_{10} acid
80°C	0	-	-	-	-	-	-	-	-	-	-	-	-	-
100°C	0.15	30.0	19.3	24.2	2.1	1.8	1.8	1.0	6.5	5.9	5.2	0	0	2.2
110°C	1.58	28.5	16.6	19.4	4.3	2.7	5.0	0.8	5.5	4.9	8.5	0.8	0.4	2.6
120°C	10.70	24.3	13.3	16.7	4.4	6.9	4.3	0.5	9.5	8.0	6.3	2.7	2.5	0.8
130°C	21,75	23.6	13.6	16.4	4.1	6.3	4.1	0.4	10	8.5	6.8	2.7	2.8	0.6

Reactions conditions: 80°C to 130°C, stirring speed 600 rpm, 15 bar O_2, decane (10g) and runtime (24 hours)

After a run of 24 hours, *n*-decane is oxidised to form several products including C_{10} alcohols, C_{10} ketones and cracked monocarboxylic acids resulting from the cleavage of a C-C bond. The C_{10} alcohols and C_{10} ketones are mainly in position 5, 4, 3, 2 and there is a very low terminal selectivity to 1-decanol and decanoic acid. The radical mechanism is not selective for the desired terminal products even at low conversion. The major positions of oxygenation functionalisation of *n*-decane during the autoxidation are in position 5, 4, 3 and 2, which will weaken the C-C bond along *n*-decane chain and can explain the presence of pentanoic acid, hexanoic acid, heptanoic acid, octanoic acid and nonaic acid which occur as a result of consecutive reactions. In such experiments reproducibility is poor because the autoxidation is

highly variable due to the quantity of impurities present in feedstock such as ROOH, olefins or trace metals [8]. High amounts of impurities will initiate the autoxidation quicker than a low level of impurities and will give a higher conversion with more products for the same runtime using the same experimental conditions. **Table 3.3** shows how the conversion and the product distribution of the reaction can change for different runs. Three different runs at 100°C and 120°C have been repeated.

Table 3.3 Reproducibility of the reaction at 100°C and 120°C.

Temp.	Conv (%)	5/4 one	3 one	2 one	5/4 ol	3 ol	2 ol	1 ol	C_5 acid	C_6 acid	C_7 acid	C_8 acid	C_9 acid	C_{10} Acid
100°C	0.15	30	19.3	24.2	2.1	1.8	1.8	1.0	6.5	5.9	5.2	0	0	2.2
100°C	0.39	32.4	20.8	21.9	1.6	3.0	2.0	1.0	3.9	3.8	2.5	5.1	0	1.9
100°C	0.28	30.9	18.3	22.2	2.7	1.7	2.8	0.8	9.0	3.8	5.4	0.5	0.3	1.6
120°C	6.12	26.1	14.9	18.5	4.7	6.5	4.2	0.5	10.2	1.1	7.2	2.6	2.5	0.9
120°C	10.70	24.3	13.3	16.7	4.4	6.9	4.2	0.5	9.5	8.0	6.3	2.7	2.5	0.8
120°C	7.34	21.4	11.6	15.8	6.1	3.9	5.7	0.5	14.1	8.7	6.1	3.5	1.6	1.0

Reactions conditions: 100°C & 120°C, stirring speed 600 rpm, 15 bar O_2, decane (10g) and runtime (24 hours)

Tables (3.4 and **3.5)** have shown the range of the results at 100°C and 120°C.

Table 3.4 Range for the conversion (%), terminal selectivity (%) and cracked acids for a run of 24 hours at 100°C.

Conversion (%)	Selectivity (%) 1-decanol	Selectivity (%) decanoic acid	Selectivity (%) cracked acids (C_5 to C_9)
0.15 to 0.39	0.8 to 1.0	1.6 to 2.2	15.3 to 19.0

The conversion can be multiplied by a factor of more than two for the same reaction with the same experimental conditions. The terminal selectivity is also not stable but stays very at a low level below 3.2 %.

Table 3.5: Range for the conversion (%), terminal selectivity and cracked acids for a run of 24 hours at 120°C.

Conversion (%)	Selectivity (%) 1-decanol	Selectivity (%) decanoic acid	Selectivity (%) cracked acids (C_5 to C_9)
6.10 to 10.70	0.5	0.8 to 1.0	23.6 to 34.0

Increasing the temperature decreases the reproducibility under the same experimental conditions. It can be noted that increasing the temperature will increase the number of consecutive reactions resulting in overoxidation of the primary products and explains the large amount cracked acids. Increasing the temperature will diminish the percentage of terminal selectivity.

During this work many blank reactions (without catalyst) were performed. The blank reaction reveals if the pot is clean after a reaction with a catalyst and whether there is any contamination. **Figure 3.3** is a summary of these results.

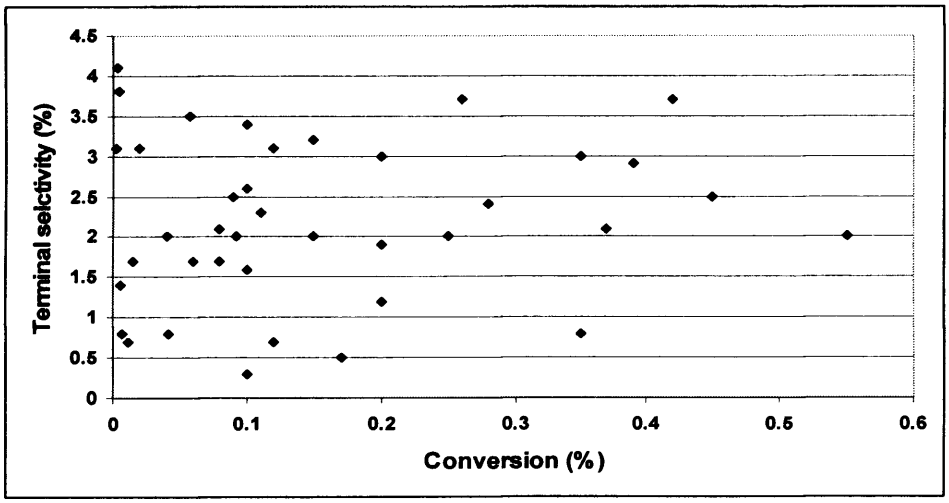

Reactions conditions: 100°C, stirring speed 600 rpm, 15 bar O_2, decane (10g) and runtime (24 hours).

Figure 3.3 Conversion (%) and terminal selectivity (%) for autoxidation.

From these results, we can see the range of the conversion for the autoxidation reaction at 100°C is between 0.05% to 0.55%. So if a blank reaction was performed with a conversion superior to 0.50% after use of a catalyst, it was assumed there is a contamination in the autoclave pot and the pot was rewashed carefully and another blank reaction was set up until a

conversion below 0.50% was observed. The value 0.5% of conversion was arbitrary decided as the maximum conversion after a run of 24h at 100°C without catalyst. This maximum conversion (0.5%) was also agreed by another team working on the same project with the same substrate and same type of autoclave at Johnson Matthey. Contamination is a major problem for the liquid phase catalysis. Contamination can promote or inhibit the conversion of the reaction, which result in wrong results and irreproducibility of data. The major cause of contamination is traces of catalyst or radical scavenger from the previous run. The second major keypoint of the **Figure 3.3** is the terminal selectivity. It can be observed that the terminal selectivity varies between 0.3% and 4.1%. These results are a very important baseline, to compare against the catalyst performance. If a run is made with a catalyst and the terminal selectivity is below 4%, it can be deduced that the catalyst does not influence the terminal selectivity of the reaction. Some points of **Figure 3.2** have been made by Yuan Shang and Sivaram Pradhan, PhD students working on the same project [9].

3.3.3. Analysis of the gas after reaction run.

At the end of the run, a miniature gas sample cylinder was attached to the autoclave to collect the gas after reaction. The gas sample was analysed using a GC fitted with a thermal conductivity detector (TCD). The target of this experiment is to check if there is production of carbon monoxide and carbon dioxide during the autoxidation.

Table 3.6 Gas analysis after run.

Analysis of the gas	Detection with FID detector
CO	0
CO_2	0

Reactions conditions: 100°C, stirring speed 600 rpm, 15 bar O_2, decane (10g) and runtime (24 hours)

No peaks corresponding to carbon monoxide or carbon dioxide were observed in the chromatogram. Only *n*-decane and oxygen were detected.

3.3.4. Time on line studies for *n*-decane autoxidation.

The autoxidation was studied for three different runtimes (8h, 16h and 24h) and the results are shown in **Table 3.7.** These runs were used to estimate the induction period of the reaction, and the primary products made by the radical mechanism. Reaction sampling is not available on the autoclave so each table entry is a different reaction rather than sampling the same reaction over time.

Table 3.7 Time on line at 100°C.

Time Hours	Conv. (%)	5/4 one	3 one	2 one	5/4 ol	3 ol	2 ol	1 ol	C_5 acid	C_6 acid	C_7 acid	C_8 acid	C_9 acid	C_{10} Acid
8h	0	-	-	-	-	-	-	-	-	-	-	-	-	-
16h	0.04	45.8	13.2	17.1	14.9	9.1	0	0	0	0	0	0	0	0
24h	0.39	32.4	20.8	21.9	1.6	3.0	2.0	1.0	3.9	3.8	2.5	5.1	0	1.9

Reactions conditions: 100°C, stirring speed 600 rpm, 15 bar O_2, decane (10g) and runtime (8, 16 and 24hours)

The results show there is an initial period where very little oxidation occurs, known as the induction period as observed in the literature by Ingold [5]. During the induction period, there is a low concentration of radical, which explains the low conversion and the concentration of radical builds up until it reaches a concentration which will allow a propagation of the radical mechanism resulting in an increase in the rate .The primary products made by this autoxidation are the internal ketones and internal alcohols (positions 5, 4, 3, 2).

Table 3.8 shows the time on line of the autoxidation reaction at higher temperature (110°C).

Table 3.8 Time on line at 110°C.

Time Hours	Conv. (%)	5/4 one	3 one	2 one	5/4 ol	3 ol	2 ol	1 ol	C_5 acid	C_6 acid	C_7 acid	C_8 acid	C_9 acid	C_{10} Acid
8h	0.1	25	16	19	3	2	3	1	13	5	6	0	0	1
16h	0.58	32	19	23	3	2	3	1	6	4	4	1	0	2
24h	1.58	28	16	19	4	2	5	1	5	5	9	1	0	2

Reactions conditions: 110°C, stirring speed 600 rpm, 15 bar O_2, decane (10g) and runtime (8, 16 and 24hours)

Increasing the temperature reduces the initiation period and a low conversion is observed after 8h.

3.3.5. Presence of hydroperoxide (ROOH) in the reaction solution.

3.3.5.1. Introduction.

The initial products of the autoxidation of alkanes are the corresponding hydroperoxides [10] formed by the free radical mechanism showed in **Figure 3.2.**

$$RH + O_2 \rightarrow RO_2H$$

RH is a hydrocarbon and RO_2H is the corresponding hydroperoxide. The reactivity of various C-H bonds decrease in the order tertiary>secondary> primary [11]. So for *n*-decane, the formation of the hydroperoxide will be easier along the chain rather than in the terminal positions.

3.3.5.2. Method used to quantify the hydroperoxide.

The concentration of hydroperoxides (ROOH) in the reaction cannot be determined directly from the GC chromatograms, as these compounds decompose in the GC column with the formation of approximately equal amounts of alcohol and ketone. If the sample of the reaction solution is treated with an excess of solid PPh_3 for 20 min at room temperature before GC

analysis, the hydroperoxide is reduced only to the corresponding alcohol [12-15]. Therefore, the difference in alcohols in the GC traces of the reaction solution before and after triphenylphosphine reductions allows to estimate the amount of hydroperoxide. If ROOH is present in the solution, the alcohol/ketone ratio of the chromatogram prior to the reduction with PPh_3 and will be different after reduction with PPh_3 (the alcohol peak will increase).

3.3.5.3. Results.

After reaction, the sample was injected twice, before treatment and after reduction with an excess PPh_3. If hydroperoxide is present, the ratio ketone/alcohol will be different between analyses. Theses results are listed in **Table 3.9**

Table 3.9 Ketones/alcohols ratio before and after treatment with PPh_3.

Reaction Time (hours)	First Injection without PPh_3	Second injection Treatment with PPh_3	ROOH Selectivity (%)
16	Ketones/alcohols=76/24	Ketones/alcohols=37/45	33
24	Ketones/alcohols=75/7	Ketones/alcohols=68/22	22

Reactions conditions: 100°C, stirring speed 600 rpm, 15 bar O_2, decane (10g) and runtime (24 hours)

After these results, it can be concluded that hydroperoxide are present in the reaction at the end of the run.

ROOH concentration was calculated by comparing the concentrations of the corresponding alcohol (R-OH) and ketone (R_H=O) in the chromatograms resulting from samples injected directly ($C`_{R\text{-}OH}$ and $C`_{RH=O}$) and from samples injected after 15 minutes of reaction with solid triphenylphosphine ($C''_{R\text{-}OH}$ and $C''_{RH=O}$). The alcohol/ketone ratio of the decomposition of alkyl hydroperoxide was assumed to be 1. The real concentration of ketone in the reaction ($C_{RH=O}$) is equal to that calculated after reduction with PPh_3. The difference in ketone concentration between both samples, $\Delta C_{RH=O} = C`_{RH=O} - C''_{RH=O}$, corresponds to the alkyl

hydroperoxide that is decomposed to ketone in the GC column. As we assumed that both alcohol and ketone are formed in a 1:1 ratio in the GC, so the alcohol that comes from alkyl hydroperoxide decomposition will be equal to $\Delta C_{RH=O}$, and its subtraction from the concentration of alcohol in the sample injected directly gives the real concentration of alcohol formed in the reaction, C_{R-OH}. The concentration of alkyl hydroperoxide in the reaction is calculated as the difference between the concentration of alcohol in the sample with PPh_3 and the real concentration of alcohol in the reaction [16].

$$C_{RH=O} = C''_{RH=O}$$

$$C_{R-OH} = C`_{R-OH} - \Delta C_{RH=O}$$

$$C_{ROOH} = C''_{R-OH} - C_{R-OH}$$

3.3.6. Radical Initiator.

3.3.6.1. Definition of radical initiator.

A lot of organic molecules are stable at elevated (>127°C) temperatures. Atoms of these compounds are connected by strong chemical bonds with bond dissociation energy (BDE) ~350-500 kJ mol^{-1}. Radical initiators are molecules bearing one weak bond with a low BDE ~100-200 kJ mol^{-1} for example a covalent bond between two oxygen atoms (O-O) [18]. When the temperature of the reaction is sufficiently high, the weakest bond of the radical initiator decomposes with homolysis and produces free radicals. These free radicals will initiate a radical reaction.

3.3.6.2. Half lives with temperature of the radical initiator.

One of the most important parameters for the choice of a radical initiator is the temperature of the reaction. The temperature determines the rate of decomposition (**Figure 3.4**) of the weakest bond of the radical initiator, which initiates the radical mechanism of the reaction.

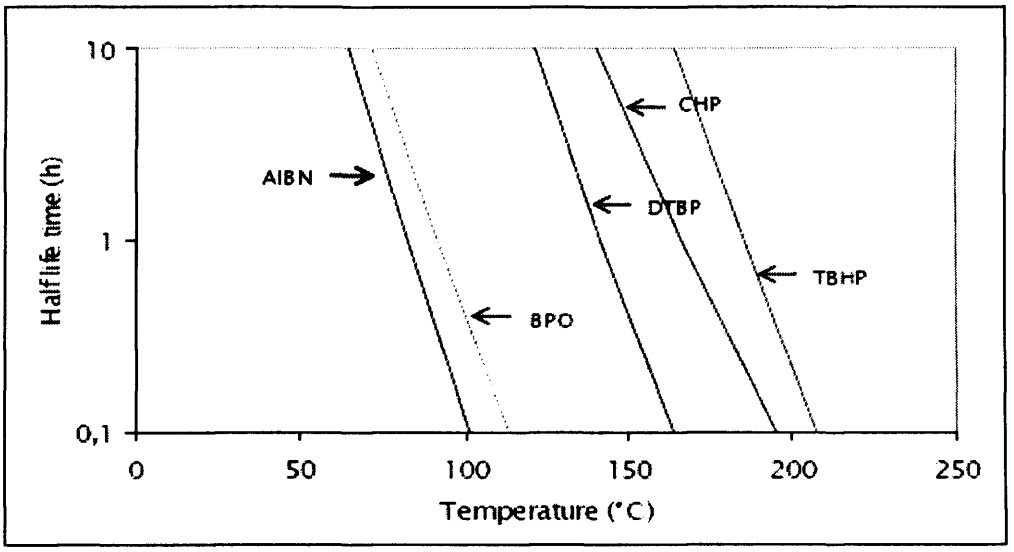

AIBN= Azobisisobutyronitrile, **TBHP**= t-Butyl hydroperoxide, **CHP**=cumylhydroperoxide, **m-CPBA**=m-Chloroperbenzoic acid,
BPO= Dibenzoyl peroxide, **DTPB** = Di-t-butyl peroxide.

Figure 3.4 Half life times of various initiators as function of temperature [19].

From the **Figure 3.4,** we can see that BPO will decompose to give radical species quicker than TBHP at the reaction temperature of 100 °C. The two different radical initiators that were tested in this work were TBHP in water (70% in water, MW=90.12) and dibenzoyl peroxide (BPO), which gives a different type and size of radical.

3.3.6.3. Activation of *n*-decane at 80°C.

The radicals initially formed by TBHP decomposition will go on to extract one hydrogen from the alkane. TBHP was added at the beginning of the reaction to explore if a small amount of radical initiator can activate *n*-decane at 80°C. **Table 3.10** is the result of three different reactions with runtimes of 8h, 16h and 24h.

Table 3.10. Conversion (%) of *n*-decane oxidation with different amount of TBHP added at the beginning of the reaction.

Mass of TBHP (g)	Conv. (%)	5/4 one	3 one	2 one	5/4 ol	3 ol	2 ol	1 ol	C_5 acid	C_6 acid	C_7 acid	C_8 acid	C_9 acid	C_{10} acid
0.05	0.12	41.5	22.1	27.9	1.5	0.7	1.5	0.1	3	0.4	0.8	0	0	0.6
0.15	1.31	45.29	22.1	28.6	0.2	0.1	0.2	0.1	0.7	0.4	0.6	0.2	0	0.8
0.30	2.24	45.5	22.1	28.6	0.2	0.1	0.2	0.1	0.7	0.5	0.6	0.3	0.1	0.8

Reaction conditions: 80°C, stirring speed 600 rpm, 15 bar O_2, decane (10g), TBHP (0.05g, 0.15g, 0.30g) and runtime (24 hours)

Without radical initiator, no reaction was observed with the same experimental conditions. Adding a radical initiator at the beginning of the reaction can promote the autoxidation reaction at 80°C. The rate of the reaction is proportional to the amount of TBHP added at the beginning of the reaction. The more radical initiator that is added at the beginning of the reaction the higher the conversion is after 24 hours. The amount of TBHP added did not influence the product distribution of the reaction.

Table 3.11. Repeat run of *n*-decane oxidation with TBHP (0.05g).

Mass of TBHP (g)	Conv. (%)	5/4 one	3 one	2 one	5/4 ol	3 ol	2 ol	1 ol	C_5 acid	C_6 acid	C_7 acid	C_8 acid	C_9 acid	C_{10} Acid
0.05	0.12	41.5	22.1	27.9	1.5	0.7	1.5	0.1	3.0	0.4	0.8	0	0	0.6
0.05	0.17	42.9	21.8	27.8	1.0	0.7	1.4	0.1	2.4	0.5	0.6	0.3	0.1	0.4

Reactions conditions: 80°C, stirring speed 600 rpm, 15 bar O_2, decane (10g), TBHP (0.05g) and runtime (24 hours)

The repeat runs (**Table 3.11**) confirm that *n*-decane can be activated at 80°C using a very small amount of TBHP at the beginning of the reaction. The terminal selectivity to 1-decanol and decanoic acid is very low after 24 hours for both reactions.

To compare the activity of BPO to TBHP operating with the same conditions, the same

number of moles of radical (**Table 3.12**) was added at the beginning of the reaction.

Table 3.12 Moles of TBHP & BPO used.

Features	TBHP	BPO
Molecular Weight	90.12	242.23
Purity	30% in water by mass	25% remainder water by mass
Mass used (g)	0.05	0.125
Mass used (g)	0.15	0.376

It has been shown in the **Figure 3.4** that BPO decomposes quicker than TBHP, so a higher conversion for the same runtime is expected.

Table 3.13 *n*-decane oxidation with different amount of BPO.

Mass of BPO (g)	Conv. (%)	5/4 one	3 one	2 one	5/4 ol	3 ol	2 ol	1 ol	C_5 acid	C_6 acid	C_7 acid	C_8 acid	C_9 acid	C_{10} Acid
0.040	0.14	15.3	9.2	10.6	21.9	11.9	14.8	2.2	4.1	2.6	4.4	0.7	1.3	0.8
0.125	0.18	16.0	9.3	10.4	23.1	12.6	15.2	2.3	1.2	0.9	4.5	2.2	1.3	1.1
0.376	0.79	16.2	9.2	9.9	23.8	13.2	14.6	3.3	1.3	1.7	3.7	0.3	1.4	1.2

Reactions conditions: 80°C, stirring speed 600 rpm, 15 bar O_2, decane (10g), BPO (0.04g, 0.125g, 0.376g) and runtime (24 hours)

As observed for TBHP, increasing the amount of BPO at the beginning of the reaction increases the conversion of the reaction after a run of 24 hours. Lower conversion is observed with the addition of BPO than with the addition of the same number of moles of TBHP beginning of the reaction.

To confirm these results, two repeat run were performed at 80°C with BPO (0.125g)

Table 3.14 Repeat run of *n*-decane oxidation with BPO (0.125g).

Time Hours	Conv. (%)	5/4 one	3 one	2 one	5/4 ol	3 ol	2 ol	1 ol	C_5 acid	C_6 acid	C_7 acid	C_8 Acid	C_9 acid	C_{10} acid
24 h	0.18	16.0	9.3	10.4	23.1	12.6	15.2	2.3	1.2	0.9	4.5	2.2	1.3	1.1
24 h	0.20	16.7	10.0	10.6	22.4	12.5	14.9	2.4	2.6	1.2	4.5	0.3	1.0	1.0

Reactions conditions: 80°C, stirring speed 600 rpm, 15 bar O_2, decane (10g), BPO (0.125g) and runtime (24 hours)

A comparative table (**Table 3.15**) allows comparison of the conversion, the terminal selectivity for 1-decanol, decanoic acid and the cracked product using TBHP or BPO as a radical initiator.

Table 3.15 Comparison of the conversion (%), internal oxygenated products and terminal selectivity (%) between TBHP and BPO at 80°C.

Radical initiator	Conversion (%)	Selectivity (%) Decanone Position 5/4/3/2	Selectivity (%) Decanol Position 5/4/3/2	Terminal Selectivity(%) 1-decanol & Decanoic acid
TBHP	0.12 to 0.17	91.5 to 92.5	3.1 to 3.7	0.5 to 0.7
BPO	0.18 to 0.20	35.7 to 37.3	49.8 to 50.9	3.4

Slightly higher conversion is observed for BPO, which can be explained by the quicker formation of radicals in the reaction. However a major difference is observed in the products profiles. More alcohol is produced using BPO as radical scavenger. So a radical initiator influences the product distribution of the autoxidation reaction.

3.3.6.4. Time on line at 100°C.

At 100°C, without a radical initiator, a long initiation period (8h) is observed. Using a radical initiator, the time of the initiation period is reduced. Three different reactions with different runtime were performed.

Table 3.16 Time on line using TBHP as radical initiator.

Time Hours	Conv. (%)	5/4 one	3 one	2 one	5/4 ol	3 ol	2 ol	1 ol	C_5 acid	C_6 acid	C_7 acid	C_8 acid	C_9 acid	C_{10} acid
8h	0.23	41.3	21.7	28.4	0.5	0.5	0.8	0.5	3.2	1.0	1.0	0.4	0.3	0.6
16h	0.38	37.2	20.4	26.1	1.1	0.7	1.4	0.3	4.5	2.5	3.1	0.3	0.4	1.9
24h	0.80	36.5	20.3	24.7	1.8	1.2	2.3	0.4	4.7	2.9	2.6	0.5	0.2	2.0

Reactions conditions: 100°C, stirring speed 600 rpm, 15 bar O_2, decane (10g), TBHP (0.05g) and runtime (8, 16, 24 hours)

Reactions, with the same reaction time were carried out with BPO as radical initiator.

Table 3.17: Time on line using BPO as radical initiator.

Time Hours	conv. (%)	5/4 one	3 one	2 one	5/4 ol	3 ol	2 ol	1 ol	C_5 acid	C_6 acid	C_7 acid	C_8 acid	C_9 acid	C_{10} Acid
1h	0.27	13.7	8.0	9.5	25.6	14.1	15.9	3.4	1.0	0.6	4.0	1.8	2.0	0.5
8h	0.35	14.2	8.1	9.3	25.0	14.0	16.2	3.0	1.6	1.0	4.2	0.3	1.6	1.4
8h	0.33	13.7	7.8	9.2	25.6	14.4	16.8	3.2	1.7	1.1	3.8	0.3	1.7	0.7
16h	0.34	15.0	8.5	9.6	24.1	13.7	16.3	3.1	1.8	1.2	3.7	0.3	1.7	1.1
24h	0.39	15.9	9.1	10.4	23.6	13.3	16.0	3.1	2.0	1.4	3.1	0.3	0.9	1.1

Reactions conditions: 100°C, stirring speed 600 rpm, 15 bar O_2, decane (10g), BPO (0.125g) and runtime (1, 8, 16, 24 hours).

After 1hour of reaction the conversion is already 0.27%, showing BPO is decomposed very quickly at 100°C.Repeat runs were performed with BPO to confirm the low conversion obtained at 24hours, compared to the conversion obtained after 1h.

Table 3.18 Repeat run of *n*-decane oxidation with BPO at 100°C.

Time Hours	Conv. (%)	5/4 one	3 one	2 one	5/4 ol	3 ol	2 ol	1 ol	C_5 acid	C_6 acid	C_7 acid	C_8 acid	C_9 acid	C_{10} Acid
24h	0.37	14.2	8.0	9.3	25.2	14.3	16.3	2.9	2.2	1.4	3.4	0.4	1.5	0.9
24h	0.39	15.9	9.1	10.4	23.6	13.3	16.0	3.1	2.0	1.4	3.1	0.3	0.9	1.1

Reactions conditions: 100°C, stirring speed 600 rpm, 15 bar O_2, decane (10g), BPO (0.125g) and runtime (24 hours).

Addition of radical initiator leads to a shorter initial induction period. BPO has a decomposition temperature lower than TBHP which will give higher conversion at shorter runtime (8h) than TBHP. BPO also gave more alcohols in the products than TBHP. **Figure 3.5** is a summary of the conversion versus time with the same molar amount of TBHP and BPO at 100°C.

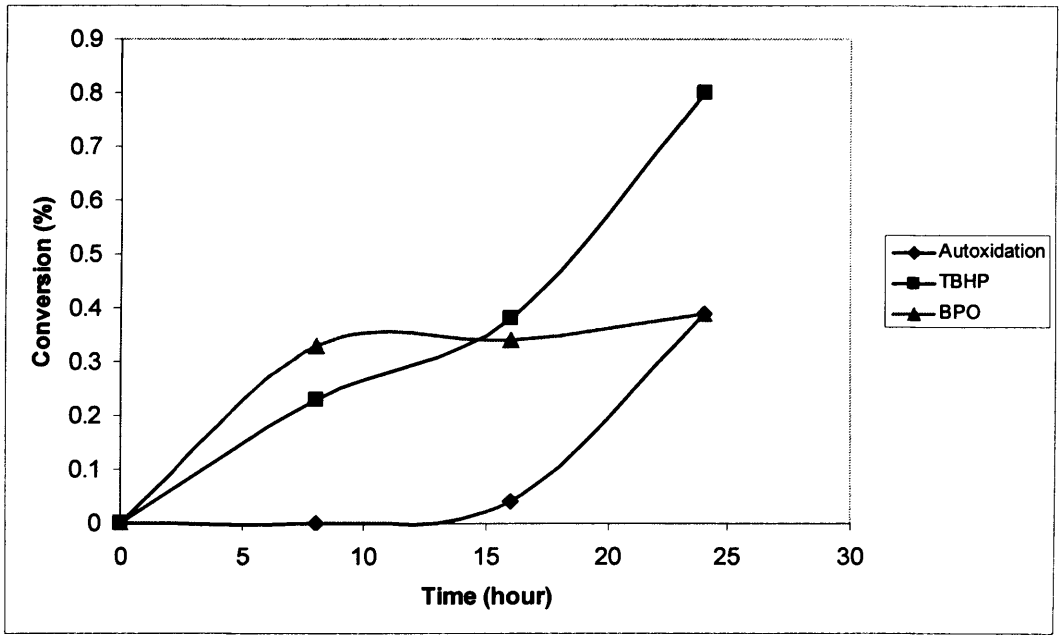

Reactions conditions: 100°C, stirring speed 600 rpm, 15 bar O_2, decane (10g), BPO (0.125g), TBHP (0.05g) and runtime (24 hours).

Figure 3.5 Time on line for autoxidation without radical initiator (blue curve), with TBHP (black curve) and with BPO (red curve).

3.3.7. Radical scavenger.

3.3.7.1. Definition.

Autoxidation can be inhibited or retarded by the addition of certain compounds known as antioxidants or radical scavengers, which lengthen the induction period [5].

In the presence of a radical scavenger, the propagation reaction is stopped by the termination step [20]. The phenyl ring will stabilise the radical.

$$RO_2^{*} + AH \rightarrow RO_2H + A^{*}$$

AH is the antioxidant and A^{*} is the radical derived from the loss of phenolic hydrogen. Stable nitroxide radicals, like 2,2,6,6-Tetramethylpiperidine-1-oxyl (PS tempo) have been also known to scavenge carbon radicals [21].

3.3.7.2. 2,6-Di-*tert*-butyl-4-methylphenol as radical scavenger.

The data for the autoxidation of *n*-decane in presence of radical scavenger are showed in the **Table 3.19.**

Table 3.19 Conversion with different amounts of 2,6-Di-tert-butyl-4-methylphenol.

Radical Scavenger	conversion (%)
None	0.1-0.4
0.050g	0
0.010g	0

Reaction conditions: 2,6-di-tert-butyl-4-methylphenol.Radical scavenger (0.0115g), 100°C, 600 rpm, 15 bar O_2, decane (10g), 24 hours

In the presence of 2,6-di-tert-butyl-4-methylphenol (BHT), the reaction was inhibited indicating that a radical process is operative.

3.3.7.3. PS-tempo as radical scavenger.

PS-tempo is 2,2,6,6-Tetramethylpiperidine-1-oxyl (tempo) supported on a polymer (polystyrene PS) prepared by Johnson Matthey. PS tempo is a bulky radical scavenger, which was used in the presence of an ion exchanged zeolites to kill the autoxidation around the catalyst but is too bulky to go inside zeolites channels to kill the reaction. So the desired target is that only the products from the reaction inside the channels of the zeolites will be present at the end of the reaction (**Figure 3.10**).

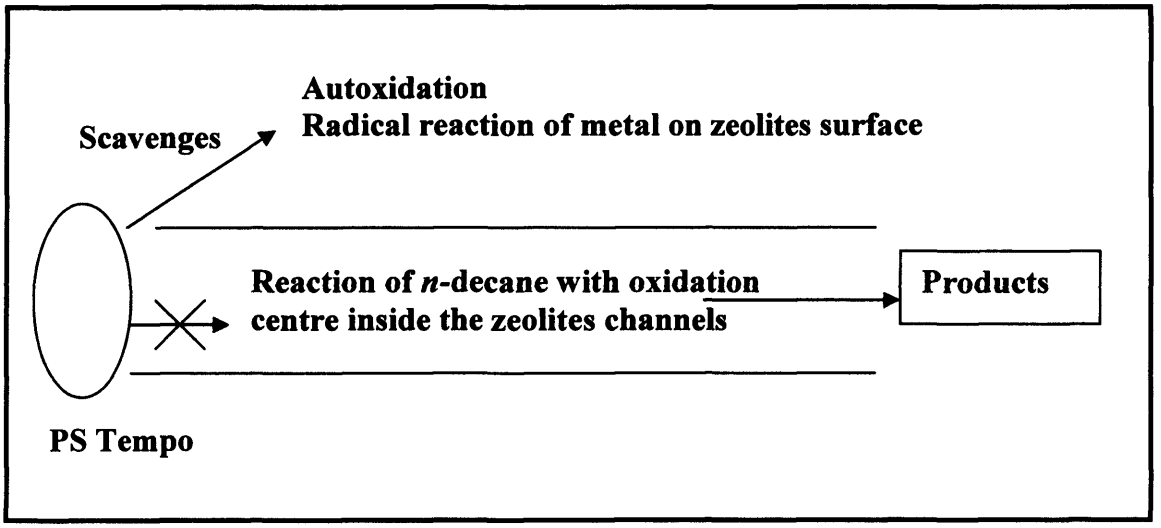

Figure 3.6 Desired action of PS-tempo with ion exchanged zeolites as catalyst

Table 3.20 Conversion (%) with different masses of PS-Tempo at different temperatures.

	Conv. (%)	Conv. (%)	Conv. (%)	Conv. (%)
Temperature	**Mass PS-tempo (50 mg)**	**Mass PS-tempo (20 mg)**	**Mass PS-tempo (5 mg)**	**Mass PS-tempo (2 mg)**
100°C	0	0	0	0
110°C	0	0	0	0
120°C	0	0	0	0.2
130°C	0	0.04	0.1	1.4

Reactions conditions: 600 rpm, 15 bar O_2, decane (10g), 24 hours, radical scavenger (50mg or 20 mg or 5 mg or 2 mg) is added at the beginning of the reaction.

Data shown in **Table 3.20** demonstrate again that temperature is an important factor for the autoxidation, and increase the temperature will result to increase the mass of radical

scavenger to inhibit the autoxidation. For example PS tempo is a very effective radical scavenger, no conversion was observed at 130°C with the addition of 50 mg of PS-tempo. The use of two different radical scavengers demonstrates that radical chemistry is involved in the present reaction, which indicates that radical chemistry is the only mechanism responsible for the autoxidation.

3.3.8. Distillation and Purification of *n*-decane.

3.3.8.1. Introduction.

The initiation step of the autoxidation mechanism is highly dependant on impurities in the reactants [3-5]. The possible effect of impurities within the *n*-decane on the autoxidation reaction was investigated. The major concern was that hydroperoxide (ROOH) impurities within the *n*-decane maybe responsible for the autoxidation reaction observed at temperatures of $\geq$ 100 °C. To remove these impurities *n*-decane was distilled and tested for autoxidation.

3.3.8.2. Method of purification.

Perrin and Armarego [22] were recommended for the method of purification of organic chemicals. This method involves shaking *n*-decane with concentrated H_2SO_4, which acts as hydroperoxide destroyer then washing with water, aqueous $NaHCO_3$, more water, then drying with $MgSO_4$, refluxing with molecular sieves distilling under pressure at 70°C under nitrogen and passing through a column of silica gel which will reduce any peroxide formed.

Immediately after purification (no storage), blank test reactions at 100°C and 120°C were carried out and compared to the same reactions with the as received *n*-decane. A glass liner was also used in some experiments to avoid contact of *n*-decane with the stainless steel autoclave walls as autoxidation can be initiated by traces of metallic species. Only a plastic

thermocouple and a magnetic bar stirrer are in contact with *n*-decane during the run. No metal is in contact with the purified *n*-decane.

3.3.8.3. Results.

The same reaction was performed with purified and unpurified *n*-decane without a glass liner at different temperatures (100°C & 120°C).

Table 3.21 Oxidation of purified and unpurified *n*-decane at 100°C.

100°C	Conv. (%)	5/4 one	3 one	2 one	5/4 ol	3 ol	2 ol	1 ol	C_5 acid	C_6 acid	C_7 acid	C_8 acid	C_9 acid	C_{10} acid
Unpurified	0.15	30.0	19.3	24.2	2.1	1.8	1.8	1.0	6.5	5.9	5.2	0	0	2.2
Purified	0.17	34.8	19.9	25.1	2.0	1.3	2.7	0.5	6.5	2.5	2.8	0.4	0.3	1.1

Reactions conditions: Purified and unpurified *n*-decane at 100°C, 24h, 15 bar oxygen, 600 rpm, no glass liner.

Table 3.22 Oxidation of purified and unpurified *n*-decane at 120°C.

120°C	Conv. (%)	5/4 one	3 one	2 one	5/4 ol	3 ol	2 ol	1 ol	C_5 acid	C_6 acid	C_7 acid	C_8 acid	C_9 acid	C_{10} acid
Unpurified	10.70	24.3	13.3	16.7	4.4	6.9	4.2	0.5	9.5	8.0	6.3	2.7	2.5	0.8
Purified	10.10	26.1	15.3	13.0	3.6	4.1	4.9	0.6	10.9	8.7	6.3	3.1	2.7	0.7

Reactions conditions: Purified and unpurified *n*-decane at 120°C, 24h, 15 bar oxygen, 600 rpm, no glass liner

These results indicate that there is no difference in the conversion and the product distribution between purified and unpurified *n*-decane for a runtime of 24 hours.

Table 3.23 Difference between unpurified without liner and purified with glass liner at 100°C.

100°C	Conv. (%)	5/4 one	3 one	2 one	5/4 ol	3 ol	2 ol	1 ol	C_5 acid	C_6 acid	C_7 acid	C_8 acid	C_9 acid	C_{10} acid
Unpurified & stainless steel	0.15	30.0	19.3	24.2	2.1	1.8	1.8	1.0	6.5	5.9	5.2	0	0	2.2
Purified & glass liner	0.29	30.4	22.8	21.9	1.6	3.0	2.0	1.0	3.9	3.8	2.5	3.1	2.0	1.9

Reactions conditions: Purified and unpurified *n*-decane at 100°C or 120°C, 24h, 15 bar oxygen, 600 rpm

Table 3.24 Difference between unpurified without liner and purified with glass liner at 120°C.

120°C	Conv. (%)	5/4 one	3 one	2 one	5/4 ol	3 ol	2 ol	1 ol	C_5 acid	C_6 acid	C_7 acid	C_8 acid	C_9 acid	C_{10} acid
Unpurified & stainless steel	10.70	24.3	13.3	16.7	4.4	6.9	4.2	0.5	9.5	8.0	6.3	2.7	2.5	0.8
Purified & glass liner	8.2	22.4	10.6	15.8	6.1	3.8	5.7	0.6	14.1	8.7	6.1	3.5	1.6	1.0

Reactions conditions: Purified and unpurified *n*-decane at 120°C, 24h, 15 bar oxygen,600rpm.

These results above suggest that the glass liner and purified *n*-decane do not prevent the self initiating autoxidation mechanism.

3.4. Discussion.

In the literature different sources of initiator are proposed for the self-initiation of the autoxidation.

- Small amount of impurities present in the feed as hydroperoxide (ROOH) or olefin [3].
- Trace of metal from the stainless steel autoclave [3].
- Heat [5]

Unless hydrocarbons are rigorously purified prior to use by the supplier, trace amounts of impurities are present in the feedstock and can initiate the autoxidation. The first impurity, which can be present in the feed are unsaturated substrates (olefins). By direct addition of oxygen to the double bond, they will produce a hydroperoxide and acts as initiator for the autoxidation [3]. This insertion is reported in **Figure 3.7.**

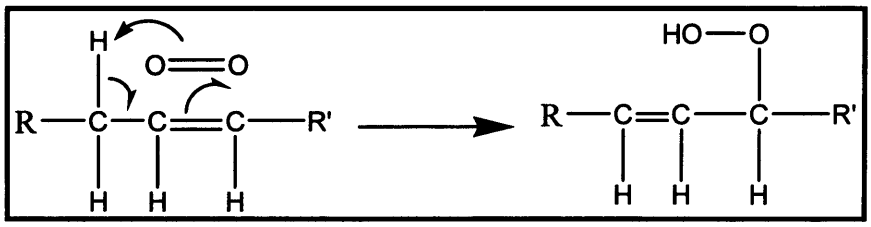

Figure 3.7 Insertion of oxygen with an olefin [3].

The second impurity which can be present in the feed are the hydroperoxide (ROOH) and can also initiate the autoxidation [3]. The hydroperoxide present in the feed or formed by direct reaction of the olefin with oxygen (**Figure 3.7**) will undergo a thermal homolytic decomposition (eq. 6), which will generate radicals (oxidation initiators), which can initiate the autoxidation reaction [3-4].

$$ROOH \rightarrow RO^* + {}^*OH \qquad \text{eq. 6}$$

During the purification *n*-decane [22], the method used a strong acid (H_2SO_4), which will decompose ROOH impurities or react with alkenes impurities. The mechanism of destruction of both species is detailed below.

1) Decomposition of ROOH to alcohols.

$$R\text{-}O\text{-}O\text{-}H + H^+ \rightarrow ROH + H_2O$$

2) Following by dehydratation.

$$ROH + H^+ \rightarrow R_1\text{-}CH{=}CH\text{-}R_2 + H_2O$$

3) Alkenes will undergo an electrophilic addition on the double bond.

$$R_1\text{-}CH{=}CH\text{-}R_2 + H_2SO_4 \rightarrow R_1\text{-}CH_2\text{-}\underset{\displaystyle SO_4H}{\underset{|}{CH}}\text{-}R_2$$

The sulphur compound formed at the end will be soluble in water, so it will be removed from the organic layer during the washing procedure. So after purification the feed is free of both ROOH species and alkenes but an autoxidation mechanism is still observed (**Table 3.24** and **Table 3.25**). Impurities are not responsible or are not the only source of the initiation of the autoxidation because the purification of the feed does not prevent the autoxidation of *n*-decane.

Another initiation source suggested in the literature is the trace of metal from reactor wall [23-25]. The mechanism is showed in eq.7 [3]

$$RH + M^{(n+1)+} \rightarrow M^{n+} + R^* + H^+ \qquad \text{eq. 7}$$

The use of glass liner, with contact with plastic stirrer and plastic thermocouple only did not avoid the autoxidation mechanism. The results are similar to those obtained without the use of a glass liner.

The last initiation source proposed in the literature is the direct radical-forming reaction between hydrocarbon and molecular oxygen [26] in which the temperature of the reaction can supply enough energy required for the formation of a radical [5]. In **Table 3.1**, conversion of the autoxidation is widely influenced by the temperature. For example, no autoxidation at 80°C for a run of 24h but a conversion of 10% at 120°C for the same run time (**Table 3.2**). Autoxidation can also be initiated deliberately by adding a radical initiator as *tert*-butyl hydroperoxide (TBHP) or benzoylperoxide (BPO) at the beginning of the reaction. The use of such radical initiator will decrease the time of the initiation step by increasing the formation rates of hydroperoxide [28]. Two different radical initiators were used in this study. The first one is *tert*-butylhydroperoxide (TBHP).The decomposition of *tert*-butylhydroperoxide is proposed in **Figure 3.8** [29].

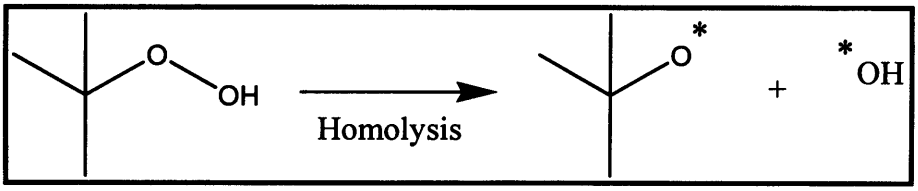

Figure 3.8 Thermal decomposition of TBHP.

The second radical initiator used is benzoyl peroxide (BPO). It is an unstable compound and produces radicals by homolytic cleavage of weak bonds simply on heating [30].

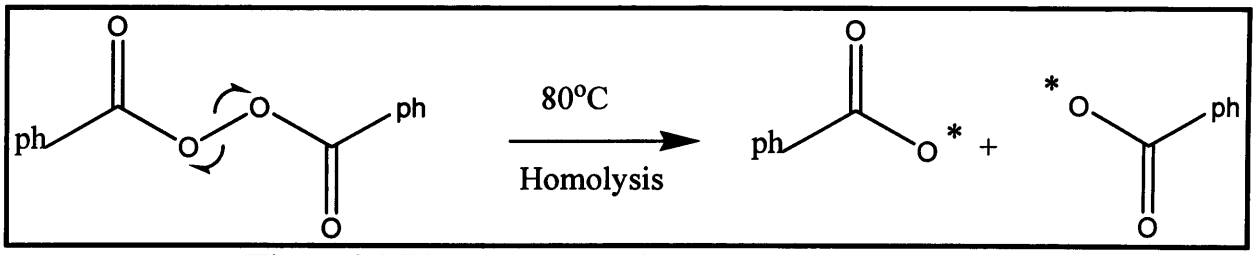

Figure 3.9 Dibenzoylpoeroxide thermal decomposition

The radicals formed from this homolysis are unstable and can break down by cleavage of a C-C bond generating CO_2 and a phenyl radical (**Figure 3.10**).

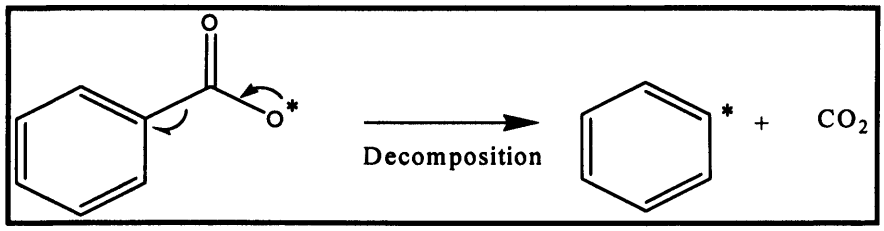

Figure 3.10 Radical elimination.

After homolytic decomposition of the radical initiator, the next step will be the abstraction by the radical of H to form the radical alkane. Eq. 8 [31] describes the reaction between linear alkane and alkoxy radical (TBHP).

$$RO^* + RH \rightarrow R^* + ROH \qquad \text{eq. 8}$$

The mechanism of the radical from dibenzoyl peroxide (BPO) decomposition with linear alkane is proposed in eq.9 [29].

$$PhCO_2^* + RH \rightarrow PhC(O)OH + R^* \qquad \text{eq. 9}$$

It can be noticed that there is a formation of benzoic acid.

After formation of the radical alkane (R*), the second step is the oxygen insertion with formation hydroperoxide [3] described in **Figure 3.11**.

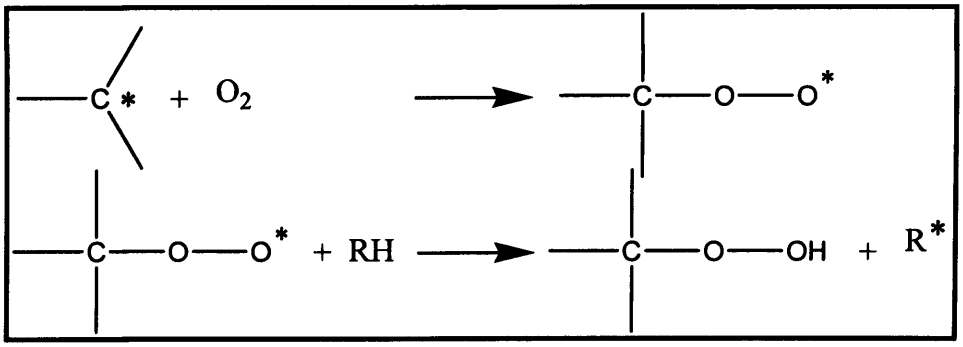

Figure 3.11 Insertion of oxygen, formation of hydroperoxide with regeneration of radical

The experiments with triphenylphosphine confirm the presence of a large amount of ROOH at the end of the reaction. The concentration of ROOH species builds up during the initiation step until it reaches a concentration, which allows the propagation step.

Radical initiators were used to reduce the long period of induction of the reaction. Tert-butyl hydroperoxide (TBHP) led to higher ROOH synthesis. Radical initiator will increase the formation rate of ROOH and will explain a shorter induction period [28]. For example no conversion is observed for the autoxidation without radical initiator after 8 hours; however the conversion is 0.23% when TBHP is added at the beginning of the reaction or a conversion of 0.33% when BPO is added at the beginning of the reaction.

The hydroperoxide species will undergo a homolytic cleavage by heat to form the free radical (RO* and OH*) [4]. In eq.10, ROOH is the hydroperoxide, RO* is the alkoxy radicals and OH* is hydroxyl radical.

$$ROOH \rightarrow RO^{*} + {}^{*}OH \qquad \text{eq.10}$$

Thermal decomposition of ROOH is influenced markedly by temperature and can explain the difference of conversion between the different temperatures [4]. These radicals (RO* and OH*) will act as oxidation initiators and will react further with alkanes or hydroperoxides or with the different products present in the mixture [3-5]. The complexity of the product profile can be explained as multi radical reactions can occur at the same time and is responsible of the scission of the C-C bond (**Figure 3.12**). The other important factor is that the primary oxygenated products made are more reactive than linear alkane. For example, alcohols or hydroperoxides are more reactive than alkanes to the dehydrogenation by a radical (OH*, RO*, R*, ROO*). **Table 3.25** compares the hydrogen bond energy dissociation between an alkane (C-H) an alcohol (RCO-H) and hydroperoxide (ROO-H).

Table 3.25 Hydrogen energy bond dissociation [32].

Hydrogen Energy bond dissociation	Energy (kcal mol^{-1})
Alkane Primary (C-H)	104
Alkane Secondary (C-H)	94.6
Alcohols (RCO-H)	86
Hydroperoxide (ROO-H)	90

The ways in which hydroperoxide decompose is summarized in **Figure 3.12** [33].

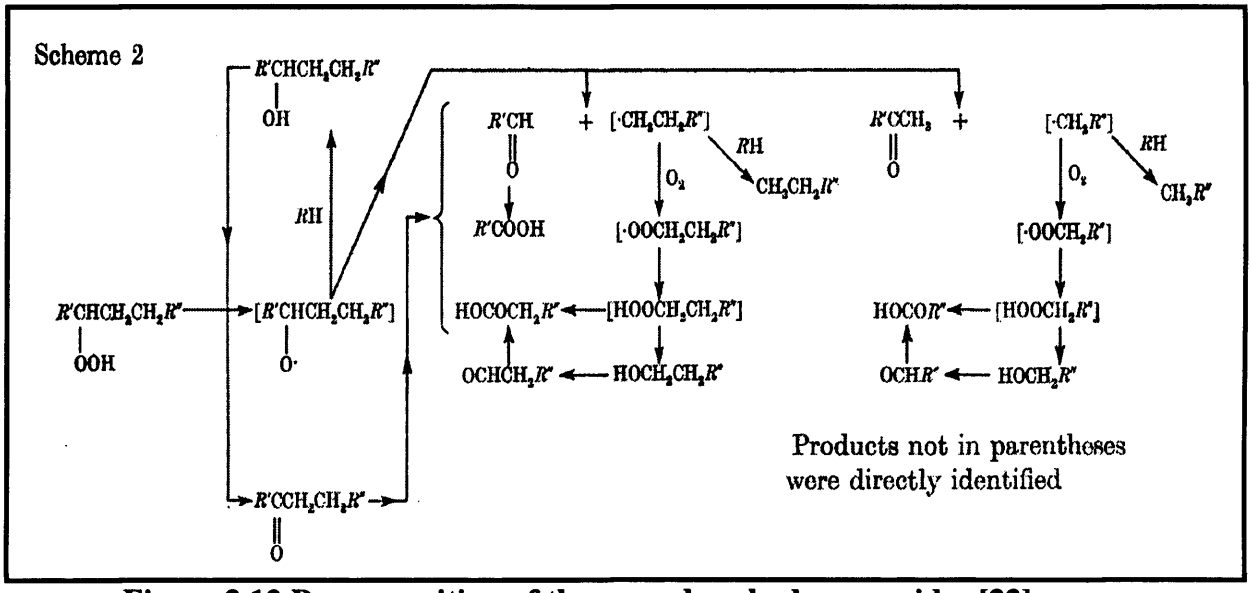

Figure 3.12 Decomposition of the secondary hydroperoxides [33].

In this scheme we can see the complexity of the radical mechanism. The first products formed are ketones and alcohols as observed in **Table 3.7** for a run of 16 hours at 100°C. Increasing the reaction time will give a more complicated product profile. As described in **Figure 3.12**, the formation of ketones will weaken the carbon-carbon bond and give C-C scission more easily and will explain the large amount of cracked products for a run of 24h with a large conversion. The terminal selectivity is very poor in each case. Under these homogeneous

conditions the regioselectivity is governed by the relative carbon hydrogen bond dissociation energies [11], which favour the oxidation on the CH_2 position on *n*-decane.

A major difference in the product profile and the conversion is observed by the use of BPO as radical initiator. The product distribution contains more alcohols and there is no major difference for the conversion after 1 hour and 24 hours runs. TBHP does not influence the decomposition of the hydroperoxide; only participate in its formation [28]. The decomposition of the ROOH will be a thermal homolytic cleavage and explain the same product profile between autoxidation (without TBHP) and autoxidation initiated with TBHP. However BPO must react with the ROOH. The explanation of these results is formation benzoic acid by the use of BPO [34-35]. Acid can do a heterolytic decomposition of the ROOH [4]. The ionic decomposition avoids the formation of the alkoxy (RO*) and hydroxyl radicals (OH*) and explains why the conversion is stable versus time. The alkoxy (RO*) and hydroxyl radicals (OH*) are also responsible for the conversion of alcohols (the hydrogen is easier to abstract than for alkanes **Table 3.25**) to ketones and explain the difference in the product profile.

The inhibitors of free radicals reduce the rate of the autoxidation [4]. The general mechanism of a radical scavenger involves a hydrogen abstraction (eq. 3). In eq.11, IH is the radical scavenger.

Autoxidation:	Initiation:	$I \rightarrow R^*$	eq.1
	Propagation:	$R^* + O_2 \rightarrow RO_2^*$	eq.2
Inhibition:		$RO_2^* + IH \rightarrow ROOH + I^*$	eq.11

The free radical (I*) is stabilized by resonance and will be insufficiently reactive to start a new autoxidation reaction. In eq. 10, hydroperoxide (ROOH) are formed and can be decomposed to alkoxy radicals (RO*) and hydroxyl radical (OH*). These radicals will also inhibited by BHT. The first radical scavenger used in this study is 2,6-di-tert-butyl-4-methylphenol (BHT) (**Figure 3.13.**).

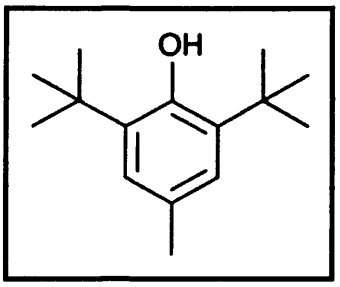

Figure 3.13 2,6-di-tert-butyl-4-methylphenol (BHT).

The phenol is surrounded by bulky substituents, which help to stabilise the radical. **Table 3.26** shows and explains why the radical formed in eq.11 will abstract a hydrogen from the radical scavenger and not from the alkane.

Table 3.26 Hydrogen bond dissociation [32].

Energy bond Dissociation	**Energy (kcal.mol^{-1})**
Primary (C-H)	104
Secondary (C-H)	94.6
Phenol (O-H)	88

The hydrogen from the phenol is easier to abstract than hydrogen from the linear alkane.

The mechanism of stabilisation with peroxyl radical is proposed in **Figure 3.14 [4].**

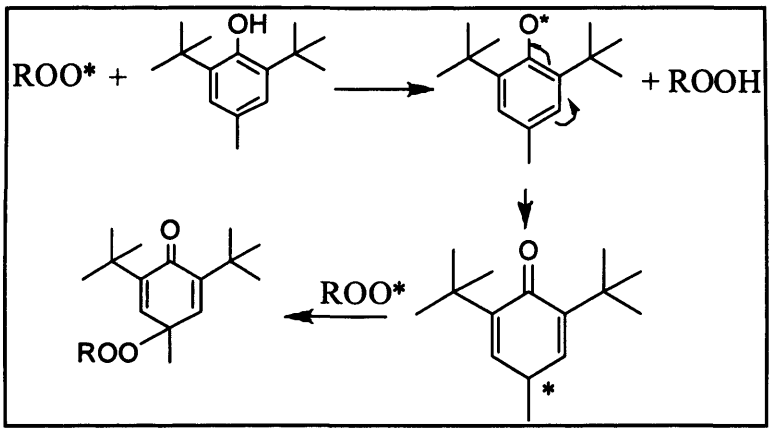

Figure 3.14 2,6-di-tert-butyl-4-methylphenol (BHT) mechanism.

It can be notice that one mol of radical scavenger can stabilise two of radical.

The other radical scavenger used is this work is PS-tempo. The mechanism of PS- Tempo is depicted in **Figure 3.15.** It scavenges the R* species and will also prevent the propagation of the autoxidation.

Autoxidation: Initiation: $I \rightarrow R^*$ eq.1

The alkyl radical will be scavenged by PS-tempo (**Figure 3.15.**)

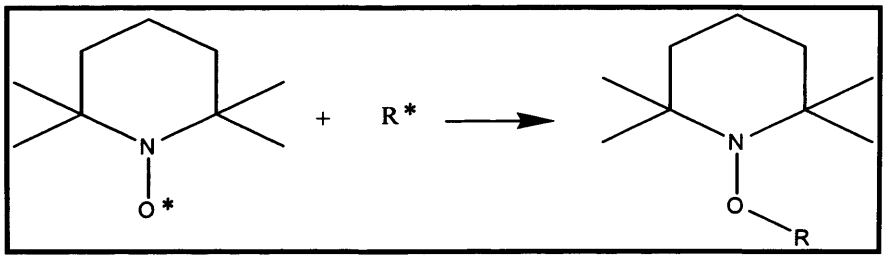

Figure 3.15 Trapping of alkyl radical by PS-tempo [36].

Autoxidation is an undesired reaction in our system because it is a radical reaction with a very poor terminal selectivity and to know how to prevent it using radical scavengers is important. For example, in the next chapters the use of a catalyst with a radical scavenger will prevent

the propagation of the autoxidation and allow the examination of only the heterogeneous mechanism from the catalyst.

3.5. Conclusion.

In summary, it has been shown that *n*-decane can react with oxygen without the presence of a catalyst via the radical mechanism of autoxidation. The products are a mixture of C_{10} oxygenated products and cracked acids. The terminal selectivity of this radical mechanism is very poor for the terminal products. The temperature does have an influence over the conversion of the reaction.Purification by distillation of *n*-decane or use of a glass liner did not avoid the autoxidation however addition of a radical scavenger can avoid the propagation of the autoxidation by trapping the radical species. Radical initiator can enhance the reaction and BPO can modify the product distribution giving more alcohols than TBHP.

3.6. References.

[1] I. Hermans, J. Peeters, P.A. Jacobs, Topics in Catalysis 48, (2008), 48.

[2] U. Schuchardt, D. Cardoso, R.Sercheli , R. Pereira , R.S. Da Cruz , M.C. Guerreiro, D. Mandelli, E.V. Spinace, E.L. Pires, Applied Catalysis A: General, 211,(2001), 1.

[3] R.A. Sheldon, J.K. Kochi, Metal Catalyzed Oxidations of Organic Compounds, Academic Press, New York (1981).

[4] C.E. Frank, Chemical Review 46, (1950), 155.

[5] K.U. Ingold, Inhibition of Autoxidation of Organic Substances in the Liquide Phase Chemical Reviews, 61, (1961), 563.

[6] I. Hermans, J. Peeters, P.A. Jacobs, Topic in Catalysis 50, (2008), 124.

[7] I. Hermans, T.L. Nguyen, P.A. Jacobs, J. Peeters, European Journal of Chemical Physics and Physical Chemistry, 6, (2005), 637.

[8] G.W. Burton, K.U. Ingold, Journal of the American Chemical Society, 103, (1981), 472.

[9] PhD students involved in this project, Y. Shang, S. Pradhan (2007).

[10] L.R. Mahoney, Angewandte Chemie International Edition, 8, (1969), 547.

[11] J.M. Thomas, R. Raja, G. Sankar, R.G. Bell, Letters to Nature, 398, (1999), 227.

[12] G.B. Shul'pin, A.N. Druzhinina, Bulletin of the Russian Academy of Sciences.41, (1992), 346.

[13] G.B. Shul'pin, G.V. Nizova, Y.N. Kozlov, New Journal of Chemistry, 20, (1996), 1243.

[14] G.P. Shul'pin, G.V. Nizova, Reaction Kinetics and Catalysis Letters, 48, (1992), 333.

[15] A.E. Shilov, G.B. Shul'pin, Chemical Review, 97, (1997), 2879.

[16] L.G. Cuervo, Thesis, Institut de Chimie de l'Université de Neuchâtel, (2003).

[17] I.W.C.E. Arends, P. Mulder, K.B. Clark, D.D.M. Wayner, Journal of Physical Chemistry , 99, (1995), 8182.

[18] E.T. Denisov, T.G. denisova and T.S. Pokidova, Handbook of Free Radical Initiators, Wiley-Interscience, (2003).

[19] J. Meijer, A. Hogt, Across Organic Review, (2006).

[21] J. Betts, The kinetics of Hydrocarbon Autoxidation in the liquid Phase, Quarterly Reviews, Chemical Society 25, (2), (1971), 265.

[22] W.L.F. Armarego, D.D. Perrin, Purification of Laboratory Chemicals, Butterworth-Heinemann, (1997).

[23] E.H. Bawnc, Discussions Faraday Society, 14, (1953), 181.

[24] A.J. Chalk, J.F. Smith, Transactions of the Faraday Society 53, (1957), 1214.

[25] V. Erofeevb, I. Sorokot, Zhurnal Prikladnoi Khimii, 33, (1960), 903.

[26] D.J. Carlsson, J. C. Robb, Transactions of Faraday Society 62, (1966), 3403.

[28] B. Modén, B. Zhan, J. Dakka, J.G. Santiesteban, E. Iglesia, Journal of Physical Chemistry C, 111, (2007), 1402.

[29] Handbook of Free Radical Initiators, E.T Denisov, T.G. Denisova, T.S. Pokidova, Wiley & Sons (2003).

[30] J. Clayden, N. Greeves, S. Warren, P. Whothers, Organic Chemistry, Oxford, (2000), 1021.

[31] B. Modén , B. Zhan , J. Dakka, J.G. Santiesteban , E. Iglesia, Journal of Catalysis 239, (2006), 390.

[32] J.A. Kerr, Bond Dissociation Energies by Kinetic Methods, Chemical Reviews 66, (1966), 465.

[33] D.M. Brown, A. Fish, Royal Society, 308, (1969), 547.

[34] M.P. Doyle, W.J. Patrie, S.B. Williams, Journal Organic Chemistry, 16, (1979), 2955.

[35] W.E. Cass, Journal of the Chemical American Society, 69, (1947), 500.

[36] A.L.J. Beckwith, V.W. Bowry and K.U. Ingold, Journal of the American Chemical Society, 114, (1992), 4983.

Chapter 4

Liquid phase oxidation of *n*-decane over vanadium magnesium oxide catalysts

4.1. Introduction.

The activation of alkanes is of fundamental importance as the activation of a CH bond allows access to a great range of more useful products. About 5% of the annual production of vanadium is used in catalysis, which is its most dominant non-metallurgical use [1]. Vanadium magnesium oxides are among the most selective and active heterogeneous catalysts for the oxidative dehydrogenation of alkane in gas phase reaction. VMgO catalysts have been broadly used for oxidative dehydrogenation of propane to propene [2-4] and butane to butadiene [5-6]. On other hand, it should be noticed that homogeneous vanadium catalysts can be efficient for long linear alkane oxidation in liquid phase to produce ketones and alcohols [7]. No literature was found on the use of solid heterogeneous VMgO catalysts for the activation of long linear alkanes in liquid phase. This chapter aims to look at the use of hetero and homogenous based vanadium systems using molecular oxygen for partial *n*-decane oxidation in liquid phase.

4.2. Experimental.

4.2.1 Preparation of VMgO catalysts.

A main method of catalyst preparation is impregnation. Impregnation occurs when the metal attaches to the oxide. It is prepared by adsorption of an active phase solution, that is, by

adding the support to a solution of the active metal. Impregnation is the most simple and widely used preparation technique for making supported vanadium oxides catalysts. Various VMgO catalysts (**Table 4.1**) were prepared via an impregnation method [8] with varying vanadium loadings.

Table 4.1 Different VMgO catalysts prepared.

Catalyst's name	Theoretical mass percentage loadings. (wt % V_2O_5)
VMgO-0 (blank)	0
VMgO-1	1
VMgO-5	5
VMgO-10	10
VMgO-20	20
VMgO-33	33
VMgO-50	50
VMgO-60	60
VMgO-70	70

4.2.2. Characterisation of catalysts.

The techniques of XRD, BET have been used to characterize the catalysts. In selected cases, ICP-MS is used to detect if there is vanadium leaching after the reaction.

4.2.3. Catalysts testing

Reactions were carried out in a high-pressure autoclave with a nominal volume of 45ml and a magnetic stirrer. VMgO solid catalyst (50 mg) and *n*-decane (10g) was heated at 80°C or 100°C degrees with a stirring speed of 600 rpm. The reaction unit was flushed once with O_2, after which the pressure was increased to 15 bar at room temperature. In selected cases time on-line studies were performed in order to explore the profile of the reaction vs. time. Reaction sampling is not available on the autoclave so each table entry is a separate experiment. In addition, some reactions were carried out with addition of radical initiator (Tert-butylhydroperoxide, TBHP, 70% in water or benzoyl peroxide, BPO, 75%, remainder

water) at the beginning of the reaction. The products were analyzed using a gas chromatograph (Varian Star 3800) fitted with a DB-WAX column. Samples were taken at the end of reactions for quantification. Internal standard (0.150 ml of 1,2,4-trichlorobenzene) was added to the product mixture before 0.2µl was injected into the GC.

4.3. Results

4.3.1. Characterisation of VMgO catalysts.

4.3.1.1. BET analysis.

The BET surface area was determined for the different VMgO catalysts. (**Table 4.2**).

Table 4.2 List the surface areas of the different vanadium loaded calcined catalysts.

Theoretical loading V_2O_5 (%)	Surface area (m^2/g)
MgO (support no calcined)	68
VMgO-0 (blank)	152
VMgO-1	147
VMgO-5	188
VMgO-10	151
VMgO-20	110
VMgO-33	81
VMgO-50	27
VMgO-60	13
VMgO-70	8

Large differences in the specific area of VMgO were obtained depending on the vanadium content. These catalysts range from low surface area to high surface area. In agreement with literature [9], the impregnation procedure led to an increase in the surface area (0-VMgO),

which increases when 5% V was added but then decreased with the increase of the V content. 188 m^2/g for 5-VMgO, 13 m^2/g for 60-VMgO while that the surface area of MgO support no calcined is the 68 m^2/g. Lower surface area than the support (MgO) that indicates blocking of some of the pores of support by vanadia crystallites [10].

4.3.1.2. XRD Analysis.

4.3.1.2.1. Different phases in VMgO catalysts.

For the gas phase reaction the proposed active phases of VMgO catalyst are the orthovanadate and pyrovanadate phases [11] (**Figure 4.1 [12]**). The active phase of the VMgO catalyst for oxidative dehydrogenation of alkanes to alkenes is the orthovanadate phase. The other phase, the pyrovanadate is more oxidising in nature due to coordination of the metal to more oxygens. The pyrovanadate phase is commonly formed at calcination temperatures greater than 500°C.

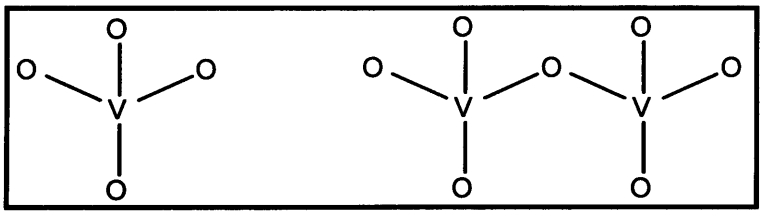

Figure 4.1 [12] ***Left***: VO_4 unit in $Mg_3(VO_4)_2$ (orthovanadate phase).
Right: V_2O_7 unit in $Mg_2V_2O_7$ (pyrovanadate phase).

4.3.1.2.2. XRD patterns of VMgO catalysts.

Figure 4.2 displays the XRD patterns of MgO not calcined (a), VMgO-0 calcined (b), VMgO-1 (c), VMgO-5 (d), VMgO-10 (e), VMgO-20 (f) and VMgO-33 (g) respectively.

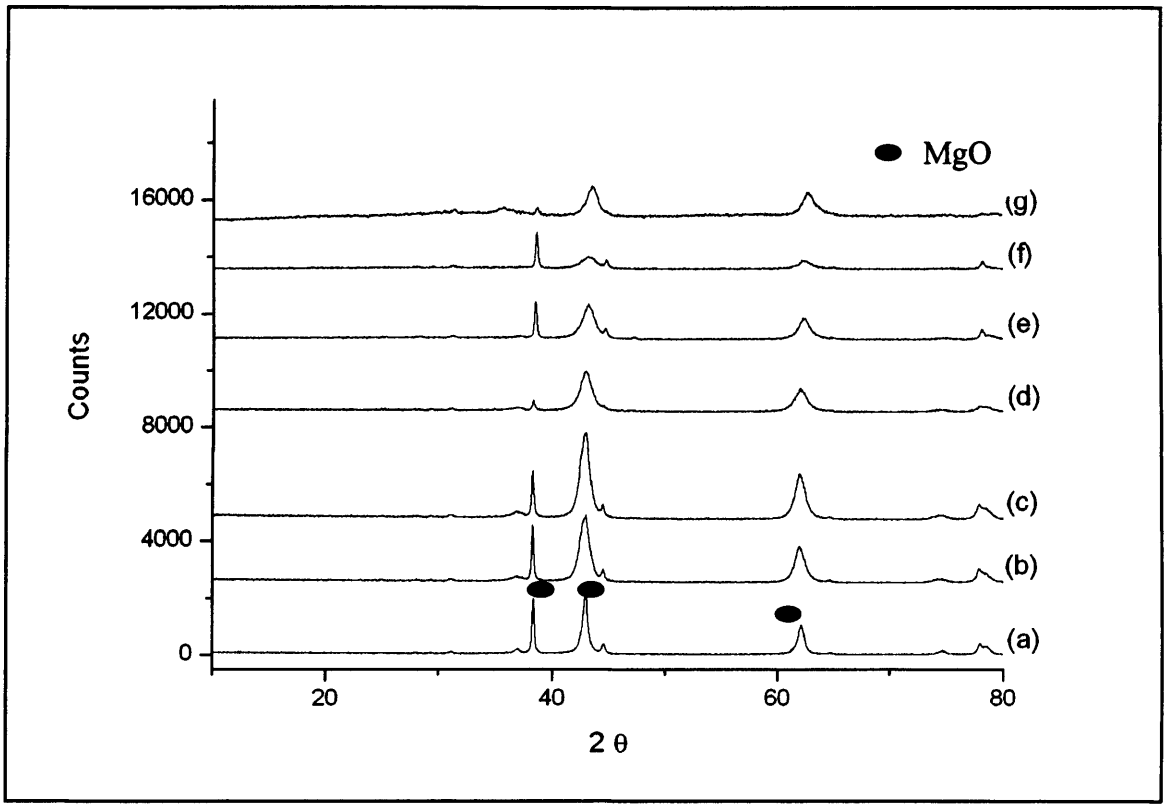

Figure 4.2 XRD patterns: MgO not calcined (a), VMgO-0 calcined (b), VMgO-1 (c), VMgO-5 (d), VMgO-10 (e), VMgO-20 (f) and VMgO-33 (g) respectively.

The XRD patterns for the low vanadium loading catalysts indicate that only diffraction peaks assigned to MgO were observed [13]. No orthovanadate phase and pyrovanadate phase are visible on **Figure 4.2** for a loading of vanadium below 33%. The intensity of the peak of MgO peaks decreased with the loading of vanadium and could be explained by the formation of amorphous or crystalline phases with small crystal sizes [14].

Figure 4.3 shows the XRD patterns of the high vanadium loading catalyst, of MgO uncalcined (a), VMgO-50 calcined (b), VMgO-60 (c) and VMgO-70 (d) respectively

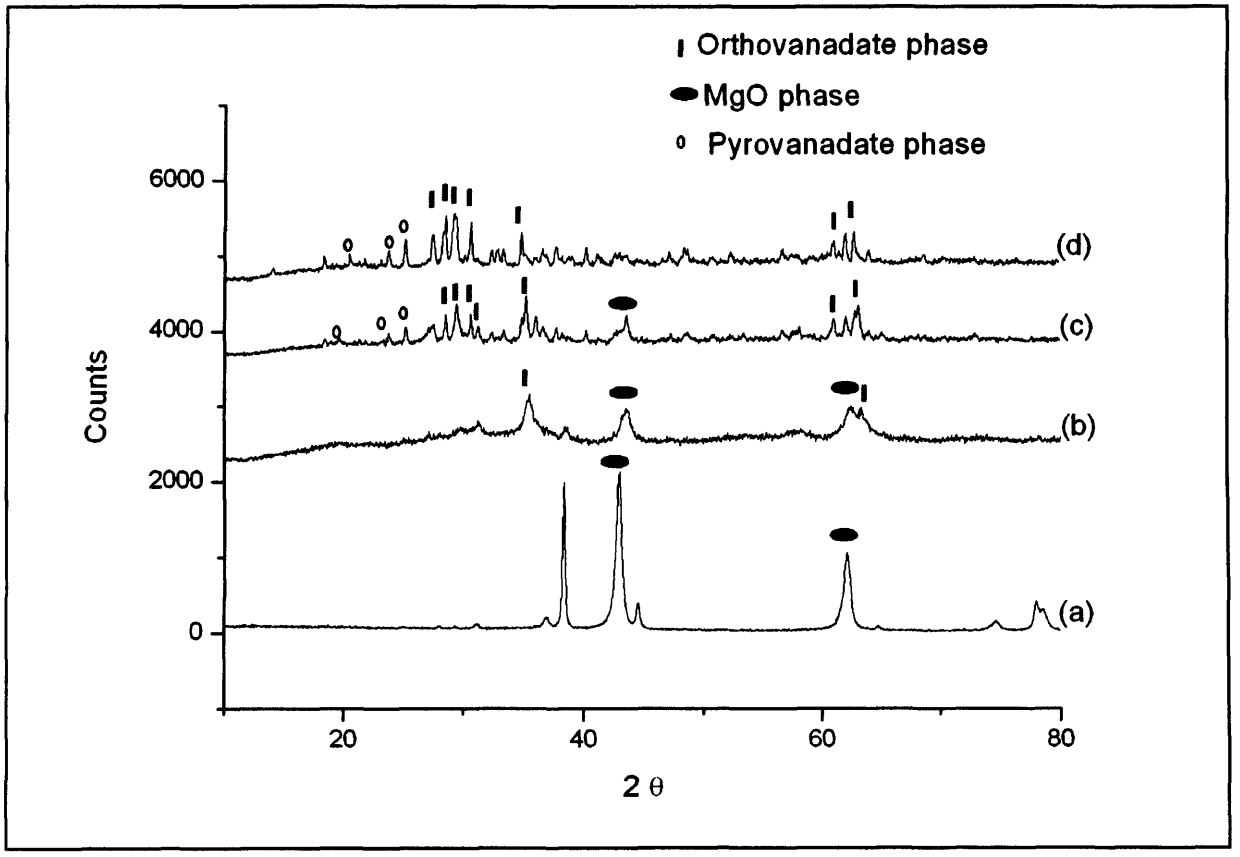

Figure 4.3 XRD patterns: MgO uncalcined (a), VMgO-50 calcined (b), VMgO-60 (c) and VMgO-70 (d) respectively.

Reflections in the XRD patterns were assigned using two references [15-16]. An only orthovanadate phase was observed for VMgO-50. The presence of both orthovanadate and pyrovanadate phase were observed for 60-VMgO and 70-VMgO. The orthovanadate phase is the predominant phase for the high vanadium loading. The number and the intensity of the peaks for each phase increase with the vanadium loading.

4.3.2. Oxidation of *n*-decane at 80°C.

4.3.2.1. Effect of vanadium loading on the conversion of *n*-decane.

In **Chapter 3**, we have seen that there is no autoxidation of *n*-decane for a 24h run at 80°C, so the target was to test the different catalysts using theses conditions to avoid the reaction of autoxidation and to promote a heterogeneous mechanism from the catalyst. **Table 4.4** is the results of these different tests.

Table 4.4 Conversion obtained for the different vanadium loaded catalysts.

Catalysts	Conversion (%)
None	0
Blank (MgO=support)	0
VMgO-1	0
VMgO-5	0
VMgO-10	0
VMgO-33	0
VMgO-50	0
VMgO-60	0.074
VMgO-70	0.1

Reactions conditions: 80°C, stirring speed 600 rpm, 15 bar O_2, decane (10g), VMgO (50 mg) and runtime (24 hours)

Table 4.4 shows that the support of the catalyst is not active and the low loading of vanadium until 50-VMgO did not show a conversion however a loading of 60% and 70% vanadium allow observing a low conversion of *n*-decane at 80°C. So these catalysts are active for the partial oxidation of *n*-decane at very low temperature (80°C).

4.3.2.2. Product profile with VMgO-70 and VMgO-60.

The products of the oxidation of *n*-decane with VMgO-70 and VMgO-60 are listed in **Table 4.5.**

Table 4.5 Product distribution using VMgO-70 and VMgO-60.

Catalyst	Conv. (%)	5/4 one	3 one	2 one	5/4 ol	3 ol	2 ol	1 ol	C_5 acid	C_6 acid	C_7 acid	C_8 acid	C_9 acid	C_{10} acid
None	0	-	-	-	-	-	-	-	-	-	-	-	-	-
VMgO-60	0.074	21.0	14.1	14.3	8.3	4.8	9.3	1.0	14.3	5.6	4.5	1.2	1.2	0.5
VMgO-70	0.1	21.2	13.6	13.8	7.5	4.7	8.4	1.0	13.6	5.9	4.4	3.5	0.8	1.4

Reactions conditions: 80°C, stirring speed 600 rpm, 15 bar O_2, decane (10g), VMgO-70 and VMgO-60 (50 mg) and runtime (24 hours).

31 peaks were detected on the GC traces for VMgO-70 at 80°C, but only C_{10} oxygenated products and cracked terminal acids were used in this work. Gas sample were collecting at the end of the reaction and analysed with a TCD detector, which showed no CO_x. Only decane and oxygen were observed. A product distribution very similar to that observed for the autoxidation mechanism, with a high level of ketones, internal alcohols in position 5, 4, 3 and 2 and cracked acids. Very low terminal selectivity is detected after 24h for both catalysts. Vanadium catalyses the oxidation of *n*-decane because the conversion is higher than the autoxidation (no conversion at 80°C). The product distribution of the autoxidation reaction and reaction with VMgO-70 are noticeably the same. One of the major problems in liquid phase is the reproducibility of the results, so repeats run were performed to confirm the activity of VMgO-70 at 80°C.

Table 4.6 Repeat runs withVMgO-70.

Catalyst	Conv. (%)	5/4 one	3 one	2 one	5/4 ol	3 ol	2 ol	1 ol	C_5 acid	C_6 acid	C_7 acid	C_8 acid	C_9 acid	C_{10} acid
VMgO-70	0.13	25.2	14.5	15.1	7.4	4.6	7.6	0.7	10.7	5.9	4.7	2.4	0.3	1.0
VMgO-70	0.11	21.2	13.6	13.8	7.5	4.7	8.4	1.0	13.6	5.9	4.4	3.5	0.8	1.4

Reactions conditions: 80°C, stirring speed 600 rpm, 15 bar O_2, decane (10g), VMgO-70 (50 mg) and runtime (24 hours)

These results confirm the activity of VMgO-70 for *n*-decane activation at 80°C.

4.3.2.3. Time on line

Time-online studies were also performed in order to plot the product profile with time. **Table 4.7** lists the data for these experiments.

Table 4.7. Product profile of the reaction versus time.

Time (h)	Conv. (%)	5/4 one	3 one	2 one	5/4 ol	3 ol	2 ol	1 ol	C_5 acid	C_6 acid	C_7 acid	C_8 acid	C_9 acid	C_{10} acid
6h	0	-	-	-	-	-	-	-	-	-	-	-	-	-
8h	0.008	32.2	20.5	23.4	8.9	6.0	9.1	0	0	0	0	0	0	0
16h	0.060	22.0	13.1	14.3	8.3	5.8	8.3	1.0	14.3	5.6	4.5	1.2	1.2	0.5
24h	0.11	21.2	13.6	13.8	7.5	4.7	8.4	1.0	13.6	5.9	4.4	3.5	0.8	1.4

Reactions conditions: 80°C, stirring speed 600 rpm, 15 bar O_2, decane (10g), VMgO-70 (50 mg) and runtime (8h, 16h, 24 h)

An induction period of 6 hours is needed before observing any conversion. A very low conversion of 0.008% is observed after 8 hours. Ketones and internal alcohols are the first products made. There is no conversion observed for the reaction without catalyst at 80°C after 24 hours, so it can be concluded that VMgO-70 promotes the oxidation of *n*-decane in liquid phase for a runtime of 24 hours.

4.3.2.4. *n*-decane oxidation over VMgO-70 catalysts with a radical initiator.

Deshpande and co-workers [17] have developed a process for the production of a mixture of alcohols and ketones by the liquid phase oxidation of higher alkanes using a catalyst system consisting of transition group metal such as palladium and support such as alumina, silica, carbon, preferably carbon in the presence of alkyl hydroperoxide as oxygen carrier. It should notice that the ratio of radical initiator to *n*-decane by weight used in this patent [17] is 1.6 (A mixture of 9.913 g TBHP in 6.247 g *n*-decane). In this case radical initiator is acting as a stochiometric oxidant (0.070 mol of *n*-decane for 0.0.70 mol of TBHP). Radical initiator is an expensive compound for the industry, so it was decided with the industrial sponsors of this project to investigate the activity of VMgO-70 with a small amount of radical initiator.

Table 4.7: *n*-decane oxidation in the presence of TBHP or BPO, VMgO-70 and TBHP or BPO with VMgO-70.

Cat.	Conv. (%)	5/4 one	3 one	2 one	5/4 ol	3 ol	2 ol	1 ol	C_5 acid	C_6 acid	C_7 acid	C_8 acid	C_9 acid	C_{10} acid
Only TBHP	0.17	42.9	21.8	27.8	1.0	0.7	1.4	0.1	2.4	0.5	0.6	0.3	0.1	0.4
VMgO-70	0.11	21.2	13.6	13.8	7.5	4.7	8.4	1.0	13.6	5.9	4.4	3.5	0.8	1.4
VMgO-70 + TBHP	0.85	32.5	17.4	19.1	6.3	3.9	6.5	0.5	4.6	2.9	3.5	1.2	0.3	1.2
VMgO-70 + TBHP	0.70	30.0	16.4	17.1	8.0	5.1	7.8	0.6	5.3	3.2	3.5	1.2	0.5	1.2
Only BPO	0.28	16.0	9.3	10.4	23.1	12.6	15.2	2.3	1.2	0.9	4.5	2.2	1.3	1.1
VMgO-70 + BPO	0.36	15.8	9.2	10.3	24.2	13.6	15.4	2.7	1.3	0.8	4.4	0.2	1.3	1.0
VMgO-70 + BPO	0.30	15.9	10.5	10.1	21.1	11.7	14.4	2.4	4.6	2.0	4.1	0.5	1.4	1.3

Reactions conditions: 80°C, stirring speed 600 rpm, 15 bar O_2, decane (10g), VMgO-70 (50 mg), 0.05g TBHP or 0.125 g BPO and runtime (24 hours)

The combination of catalyst and TBHP is a benefit for the conversion. For the terminal selectivity, no improvement is achieved using TBHP with VMgO-70. With BPO, a large amount of alcohols is observed in position 5, 4, 3, 2 which is not observed using TBHP. The conversion obtained with BPO with and without catalyst for a run of 24 hours is very similar indicating VMgO-70 is inactive with BPO present.

4.3.2.5. Investigation of the role of the oxidant.

Different experiments have been carried out to try to understand the origin of the oxygen in the products at the end of the reaction. Three different sources are susceptible to give oxygen.

The first one is from the gas O_2, the second one is from the lattice of VMgO and the last one is from the oxygen present in the radical initiator. Different experiments have been made with inert atmosphere to asses the origin of the oxygen.

Table 4.8 Mechanism investigation.

Experiment Number	Catalyst VMgO-70	Oxidant 15 bar	TBHP (g)	T (°C)	Conv. (%)
1	No	He	0.015	80	0
2	0.05g	He	0.05	80	0
3	0.05g	He	0.012	80	0
4	Excess 0.5g	He	0.15	80	0

Reactions conditions: 80°C, stirring speed 600 rpm, 15 bar O_2, decane (10g), VMgO-70 (0.05g or 0.5g), TBHP (0.015, 0.05 and 0.012) and runtime (24 hours)

Entry 1 in **Table 4.8** shows that without catalyst and oxygen, but with TBHP present, there is no product, so radical initiator and alkane can not react together to give oxygenated products. The role of TBHP [18] in the solution is to form the radical species

$$^{t}BuOO^{*} + RH \rightarrow R^{*} + {}^{t}BuOOH$$

This is normally followed by O_2 insertion to give the hydroperoxide species (ROOH) but the reaction was performed in an inert atmosphere so no oxygen available. So TBHP does not supply oxygen to form the oxygenated products.

Entry 2 and 3 in **Table 4.8** showed that with the presence of VMgO and TBHP without oxygen, there still no conversion. An excess of catalyst (ten times the normal amount) was tested in experiment 3 to give more oxygen available from the lattice of the catalyst, which could react by direct docking with alkane and give a small amount of oxygenated products but no conversion is observed. So we can conclude that the initiation step of the reaction is from the rea ction between oxygen gas with alkane or an alkyl radical to give hydroperoxide

(ROOH). No catalyst is needed for this initiation step. The limiting rate of the autoxidation [19] is due to the production of a steady-state concentration of hydroperoxide (ROOH).

4.3.2.6. Test calcined and uncalcined catalysts (VMgO-70).

In order to determine if the phases present after calcination in VMgO-70 are responsible for the activity of the catalyst at 80°C, the same reaction was performed with calcined and uncalcined catalysts. The data for these results are shown in **Table 4.9.**

Table 4.9 Conversion and product profile with VMgO-70 calcined and uncalcined.

Cat.	Conv. (%)	5/4 one	3 one	2 one	5/4 ol	3 ol	2 ol	1 ol	C_5 acid	C_6 acid	C_7 acid	C_8 acid	C_9 acid	C_{10} acid
calcined	0.10	21.2	13.6	13.8	7.5	4.7	8.4	1.0	13.6	5.9	4.4	3.5	0.8	1.4
Not calcined	0.02	23.0	15.0	12.9	8.2	5.2	9.1	1.0	10.3	4.4	4.1	3.4	3.5	0

Reactions conditions: 80°C, stirring speed 600 rpm, 15 bar O_2, decane (10g), VMgO-70 calcined and uncalcined (0.05g) and runtime (24 hours)

Calcined VMgO-70 gave higher conversion than uncalcined VMgO-70. It is a more active catalyst after calcination for the oxidation of *n*-decane. The product distributions for both catalysts are similar.

4.3.2.7. Leaching test at 80 °C.

Some experiments have been performed to determine if the observed catalysis of VMgO-70 at 80 °C is due to the leaching of vanadium into the solution generating an active homogeneous catalyst. In order to test for the leaching, the solution was filtered off at the reaction temperature after different runtime of reaction (1h and 8h) in order to prevent any soluble vanadium from readsorbing onto the catalyst surface on cooling [20]. The filtrate was put back in the autoclave to react further with any soluble vanadium present in the reaction

solution but no heterogeneous catalyst. The results are summarised in Table 4.10 and Table 4.11. After removal of the catalyst by filtration after 1h or 8h, the filtrate was run for 23h or 16h respectively, which allow a comparison of conversion to a run with a catalyst during 24h.

Table 4.10 Removal of the catalyst by filtration after 1 h reaction.

Time (h)	Conv. (%)	5/4 one	3 one	2 one	5/4 ol	3 ol	2 ol	1 ol	C_5 acid	C_6 acid	C_7 acid	C_8 acid	C_9 acid	C_{10} acid
1	0	-	-	-	-	-	-	-	-	-	-	-	-	-
23	0.012	20.5	16.4	16.2	11.1	5.9	11.7	1.1	10.7	3.2	3.2	0	0	0
VMgO-70 (24 h)	0.13	25.2	14.5	15.1	7.4	4.6	7.6	0.7	10.7	5.9	4.7	2.4	0.3	1.0

Reactions conditions: 80°C, stirring speed 600 rpm, 15 bar O_2, decane (10g), VMgO-70 (0.05g), filtration at 80°C after 1h run and filtrate put back for 23h.

When the catalyst is removed after 1 hour, no conversion is observed. The conversion without catalyst is lower than the conversion with catalyst.

Table 4.11 Removal of the catalyst by filtration after 8 h reaction.

Time (h)	Conv. (%)	5/4 one	3 one	2 one	5/4 ol	3 ol	2 ol	1 ol	C_5 acid	C_6 acid	C_7 acid	C_8 acid	C_9 acid	C_{10} acid
8	0.005	32.2	20.5	23.4	8.9	6.0	9.1	0	0	0	0	0	0	0
16	0.014	24.2	27.4	17.2	21.9	9.7	6.8	11.4	1.2	0	0	0	0	0
VMgO-70 (24 h)	0.13	25.2	25.2	14.5	15.1	7.4	4.6	7.6	0.7	10.7	5.9	4.7	2.4	0.3

Reactions conditions: 80°C, stirring speed 600 rpm, 15 bar O_2, decane (10g), VMgO-70 (0.05g), filtration at 80°C after 8h run and filtrate put back for 23h.

No autoxidation was detected using these experimental conditions and a conversion of 0.13% is observed using VMgO-70 catalyst. The first leaching test (**Table 4.10**), corresponding to a filtration of the catalyst after 1 hour, shows a conversion 10 times lower than the catalyst. One of the reasons could be that a small amount of vanadium leaches into a solution, but it is not

enough to cause the observed catalysis. The second leaching test (**Table 4.10**) was done after 8hours. In **Table 4.7**, an induction period of 8 hours is needed before to see a very small conversion. So the vanadium may take 8 hours to leach into the solution and this is responsible for the conversion, but like it is observed in the second leaching test, the conversion is 10 times lower than the conversion achieved by VMgO-70 after 24 hours. So the induction period of 8 hours is not due to the times of the catalyst to leach in the solution.

4.3.2.8. Recycling of VMgO-70 at 80°C.

A first run with VMgO-70 was performed at 80°C during 24 hours. After the first reaction the catalyst was recovered, by filtration and dried in air. A second run with the same catalyst was performed.

Table 4.12 Conversion for the recycling experiments.

Catalyst	Conversion (%)
Fresh catalyst	0.13
Recycling catalyst	0.11

The recycling experiment has showed that VMgO-70 catalyst does not lose its activity after a second run and can be reused after reaction a second time.

4.3.3. Oxidation of *n*-decane at 100°C.

4.3.3.1. Activity of VMgO-70.

After the interesting results obtained at 80°C, it was decided to see the effect of increasing the temperature on the conversion and the product distribution. Increasing the temperature can promote the activity of the catalyst but in this work it will promote as well the autoxidation of

n-decane described in **chapter 3**.

Table 4.13 Comparison of the activity of VMgO-70 to autoxidation at 100°C.

Cat.	Conv. (%)	5/4 one	3 one	2 one	5/4 ol	3 ol	2 ol	1 ol	C_5 acid	C_6 acid	C_7 acid	C_8 acid	C_9 acid	C_{10} Acid
Blank	0.15	30.0	19.3	24.2	2.1	1.8	1.8	1.0	6.5	5.9	5.2	0	0	2.2
Blank Repeat	0.39	32.4	20.8	21.9	1.6	3.0	2.0	1.0	3.9	3.8	2.5	5.1	0	1.9
VMgO-70	3.90	24.4	13.1	16.6	4.4	2.6	4.4	0.5	14	8.2	5.6	4.2	0.4	1.6
VMgO-70 Repeat run	5.0	24.0	12.8	16.0	4.6	3.0	4.6	0.4	13.8	8.0	6.2	4.3	0.5	1.5

Reactions conditions: 100°C, stirring speed 600 rpm, 15 bar O_2, decane (10g), no catalyst or VMgO-70 calcined (0.05g) and runtime (24 hours).

When no catalyst is present there is a limited autoxidation of the *n*-decane (0.15% of conversion) while the effect of the vanadium loading in terms of catalytic performance is immediately obvious with the VMgO-70 sample showing a conversion of 3.9 % to 5.0% over a 24 hours period. It is interesting to note that the product distribution profile is the same for all four reactions, which may indicate that the reaction mechanism or at least the controlling factor for the regio-selectivity is the same in each case. The enhanced reaction rate for the VMgO-70 must be controlled by the thermodynamics of the C-H bond dissociation as the case for the autoxidation, which decrease from 104 kcal mol^{-1} to 94.6 kcal mol^{-1} in going from primary to secondary carbon, the corresponding selectivity increase [21].

4.3.3.1.1. Time on line.

A time on line study for VMgO-70 (**Table 4.14**) shows an initiation period of at least 8 hours while an active species is generated (This is also the case for the autoxidation reaction)

Table 4.14 Time on line study.

Time (h)	Conv. (%)	5/4 one	3 one	2 one	5/4 ol	3 ol	2 ol	1 ol	C_5 acid	C_6 acid	C_7 acid	C_8 acid	C_9 acid	C_{10} acid
4	0	-	-	-	-	-	-	-	-	-	-	-	-	1.1
8	0.20	23.3	13.9	14.5	7.3	4.7	8.5	1.2	9.3	5.8	7.3	2.6	0.4	1.1
16	1.32	23.5	14.4	15.1	5.7	3.7	5.4	0.6	12.1	7.3	6.4	3.8	0.4	1.6
24	5.0	24.0	12.8	16.0	4.6	3.0	4.6	0.4	13.8	8.0	6.2	4.3	0.5	1.5

Reactions conditions: 100°C, stirring speed 600 rpm, 15 bar O_2, decane (10g), VMgO-70 calcined (0.05g) and runtime (24 hours).

The product profile for low conversion (8 hours run) is the same as observed at higher conversion (5%) for ketones, alcohols and cracked acids. The nature of this induction period could be due to the establishing of an active species.

4.3.3.1.2. Activity of VMgO-70 with a radical initiator.

The activity of VMgO-70 with the presence of a radical initiator was investigated at 100°C. Results are summarised in Table **4.15** and **4.16**.

Table 4.15 Activity of VMgO-70 with the presence of a radical initiator.

Cat.	Conv. (%)	5/4 one	3 one	2 one	5/4 ol	3 ol	2 ol	1 ol	C_5 acid	C_6 acid	C_7 acid	C_8 acid	C_9 acid	C_{10} Acid
Only BPO	0.39	15.9	9.1	10.4	23.6	13.3	16.0	3.1	2.0	1.4	3.1	0.3	0.9	1.1
VMgO-70	5.0	24.0	12.8	16.0	4.6	3.0	4.6	0.4	13.8	8.0	6.2	4.3	0.5	1.5
VMgO-70 + BPO	0.36	14.7	8.5	9.4	23.8	13.6	15.7	2.7	2.9	1.8	3.4	0.5	1.8	1.2
VMgO-70 + BPO	0.39	14.6	8.4	9.6	23.7	13.7	16.3	3	2.8	1.7	3.0	0.5	1.8	0.9
Only TBHP	0.80	36.5	20.3	24.7	1.8	1.2	2.3	0.4	4.7	2.9	2.6	0.5	0.2	2.0
VMgO-70 + TBHP	4.82	25.2	13.3	16.5	4.6	2.8	4.4	0.4	13.6	0.4	7.5	5.8	3.9	0.5
VMgO-70 + TBHP	4.43	25.1	13.2	16.6	4.3	2.6	4.0	0.3	13.8	7.9	5.9	4.2	0.5	1.5

Reactions conditions: 100°C, stirring speed 600 rpm, 15 bar O_2, *n*-decane (10g), VMgO-70 (50 mg), 0.05g TBHP or 0.125 g BPO and runtime (24 hours)

Table 4.16 Product profile comparison.

Catalyst	Ketones (%)	Internal Alcohols (%)	Terminal Selectivity (%)	Cracked acids (%)
Only BPO	35.4	52.9	3.1	7.7
VMgO-70	52.8	12.2	1.9	32.8
VMgO-70 + BPO	32.6	53.1	3.9	10.4
Only TBHP	81.5	5.3	2.4	10.9
VMgO-70 + TBHP	55	11.8	1.8	32.3

The addition of TBHP at the beginning of the reaction showed an activity similar to VMgO on its own. However no difference has been seen using VMgO-70 and BPO. It is interesting to note that the products profile is different when BPO is used as radical initiator for the reaction. With BPO more internal alcohols than ketones in the product profile. The reverse is observed for VMgO-70 alone, VMgO-70 with TBHP. A very slight increase of the selectivity of 1-decanol using BPO is also detected but still below the baseline described in **Chapter 3** for the autoxidation at 100°C, which showed that the terminal selectivity can oscillate between 0.3 to 4.1 %.

4.3.3.1.3. Use a radical scavenger.

The use of a radical scavenger (**Table 4.17**) can help identify whether radical species are kept to the reaction mechanism. If there is conversion that means it is not a radical mechanism, if there is an inhibition of the reaction that means the reaction occurs via a radical mechanism.

Table 4.17 Reaction with radical scavenger.

Catalyst	Mass of radical scavenge (g)	Conversion (%)
None	0.010	0
VMgO-70	0	5.0
VMgO-70	0.15	0
VMgO-70	0.010	0

Reactions conditions: 100°C, stirring speed 600 rpm, 15 bar O_2, decane (10g), VMgO-70 (50 mg), radical scavenger 2,6-Di-tert-butyl-4-methylphenol, runtime (24 h).

The mechanism of the reaction was probed through the use of a radical scavenger (2,6-Di-tert-butyl-4-methylphenol), which stopped all reaction in both the autoxidation reaction and VMgO-70 catalysed experiments. The mechanism is therefore clearly radical based in both cases but the nature of the active species therefore remains a vital question to be answered.

4.3.3.1.4. Recycling of VMgO-70 catalyst at 100 °C.

At the end of the run, the catalyst was recovered and its activity was tested in second run. The target of this experiment is to compare the activity of fresh catalyst and recycled catalyst. The test was carried out twice. **(Table 4.18)**

Table 4.18 Comparison between fresh and reused catalyst.

	Fresh VMgO-70 Conversion (%)	Re-used catalyst Conversion (%)
First reaction	4.4	4.3
Repeat Reaction	4.7	4.4

Reactions conditions: 100°C, stirring speed 600 rpm, 15 bar O_2, decane (10g), VMgO-70 (0.05g) and runtime (24 hours).

No significant change between both experiments, meaning VMgO-70 does not lose its activity after a run of 24 hours and can be reused for another run.

4.3.3.1.5. Activity VMgO-70 precursor (uncalcined).

The activity of the uncalcined catalyst was also investigated at 100°C and its activity was compared to the calcined catalysts. The data are reported in **Table 4.19.**

Table 4.19 Activity of calcined VMgO-70 and VMgO precursor.

Cat.	Conv. (%)	5/4 one	3 one	2 one	5/4 ol	3 ol	2 ol	1 ol	C_5 acid	C_6 acid	C_7 acid	C_8 acid	C_9 acid	C_{10} acid
No calcined	4.8	25.0	13.2	15.5	4.1	2.4	4.6	0.4	14.8	8.3	5.5	4.3	0.4	1.5
calcined	5.0	24.0	12.8	16.0	4.6	3.0	4.6	0.4	13.8	8.0	6.2	4.3	0.5	1.5

Reactions conditions: 100°C, stirring speed 600 rpm, 15 bar O_2, decane (10g), VMgO-70 (0.05g) and runtime (24 hours).

The results are very similar for both catalysts, meaning VMgO-70 does need to be calcined to achieve a conversion of 5% for a run of 24 hours. The next step to understand and clarify the mechanism of VMgO-70 will be the leaching test.

4.3.3.1.6. Effect of catalyst removal at different runtimes.

Experiments were performed to investigate whether leaching of the catalyst was responsible for the catalyst activity. The calcined catalyst was removed by hot filtration at various periods with the reaction mixture returned to the pot to complete the 24 hours reaction period (**Table 4.20, 4.21 and 4.22**). Blank reactions were performed before the leaching tests in order to check there was no contamination from the previous run.

Table 4.20 Effect of catalyst removal after 15 minutes.

Time	Conversion (%)
After 15 min	0
23h45	3.4

Filtration after 15 min of reaction at 100°C and put back the mixture (23h45 min) 100°C, 600 rpm, 15 bar O_2, decane (10g)

Table 4.21 Effect of catalyst removal after 8 hours.

Time	Conversion (%)
After 8 h	0.08
24h	2.08

Filtration after 8h of reaction at 100°C and put back the mixture 16h, 100°C, 600 rpm, 15 bar O_2

Table 4.22 Effect of catalyst removal after 16 hours.

Time	Conversion (%)
After 16 h	1.05
24h	3.50

Filtration after 16h of reaction at 100°C and put back the mixture 8h, 100°C, 600 rpm, 15 bar O_2

A level of conversion well above that recorded without catalyst were obtained even when the mixture was exposed to the VMgO-70 catalyst for only 15 minutes, showing the process to be homogeneous in nature rather than occurring on the surface of VMgO. Assuming it is the leached vanadium that is active and then this shows the leaching of the material to be a fast step (clearly happening to a large extent within the first 15 minutes).

4.3.3.1.7. ICP-MS of the filtrate at different runtimes.

In order to quantify the amount of V leaching from VMgO-70, sample of the organic layer after different runtimes were submitted to ICP-MS. The data are reported in **Table 4.23**.

Table 4.23 Amount of vanadium detected by ICP –MS after different runtimes.

Runtime (hours)	Vanadium (ppm)	Conversion (%)
8	0.8	0.20
16	<0.5	1.32
24	<0.5	5.0
32	<0.5	8.1

Reactions conditions: 100°C, stirring speed 600 rpm, 15 bar O_2, decane (10g), VMgO-70 (0.05g) and runtime (8h, 16h, 24h and 32h).

Measurement of V content (ICP-MS) of the reaction mixture following removal of the solid by filtration, showed the presence of vanadium in a concentration of <0.8 ppm in *n*-decane. The leaching does not increase with the reaction time. A tiny amount of vanadium leached in the solution and is responsible for the activity of the catalyst at 100°C. Less than 0.5 ppm of homogeneous vanadium is responsible of the conversion. VMgO-70 is not a heterogeneous catalyst at 100°C.

4.3.3.2. Activity of a homogeneous vanadium catalyst.

4.3.3.2.1. Vanadium oxytriethoxide as homogeneous catalyst.

In order to reproduce the leaching of VMgO-70, the activity of small amounts of homogeneous vanadium was tested through the use of a homogeneous vanadium source V, which is vanadium oxytriethoxide $VO(OC_2H_5)_3$ (**Figure 4.4**) .

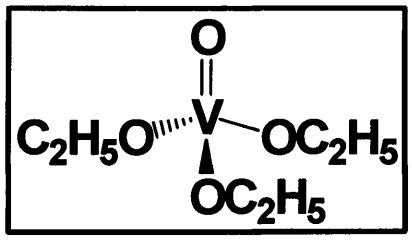

Figure 4.4 Vanadium oxytriethoxide (oxidation state + 5).

A homogeneous vanadium catalyst has already been reported for the oxidation of linear alkane in liquid phase [7]. Two different concentrations 0.1 ppm and 0.4 ppm of homogeneous vanadium were tested as catalyst for the oxidation of *n*-decane at 100°C.

Table 4.24 Activity of 0.1 ppm of vanadium oxytriethoxide.

Time (h)	Conv. (%)	5/4 one	3 one	2 one	5/4 ol	3 ol	2 ol	1 ol	C_5 acid	C_6 acid	C_7 acid	C_8 acid	C_9 acid	C_{10} acid
8	0	-	-	-	-	-	-	-	-	-	-	-	-	-
16	0.07	23.5	14.4	16.1	5.7	3.7	5.4	0.6	12.1	7.3	5.4	3.8	0.4	1.6
24	0.64	23.0	14.5	16.6	4.4	2.6	4.4	0.5	10.0	8.2	5.6	4.2	4.4	1.6

Reactions conditions: 100°C, stirring speed 600 rpm, 15 bar O_2, decane (10g), 0.1 ppm of vanadium oxytriethoxide and runtime (8h, 16h and 24h).

Table 4.25 Activity of 0.4 ppm of vanadium oxytriethoxide.

Time (h)	Conv. (%)	5/4 one	3 one	2 one	5/4 ol	3 ol	2 ol	1 ol	C_5 acid	C_6 acid	C_7 acid	C_8 acid	C_9 acid	C_{10} acid
8	0.16	22.2	12.6	13.8	7.5	4.7	8.4	1.0	13.6	5.9	4.4	3.5	0.8	1.4
16	1.9	24.4	13.1	16.6	4.4	3.6	3.4	0.5	14.0	8.2	5.6	4.4	0.3	1.5
24	3.71	24.3	13.2	16.6	4.5	2.8	4.4	0.5	14	8.2	5.6	3.9	0.4	1.6

Reactions conditions: 100°C, stirring speed 600 rpm, 15 bar O_2, decane (10g), 0.1 ppm of vanadium oxytriethoxide and runtime (8h, 16h and 24h).

This homogeneous species in a concentration of 0.4 ppm shows good activity (3.71 %) over a period of 24 hours. With a lower loading of 0.1 ppm, the conversion is reduced to 0.64 %. A similar product distribution is observed with a majority of ketones, internal alcohols and cracked acids.

4.3.3.2.2. Radical scavenger with homogeneous vanadium catalyst.

In order to elucidate if the mechanism of the homogeneous vanadium is a radical mechanism, radical scavenger was added at the beginning of the reaction. This test has been carried out twice (**Table 4.26**).

Table 4.26 Activity of vanadium salt with a radical scavenger.

Radical scavenger (g)	Time (h)	Conv. (%)
0.0115	24	0
0.0115	24	0

Reactions conditions: 24h, 100°C, 600 rpm, 15 bar O_2, decane (10g), 0.4 ppm V and 2, 6-Di-tert-butyl-4-methylphenol ($C_{15}H_{24}O$) (0.0115g) were added at the beginning of the reaction.

No conversion after 24 hours with a radical scavenger, which demonstrates that the mechanism is a radical mechanism.

4.3.3.3 Comparative data

A summary of the time on line at 100°C is presented in **Table 4.27** for the autoxidation, VMgO-70 and the homogeneous vanadium salt.

Table 4.27 Summary of time on line for autoxidation, VMgO-70 and the homogeneous vanadium salt.

Catalyst	Conv. (%) at 8 hours	Conv. (%) at 16 hours	Conv (%) at 24 hours
0.1 ppm	0	0.07	0.64
0.4 ppm	0.16	1.85	3.71
VMgo-70	0.06	1.5	3.4
Blank	0	0.04	0.18

It can be seen data for 0.4 ppm $VO(C_2H_5)_3$, map relatively well onto the data for VMgO-70, with both showing a similar induction period of 8 hours.

4.4. Discussion.

At 80°C, no autoxidation is observed for a run of 24 hours (**Table 4.4**), meaning no conversion of *n*-decane without catalyst. **Figure 4.3** showed that a minimum loading of 60% is needed to observe in the XRD pattern the formation of active phases after calcination. A loading of 60% of vanadium is also the minimum loading to see a conversion of *n*-decane at 80°C (**Table 4.4**). The conversion after 24 hours for uncalcined VMgO-70 is ten times lower than VMgO-70 calcined (**Table 4.9**). From the literature [10] pyrovanadate ($Mg_2V_2O_7$) active phase is common for calcination temperatures greater than 500°C [11]. The appearance of the active phase on the XRD pattern matches with the appearance of activity of VMgO catalyst for the oxidation of *n*-decane.

The question about the true nature of the catalytic reaction (homogeneous or heterogeneous) is a serious one [21-22]. A heterogeneous catalyst which simply releases its active species into solution is likely to have limited practical use [20]. **Table 4.12-4.18** show that VMgO-70 does not lose its activity after recovering the catalyst from the first run and retesting for a second time with the same experimental conditions. The conventional recycling of catalysts several times without significant loss of activity is not a sufficient proof of heterogeneity [20]. The catalyst may act as reservoir, which slowly releases its active centres over the course of several reactions.

Sheldon *et al.* [20] proposed three situations with the respect to leaching of a metal from a catalyst into the solution. Firstly, the metal may leach but is not an active homogeneous catalyst, secondly the metal leaches and does form an active homogeneous catalyst, and thirdly the metal does not leach and the observed catalysis is truly heterogeneous.

Appropriate rigorous tests [20] for heterogeneity have been performed (**Table 4.10-4.11 and 4.20-4.21-4.22).** To test for leaching we filtered the catalyst and allowed the filtrate to react further. Filtration was performed at the reaction temperature in order to avoid readsorption of solubilized vanadium on cooling. Sheldon et al. [20] have found that after hot filtration, the mother liquor (filtrate) reacted further at roughly the same rate as that observed when the catalyst was not filtered. In contrast, if the mixture was allowed to cool to ambient temperature prior to catalyst filtration, the procedure generally followed when testing for leaching, little further reaction was observed. At 80°C the leaching tests (**Table 4.10-4.11**) have showed that the filtration of the catalyst after 1h or 8h did not stop the conversion of *n*-decane. The combination of these results is a strong indication that a heterogeneous mechanism occurs at 80°C. This does not rule out a slow but practically insignificant leaching.

The major difference between the reaction at 80°C and 100°C is the results of the leaching test. At 100°C, the leached vanadium is responsible for the conversion. The leaching test after 15 min at 100°C showed that leaching is much more rapid than the catalysed reaction itself (no conversion after 15 minutes), in which case there would be exclusively homogeneous catalysis [20]. The test with homogeneous vanadium with the same concentration of vanadium detected by ICP-MS is a strong indication that the leachate of vanadium is responsible of the activity. The reaction profile (conversion and product distribution) was almost identical which leads to the inevitable conclusion that all the observed activity can be attributed to homogeneous vanadium leached from VMgO-70 at 100°C.

The addition of *tert*-butyl hydroperoxide (TBHP) led to a marked increase in *n*-decane oxidation, predominately because ROOH species are formed more rapidly by the use of TBHP [18].

$$^{t}BuO^{*} + RH \rightarrow R^{*} + {}^{t}BuOOH$$

Following by O_2 insertion

$$R^{*} + O_2 \rightarrow ROO^{*}$$

$$ROO^{*} + RH \rightarrow ROOH + R^{*}$$

However, the combination of benzoyl peroxide and VMgO-70 does not promote the conversion of the reaction (**Table 4.15**). The same conversion is observed with and without catalyst, which means that VMgO is inactive.

The first possibility is BPO is doing a deactivation of the catalyst and will explain this result. BPO and TBHP give rise to very different intermediate free radicals. BPO undergoes homolytic O-O cleavage giving first to form benzoyloxy radicals [23] described in **Chapter 3**.

$$PhOCO\text{-}OCOPh \rightarrow 2\ PhCO\text{-}O^{*}$$

The benzoyl peroxide may undergo a variety of reactions besides [23] including decomposition to the phenyl radical and carbon dioxide and radical combination.

$$PhCO\text{-}O^{*} \rightarrow Ph^{*} + CO_2$$

$$PhCO\text{-}O^{*} + Ph^{*} \rightarrow PhCOOPh$$

The phenyl radical is classified as a rather nucleophilic free radical [BPO]. By contrast, TBHP gives rise principally to t-Bu-O* and HO*, both are classified as electrophilic radicals [24]. Thus phenyl radical will attack centres of relatively low electron density, in inorganic situations this often means binding to co-ordinatively unsaturated centres and this could mean binding to active sites on oxidation catalysts (thereby killing the catalysis). Electrophilic radicals such as t-Bu-O* will preferentially favour H-abstraction; in VMgO it may be difficult for it to find a suitable site and so the effect on catalysis is invisible.

The second possibility is the formation of benzoic acid which performs an acid catalysed decomposition of ROOH. After the homolytic cleavage, the benzoyl radical can react with *n*-decane and remove a proton from the alkane to form benzoic acid [25]. ROOH is the first species formed during the oxidation of alkane in liquid phase [18] and acid sites (acid benzoic) will catalyse ROOH heterolytic decomposition and in the same time avoid the propagation of the hydroxyl (OH*) and alkoxyl radical (RO*) the reaction [26-27] as described in **Chapter 2**.

The mechanism study shows that the initiation step of the reaction is a reaction between oxygen and *n*-decane. An initiation period of 6 hours is needed at 80°C and 4 hours at 100°C . The induction period is the time needed with the experimental conditions used to reach the minimum concentration of hydroperoxide (ROOH), which allows the propagation step of the mechanism [19]. The initiation is a radical reaction between *n*-decane and oxygen and will undergo the rules of the autoxidation reaction (CH_2 easier to oxidise than CH_3) [29] and will explain the poor terminal selectivity. The time on line studies at 80°C and 100°C have showed the poor activity of the catalyst during the first 8 hours of the reaction followed by an increase in the rate. From the leaching test, it can be seen clearly that 8 hours is not the time needed by VMgO-70 to leach in the solution. The reaction in inert atmosphere with an excess of catalyst show no conversion so there is no direct docking of RH onto the VMgO-70 catalyst. The metal catalysed decomposition of ROOH by V^{5+} [30] can involve homolotic pathways via free radical intermediates and/or heterolytic oxygen transfer processes. V^{5+} can exhibit acitivity for both reactions and the homolytic and heterolytic pathways give the same products.

Figure 4.5 Homolytic and heterolytic decomposition of ROOH by vanadium [30].

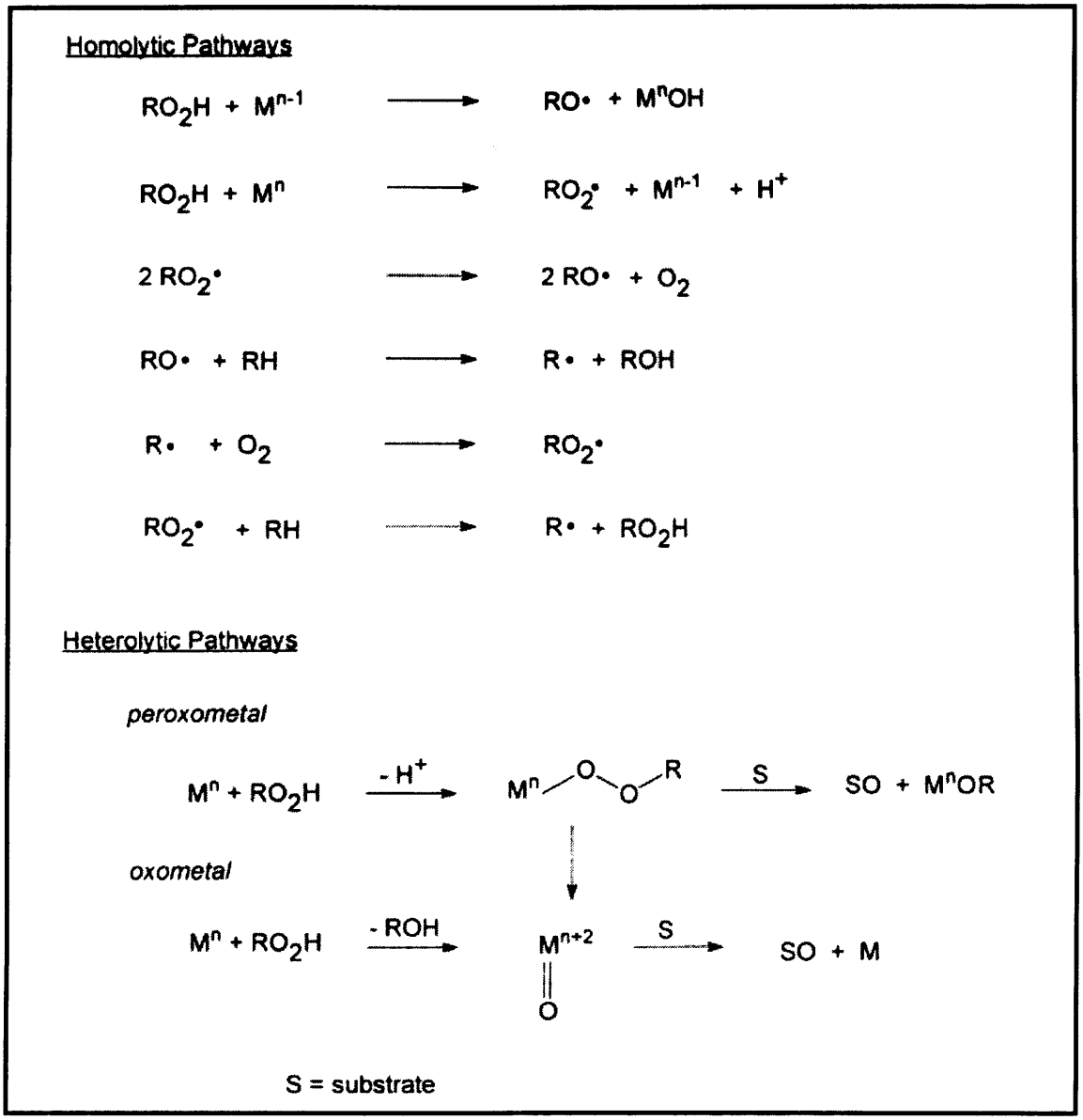

The test (**Table 4.17**) with a radical scavenger indicates a free radical mechanism and the loss of conversion using an inert gas (**Table 4.8**) suggest a homolytic pathway. The propagation of the different radical from the homolytic decomposition of the hydroperoxide (ROOH) by vanadium will act as oxidation initiators for further oxidative reaction.

4.5. Conclusion.

The target of the work is to find out a heterogeneous catalyst which can oxidise *n*-decane in terminal position to form 1-decanol in liquid phase. These results of this chapter have showed that VMgO catalyst with a minimum loading of vanadium can catalyse the oxidation of *n*-decane at 80°C and 100°C with oxygen and give better conversion than the autoxidation but did not increase the terminal selectivity. It can be conclude that vanadium is an active catalyst for the oxidation of alkanes homogeneously and heterogeneously at low temperatures in liquid phase but did not play a significant role in the product distribution, which is similar to those observed for the autoxidation with a modest terminal selectivity.

4.6. References.

[1] B. M. Weckhuysen, D.E. Keller, Catalysis Today 78, (2003), 25.

[2] X. Gao, P. Ruiz, Q. Xin, X. Guo, B. Delmont, Journal of Catalysis 148, (1994), 56.

[3] P.M. Michalakos, M.C. Kung, H.H. Kung, Journal of American Chemical Society, Division of Petroleum Chemistry 37, (1992), 1201.

[4] R. Burch, E.M. Crabb, Applied Catalysis A: General, 100 (1), (1993), 111.

[5] A.A. Lemonidou, Applied Catalysis A: General, 216, (2001), 277.

[6] M.A. Chaar, D. Patel, M.C. Kung, H.H. Kung, Journal of Catalysis 105, 2, (1987), 483.

[7] G. Süss-Fink, L. Gonzalez, G.B. Shul'pin, Applied Catalysis A: General, 217, (2001) 111.

[8] H. B. Friedrich, N. Govender, M. R. Mathebula, Applied Catalysis A: General, 297, (2006), 81.

[9] R.X. Valenzuela, V. Cortes Corberan, Topics in Catalysis 11/12, (2000), 153.

[10]M.D. Argyle, K. Chen, A. T. Bell, E. Iglesia., Journal of Catalysis, 208, (2002) 139.

[11] M.A. Chaar, D. Patel, M.C. Kung, H.H. Kung, Journal of Catalysis, 105, (1987), 485.

[12] P.M. Michalakos, M.C. Kung, I. Jahan and H.H. Kung, Journal of Catalysis, 140, (1993), 226.

[13] A. Corma, J.M. Lopez Nieto, N. Parades, Journal of Catalysis, 144, (1993) 425.

[14] Y. Sakurai, T. Suzaki, K. Nakagawa, N. Ikenaga, H. Aota and T. Suzuki, Journal of Catalysis 209, (2002), 16.

[15] B. Solsona, A. Dejoz, M.I. Vázquez, F. Márquez , J.M. López Nieto, Applied Catalysis A: General 208, (2001), 99.

[16] A. Burrows, C.J. Kiely , J. Perregaard , P.E. Højlund-Nielsen , G. Vorbeck , Catalysis Letters 57 , (1999), 121.

[17] R. Deshpande, R. Madhukar, H. Vilas, V. Raghunath, U.S. Patent No. 976737, (2004).

[18] B. Modén, B. Zhan , J. Dakka, J.G. Santiesteban, E. Iglesia, Journal of Catalysis 239, (2006), 390.

[19] Y. Kamiya, K.U. Ingold, Canadian Journal of Chemistry, 42, (1964), 242.

[20] R. A. Sheldon, M. Wallau, I.C.E. Arends and U. Schuchardt, Accounts of Chemical Research, 31, (1998), 485.

[21] Y. Deng, C. Lettmann, W.F. Maier, Applied Catalysis A: General 214, (2001) 31.

[22] M. Besson, P. Gallezot, Catalysis Today 81, (2003), 547.

[23] Encyclopedia of polymer science and engineering, volume 11, Mark, Bikales, Overberger, Menges, Wiley & Sons, New York, (1988).

[24] Personnal Communication: Professor Donald bethel, Emeritus Professor of Physical Organic Chemistry, University of Liverpool.

[25] E.T. Denisov, T.G. denisova and T.S. Pokidova, Handbook of Free Radical Initiators, Wiley-Interscience, (2003).

[26] H. Sun, F. Blatter, H. Frei, Journal of American Chemical Society, 118, (1996), 6873.

[27] N. Kuprowicz, J.S. Ervin, S. Zabarnick, Fuel, 83, (2004), 1795.

[28] B.M. Weckhuysen, D.E. Keller, Catalysis Today, 78, (2003), 25.

[29] J. M. Thomas, R. Raja, G. Sankar, R.G. Bell, Nature, 398, (1999), 227.

[30] R.A. Sheldon, I.W.C.E. Arends, H.E.B. Lempers, Catalysis Today, 41, (1998), 387.

Chapter 5

Liquid phase oxidation of *n*-decane over zeolite catalysts

5.1. Introduction.

Zeolites or molecular sieves are ideal catalytic materials for shape selective catalysis because they contain channels of varying size and shape, which can influence selectivity in catalytic reactions [1-4]. To assess the role of spatial constraints on regioselectivity, different sizes of pores were used. The characteristics of the different zeolites used in this study are listed in **Table 5.1**.

Table 5.1 Characteristics of selected zeolites.

Zeolites	Nominal cation	SiO_2/ Al_2O_3 mole ratio	Size of the pores (Å) [5]
Modernite	Ammonium	20	7
Y-zeolites	Hydrogen	80	8
ZSM-5	Ammonium	23, 30, 80, 280	5

Mordenite, Y and ZSM-5 zeolites have different SiO_2/Al_2O_3 mole ratios, which allows different loading of redox-active cations [6]. The kinetic diameter of a linear hydrocarbon is 4.3 Å [7]. This indicates that *n*-decane has access to the micropore of all the zeolites (ammonium or hydrogen form) tested. Silanation or ion exchange with cobalt of zeolites can block the entrance of the pores and make it more difficult for *n*-decane to go inside the channels. The geometric constraints of zeolites were used with the aim of controlling the selective heterogeneous functionalisation of *n*-decane in liquid phase with oxygen.

5.2. Experimental.

5.2.1. Preparation of proton zeolites.

Zeolites have negatively charged frameworks [8], which is compensated by a nominal cation. The zeolites were initially heated to 500°C for 3 h in air to remove organic templates left used after the synthesis of the zeolites and to obtain the proton form of the zeolites [9].

5.2.2. Preparation of cobalt zeolites.

Co-zeolites were exchanged by solid state ion exchange (SSIE) [6]. Different Co/Al ratios were prepared. **Table 5.2 and 5.3** are a summary of the different theoretical cobalt loaded zeolites. Two different rates of increasing the temperature (20°C per minute and 3°C per minute) were investigated during the solid state ion exchange process. A long washing process was used to prevent non exchanged metal being present, which can act as a homogeneous catalyst in liquid phase (see **Chapter 2**). The oxidation state of cobalt is Co^{2+}.

Table 5.2 List of different Co-zeolites prepared with a calcination rate of 20°C/min.

Zeolites	SiO_2/ Al_2O_3 mole ratio	Theoretical Co/Al ratio
Modernite	20	1
Y-zeolites	80	1
ZSM-5	280	1
ZSM-5	80	1
ZSM-5	30	0.1, 0.2, 1 and 2
ZSM-5	23	0.1, 0.2, 1 and 2

Table 5.3 List of different Co-ZSM-5 prepared with a calcination rate of 3°C/min.

Zeolites	SiO_2/ Al_2O_3 Mole ratio	Theoritical Co/Al ratio
ZSM-5	30	0.1-Co
		1-Co

The number before the catalyst is the ratio of cobalt/aluminium used in the physical mixture at the beginning of the solid state ion exchange. (0.1-Co-ZSM-5 will be used for a catalyst, which has been prepared with an initial physical mixture of Co/Al with a ratio of 0.1)

5.2.3. Preparation of silanated zeolites.

During the solid state ion exchange, cobalt can be deposited on the surface of the zeolites or inside the channels. Cobalt on the surface will give an unselective reaction (no geometric constraint). Silanation decreases the number of sites available to anchor cobalt on the external surface of the zeolites and will favour the incorporation of cobalt inside the pores, which may then give a selective reaction using the spatial constraints [10]. After silanation, silanated zeolites were ion exchanged with a theoretical ratio Co/Al equal to one. The effect of silanation on the structure and catalytic behaviour of ZSM-5 with a SiO_2/ Al_2O_3 mole ratio of 23, 30 and 80 has been investigated (**Table 5.4**).

Table 5.4 List of different silanated zeolites prepared.

Zeolites	SiO_2/ Al_2O_3 Mole ratio	Theoritical Co/Al loading after silanation
ZSM-5	23	1
ZSM-5	30	1
ZSM-5	80	1

5.3. Catalyst characterization.

The techniques of XRD, BET, TGA and XPS have been used to characterize the catalysts. ICP-MS was used to detect the cobalt loading after preparation.

5.3.1. X-ray diffraction.

5.3.1.1. Introduction.

The following section describes the analysis of the samples using XRD. The crystallinity measured by XRD of the samples was calculated using the following formula [11-12].

Crystallinity (%)= [(sum of the 3 major peaks of Co-zeolites)/(sum of the 3 major peaks of H-zeolites)] X 100

The calculations are based on the three major peaks occurring at 23.06, 23.26 and 24.31 degrees 2 Theta on the XRD diffractogram. The proton form of the sample was considered as a reference sample for these calculations. The proton form was run twice and a percentage of crystallinity of 99% was found with repeat examinations showing a very low percentage error for the sample. However there is a problem associated with this crystallinity measured by XRD method in that the intensities of the peaks for ion exchanged zeolites are influenced by the in-going cation [13-14]. The intensity of the reflections peaks of the exchanged zeolites decrease compared to the zeolites framework XRD pattern.

5.3.1.2 Cobalt zeolites prepared by SSIE with a calcination rate of 20°C per minute.

The X-ray diffractograms of H-mordenite calcined and 1-Co-mordenite catalysts are shown in **Figure 5.1.** The quantity of material used for each XRD diffractograme is 0.3g.

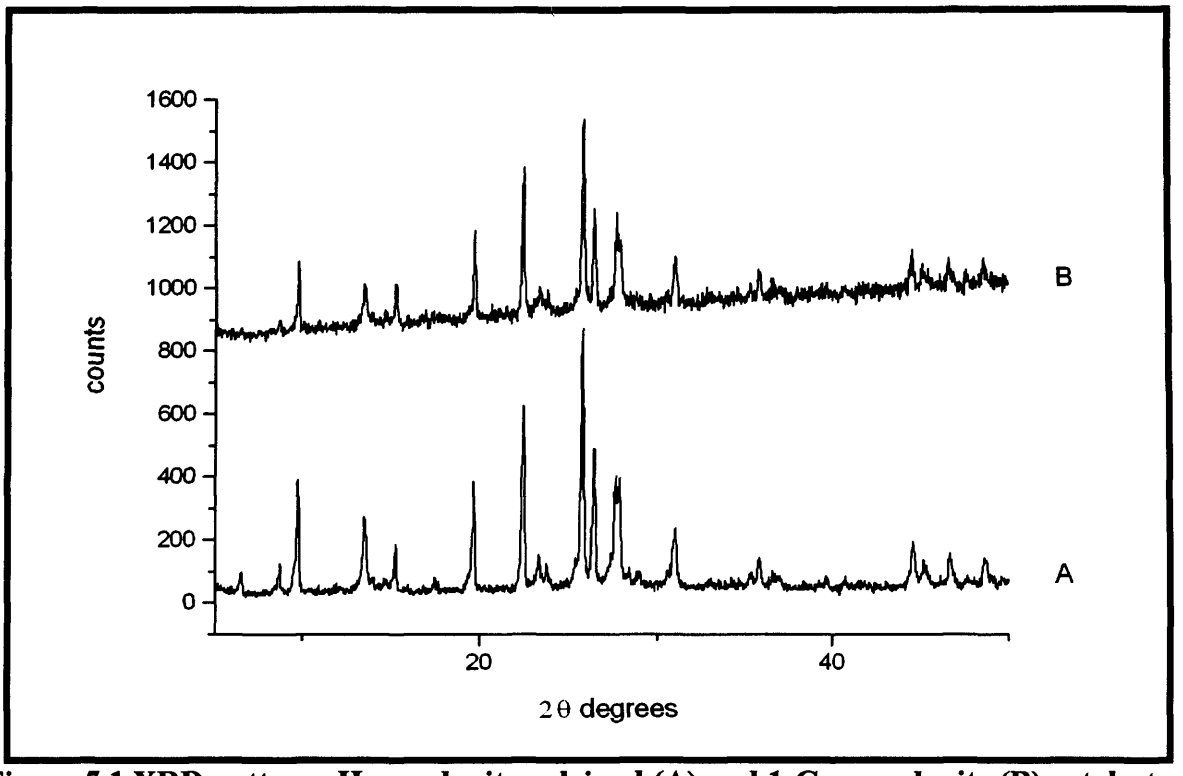

Figure 5.1 XRD patterns H-mordenite calcined (A) and 1-Co-mordenite (B) catalysts.

Crystallinity (%) = 69 %

This data indicated that the cobalt-modified samples did not exhibit detectable shifts of peaks with respect to the parent zeolites (H-mordenite). However, a decrease of line intensities can be seen. 31 % of the crystallinity measured by XRD is lost after solid state ion exchange with cobalt.

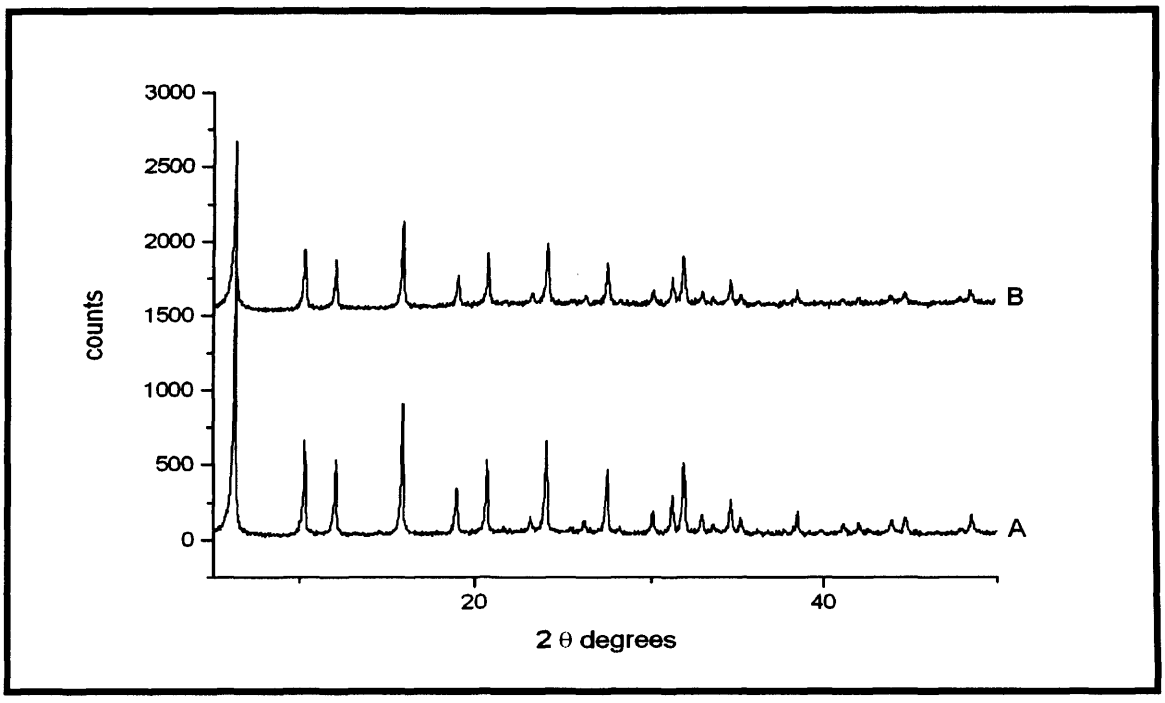

Figure 5.2 XRD patterns of H-Y zeolite (A) and 1-Co-Y-zeolite (B).

Crystallinity (%) = 65 %

For 1-Co-Y zeolites the diffraction peaks obtained are only attributed to zeolite structure, in particular, no cobalt species could be identified. 35 % of the crystallinity measured by XRD is lost after solid state ion exchange with cobalt.

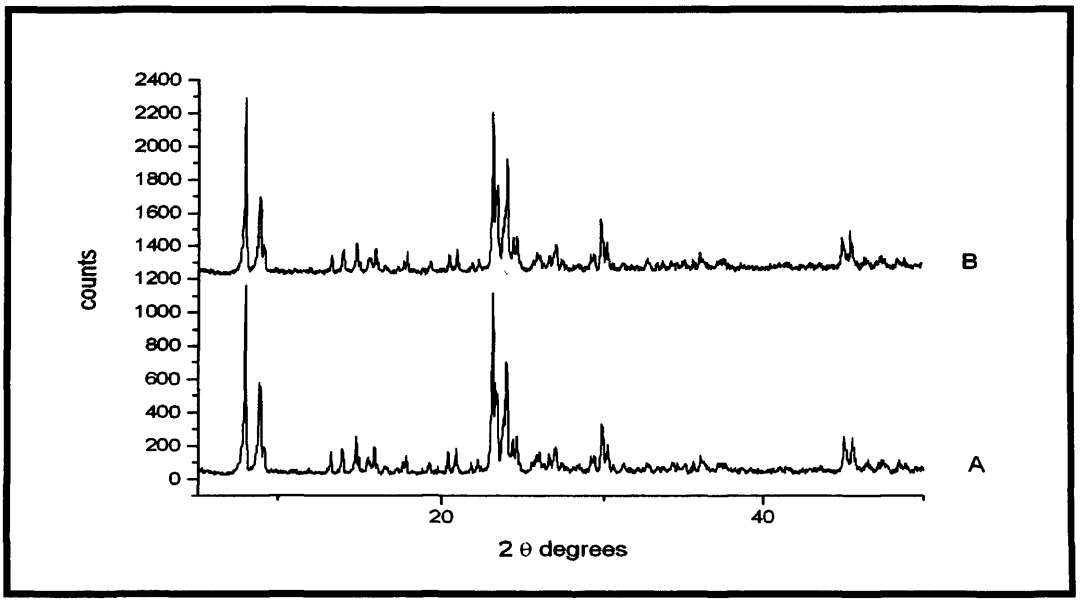

Figure 5.3 The XRD patterns of H-ZSM-5 (SiO_2/ Al_2O_3=280) (A) and 1-Co- ZSM-5 (B) (SiO_2/ Al_2O_3=280).

Crystallinity (%) = 95 %

Crystallinity measured by XRD is retained after ion exchange with a theoretical loading of 1-Co/Al with a ZSM-5 which has a SiO_2/ Al_2O_3 molar ratio of 280. No additional reflections are observed after preparation.

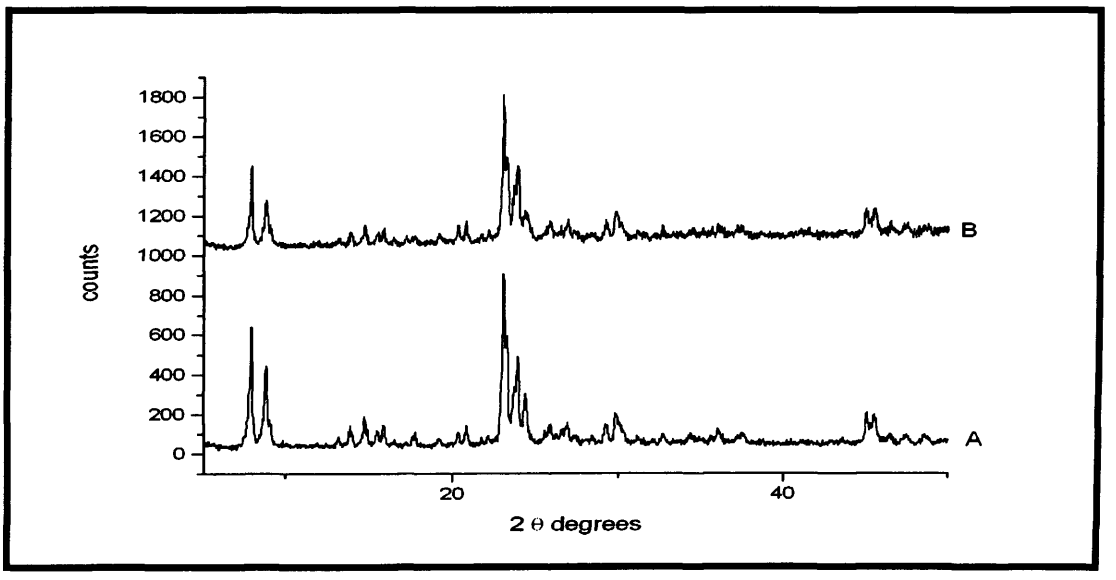

Figure 5.4 The XRD patterns of H-ZSM-5 (SiO_2/ Al_2O_3 =80) (A) and 1-Co-ZSM-5 (B) (SiO_2/ Al_2O_3 =80).

Crystallinity (%) = 81 %

A lower crystallinity measured by XRD for SiO_2/Al_2O_3 molar ratio of 80 is observed after ion exchange with a theoretical loading of 1-Co/Al than with H-ZSM-5 (SiO_2/Al_2O_3 =280). It should be noted that the theoretical loading of cobalt (1-Co/Al) for both H-ZSM-5 (SiO_2/Al_2O_3 =280 and SiO_2/Al_2O_3 =80) is the same but the amount of cobalt loaded in H-ZSM-5 with a molar ratio of SiO_2/Al_2O_3 =80 is higher than ZSM-5 with a molar ratio of SiO_2/Al_2O_3 =280.

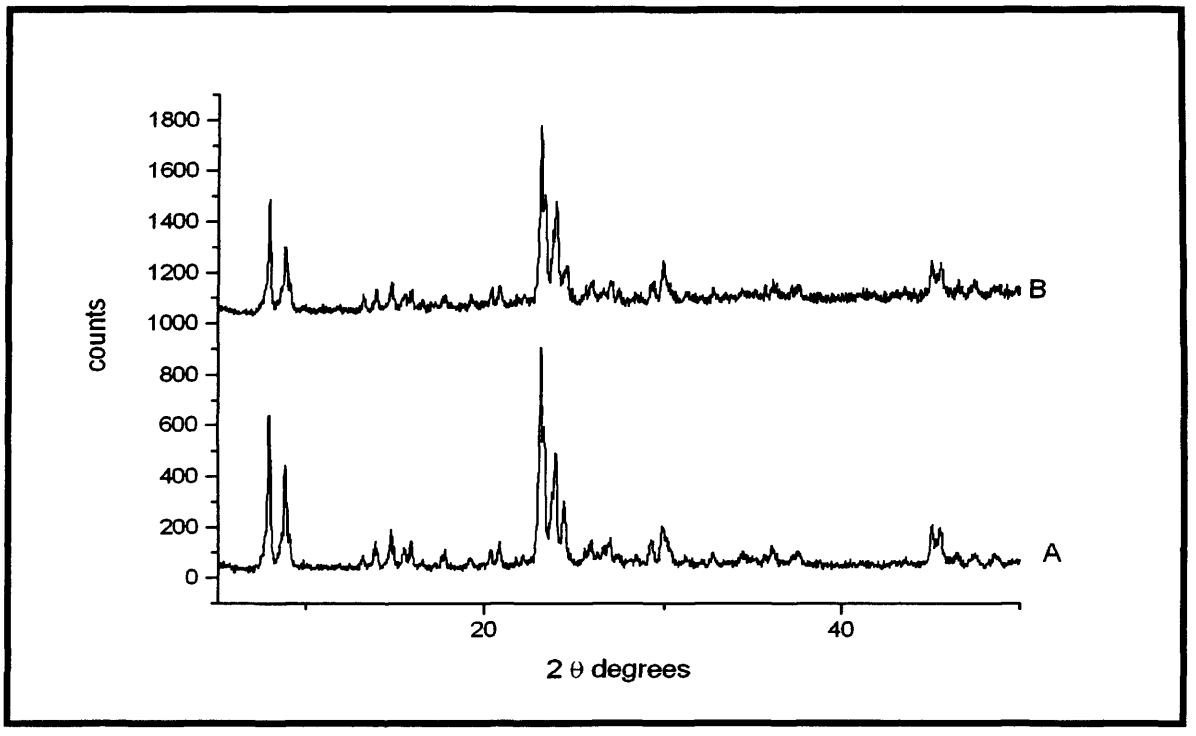

Figure 5.5 The XRD patterns of Si-ZSM-5 (SiO_2/Al_2O_3 =280) (A) and 1-Co-silanated ZSM-5 (B) (SiO_2/Al_2O_3 =280).

Crystallinity (%) = 80 %

The XRD of 1-Co-silanated-ZSM-5 and silanated ZSM-5 are given for comparison (**Figure 5.5**). XRD measurements revealed the same structure and a decrease in crystallinity of 20%.

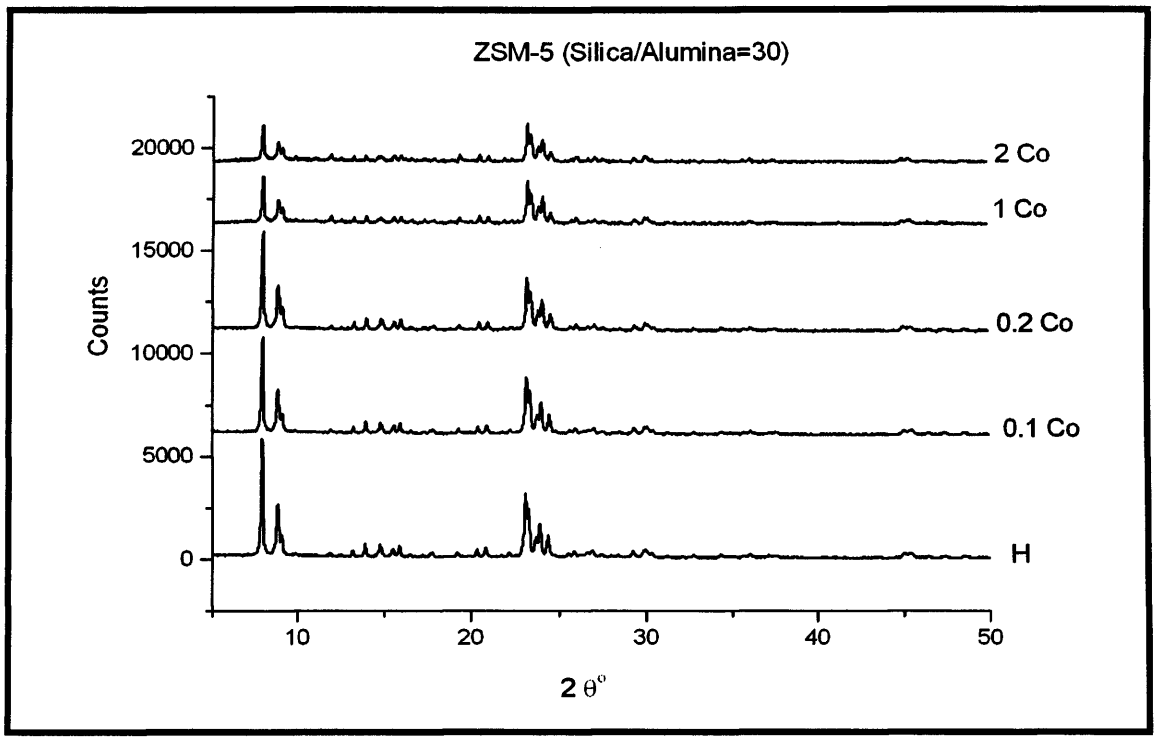

Figure 5.6 The XRD patterns of ZSM-5 (SiO_2/ Al_2O_3 =30) of the different loading of cobalt, H-ZSM-5 (H), 0.1 cobalt loading (0.1-Co), 0.2 cobalt loading (0.2-Co), 1 cobalt loading (1-Co), 2 cobalt (2-Co) loading.

From the XRD analyses (**Figure 5.6**), ZSM-5 was identified as the only crystalline phase. The XRD patterns show that when the amount of cobalt is increased by solid state ion exchange a greater loss of crystallinity is observed. The crystallinity of the samples, as determined by XRD is shown in **Figure 5.8** for these samples.

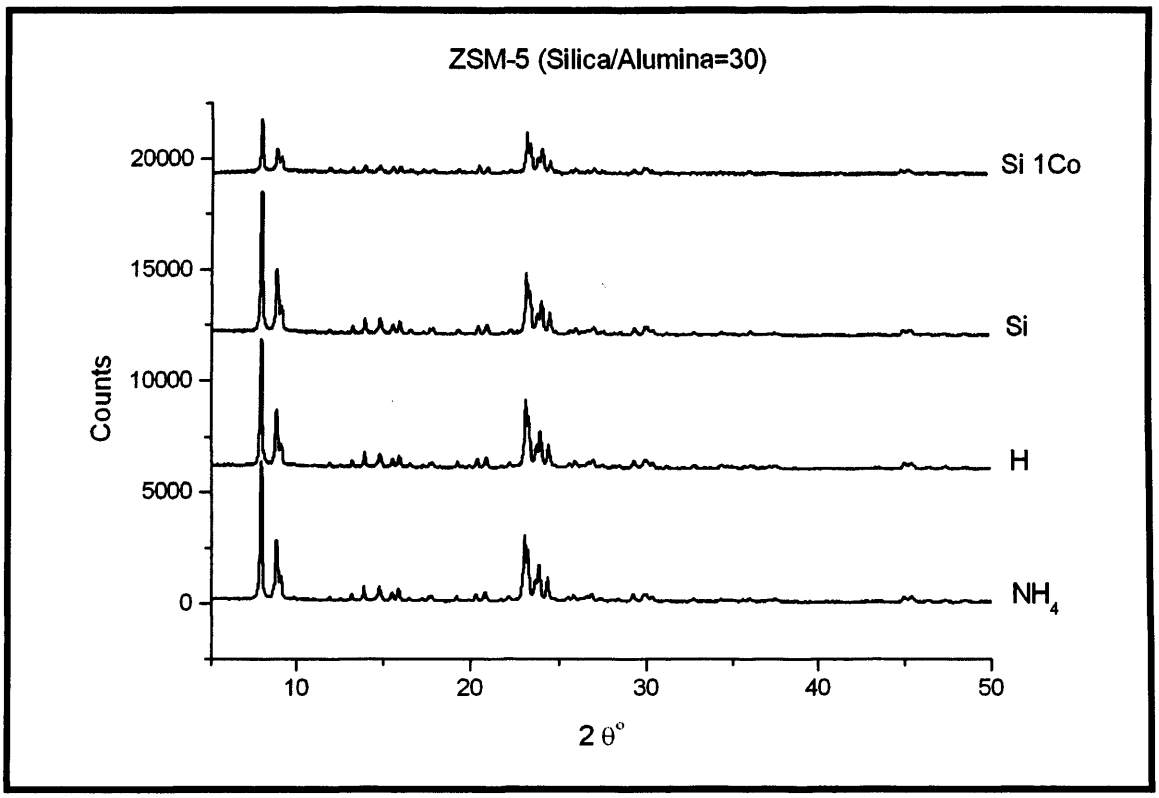

Figure 5.7 The XRD patterns of ZSM-5 (SiO_2/ Al_2O_3 =30), NH_4-ZSM-5 (NH_4), H-ZSM-5 (H), silanated-ZSM-5 (Si), 1-Co/Al after silanation (Si-1-Co).

No changes were observed between the proton forms (H) and the silanated sample (Si) meaning the silanation under these conditions does not affect the structure of the zeolites. However the solid state ion exchange with cobalt decreases the crystallinity of the zeolites although no additional peaks from the silanation and cobalt exchange were observed. From **Figure 5.7**, it easy to see that the silanation decreases the crystallinity of the zeolites.

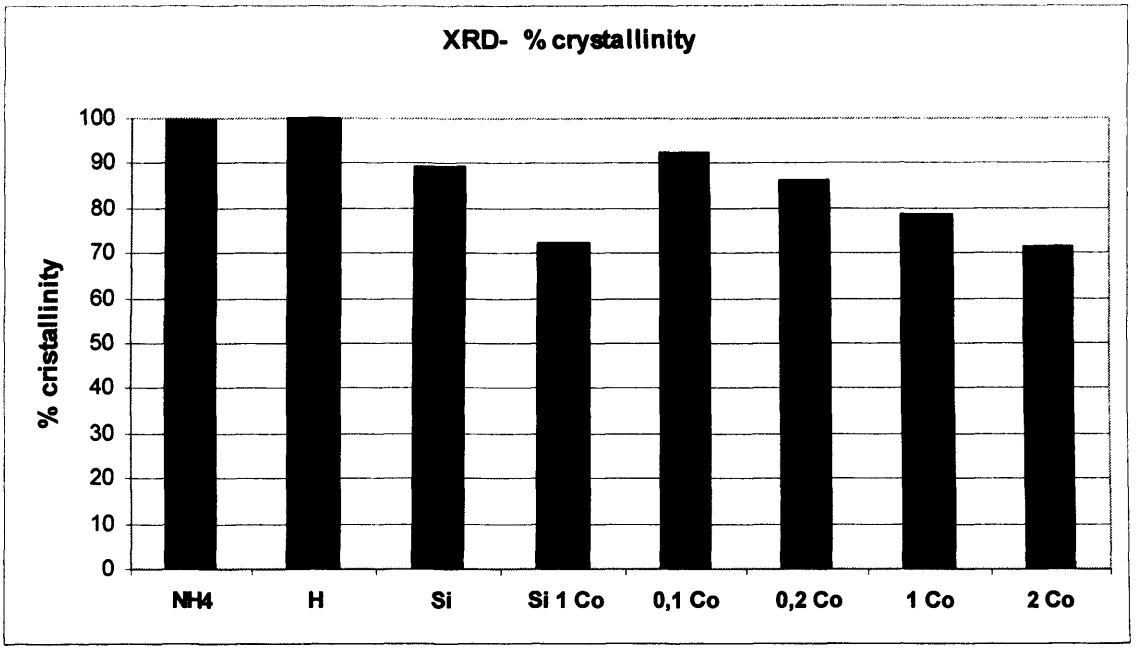

Figure 5.8 Percentage of crystallinity of each zeolites (SiO_2/ Al_2O_3 = 30).

From the **Table 5.8**, it can be observed that the percentage crystallinity decreases gradually with cobalt loading. This may due to the quick evolution of HCl/H_2O during the calcination step of the solid state ion exchange leading to the dealumination or the high temperature used for its preparation [15]. It may also due to a distortion of the zeolites surface by insertion cobalt incorporation in the pores.

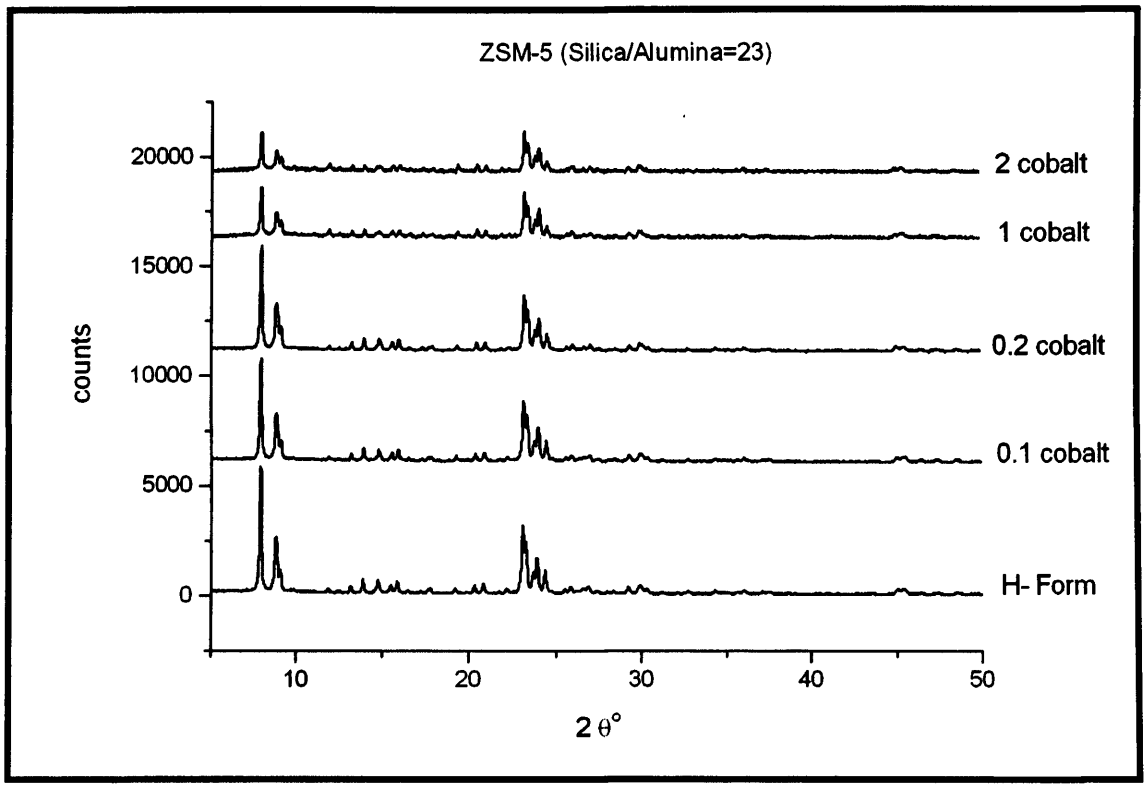

Figure 5.9 display the XRD patterns of ZSM-5 (SiO_2/ Al_2O_3 =23) of the different loading of cobalt, H-ZSM-5 (H), 0.1 cobalt loading (0.1-Co), 0.2 cobalt loading (0.2-Co), 1 cobalt loading (1-Co), 2 cobalt (2-Co) loading.

As observed for the ZSM-5 with a SiO_2/Al_2O_3 = 30, when more cobalt is loaded in the zeolites the intensity of the peaks decreases by a larger amount, indicating a greater loss of crystallinity in the sample.

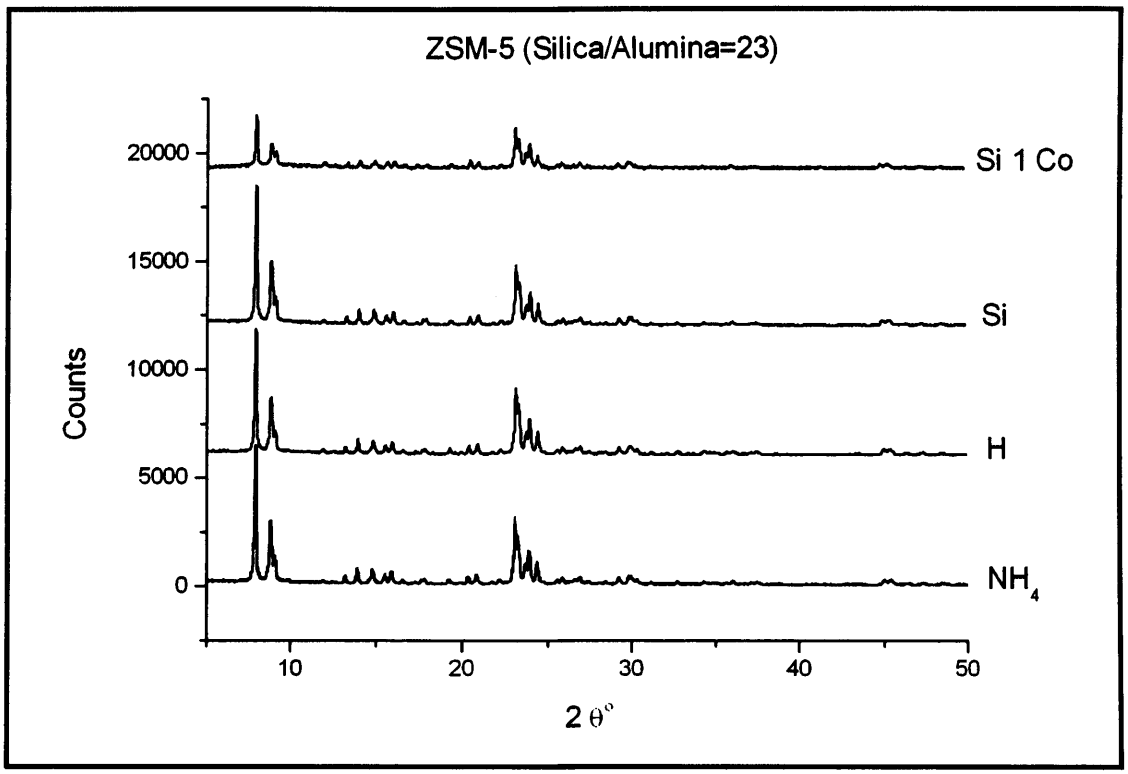

Figure 5.10 display the XRD patterns of ZSM-5 (SiO_2/Al_2O_3 =23), NH_4-ZSM-5 (NH_4), H-ZSM-5 (H) , silanated-ZSM-5 (Si), 1-Co/Al after silanation (Si-1-Co).

There are no additional peaks observed in the pattern after silanation indicating the passivation of the external surface of the zeolites, does not lead to an additional crystalline phase and a high crystallinity (89%) is maintained.

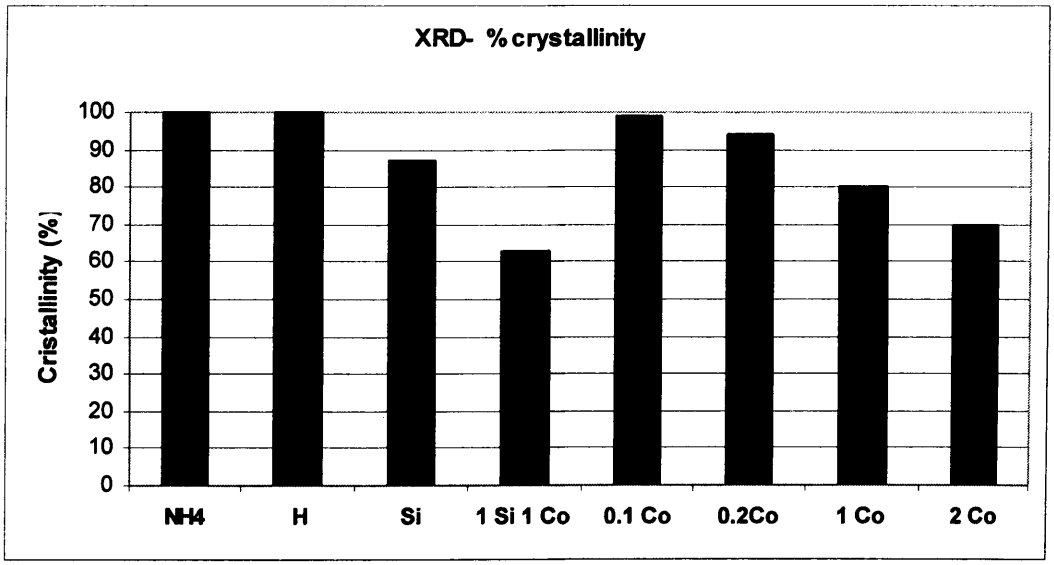

Figure 5.11 Percentage of crystallinity of each zeolites (SiO_2/Al_2O_3= 23).

When we compare the results for the crystallinity for the ZSM-5 with a silica ratio 23 and 30 (**Table 5.7**), it can be seen in both cases that the crystallinity measured by XRD decreases with cobalt loading. Lower crystallinity is observed for the same loading of Co/Al for a silanated zeolites than unsilanated.

5.3.1.3. Cobalt zeolites prepared by SSIE with a calcination rate of 3°C per minute.

During the calcination step of the solid state ion exchanged [16], $CoCl_2.6H_2O$ is melted with the evolution of HCl/H_2O , which can lead to dealumination of the zeolites and may be responsible for the lose of crystallinity observed in the previous sample when cobalt loading is increased. To try to eliminate this effect, a lower temperature rate (3°C /min) with a very thin bed (~0.5 cm) was used (**Figure 5.12**).

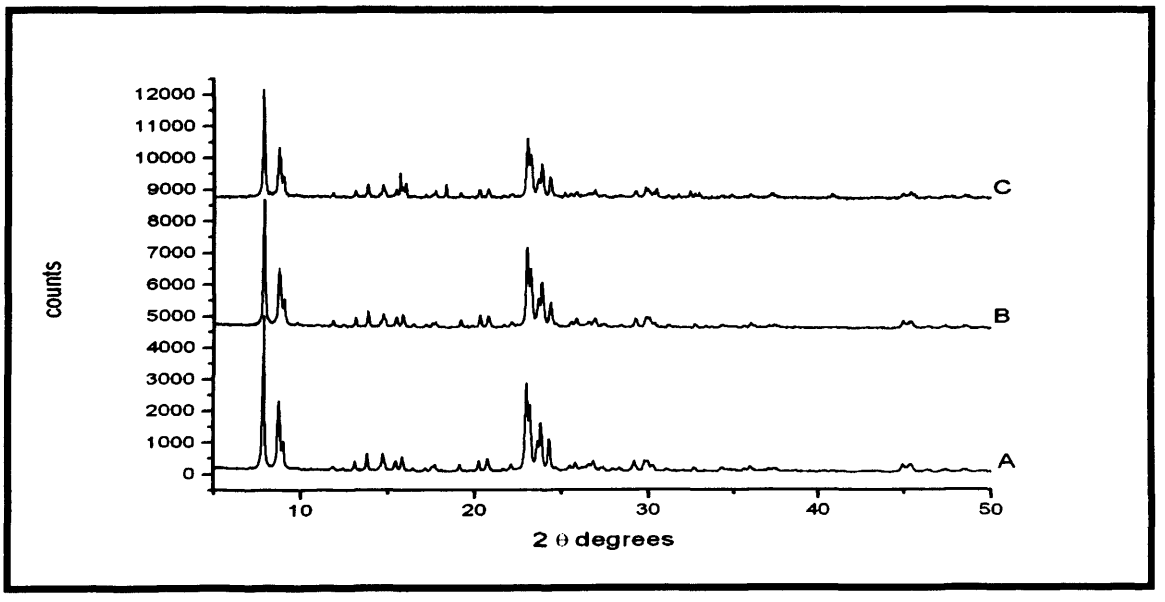

Figure 5.12 display the XRD patterns of ZSM-5 (SiO_2/ Al_2O_3 =30), H-ZSM-5 (A), 0.1-Co ZSM-5 (B), 1-Co-ZSM-5 (C).

Table 5.5 Comparison of the crystallinity.

Theoretical loading	Crystallinity (%) (3°C / min)	Crystallinity (%) (20°C/ min)
0.1-Co	93	92
1-Co	83	78

Decreasing the heating rate of the calcination step of the solid state ion exchange with a very thin bed does not improve the crystallinity of the sample after solid state ion exchanged. Very similar results are observed for both rates used.

5.3.2. Thermal Gravimetric Analysis (TGA).

After the washing procedure of the solid state ion exchange, the zeolites were dried in air at room temperature. Zeolites are hydrophilic and can adsorb water [17]. Before performing BET and micropore analysis of the different zeolites, TGA was carried out in order to determine the time and the temperature to outgas the samples for BET analysis to remove the water from the pores. TGA was also used to determine the time to heat the zeolites before catalyst testing.

Table 5.6 Percentage by mass of water lost for different zeolites.

Catalyst	Water lost by masses (%)
NH_4-ZSM-5 ($SiO_2/Al_2O_3 = 30$)	5.6 %
NH_4-ZSM-5 ($SiO_2/Al_2O_3 = 23$)	8.2 %
1-Co-ZSM-5 ($SiO_2/Al_2O_3 = 30$)	7.4 %
2-Co-ZSM-5 ($SiO_2/Al_2O_3 = 23$)	11.5 %

Table 5.6 shows that a large amount by mass of water can be retained by the zeolites from the washing procedure or from the atmosphere. A maximum temperature of 300 °C was used to avoid the decomposition of the ammonium ion to the proton form which occurs at 400 °C. To

ensure no residual moisture was present on the zeolite catalyst, they were transferred into the reactor immediately after treatment in dry air at 300°C for 5h. Correct outgasing of the sample before BET and micropore volume analysis is an important step. Following the TGA experiments, the outgasing method used for BET and micropore volume analysis was maintained at 300°C overnight before analysis.

5.3.3. BET and micropore volume.

BET analysis and porosity measurements were carried out using Autosorb apparatus at −196 °C with liquid nitrogen. The internal surface of the zeolites is highly accessible and can compose more than 98% of the total surface area [18].

Table 5.7 Surface area and micropore volume of the proton form zeolites.

H-Zeolites	Surface Area (m^2/g)	Pore Volume (cm^3/g)
Modernite (SiO_2/ Al_2O_3=20)	457	0.152
Y-zeolites (Silica/Alumina=80)	809	0.253
ZSM-5 (SiO_2/ Al_2O_3=23)	529	0.145
ZSM-5 (SiO_2/ Al_2O_3=30)	494	0.119
ZSM-5 (SiO_2/ Al_2O_3=80)	487	0.178
ZSM-5 (SiO_2/ Al_2O_3=280)	461	0.140

Zeolites have a very high surface area. To estimate the experimental error of these data on the surface area and the pore volume, the same samples (ZSM-5 with a silica /alumina =280) were run twice. The first surface area found was 461 m^2/g and the second surface area found is 447 m^2/g, so a difference of 14 m^2/g which gives an error percentage of 3 %. For the pore volume the first result is 0.140 cm^3/g and the second result is 0.136 cm^3/g, so a difference of 0.004 cm^3/g, which gives an error percentage of 2.9 %.

Table 5.8 Surface area and micropore volume after solid state ion exchange with a physical mixture of 1-Co/Al.

1-Co-Zeolites	Surface Area (m^2/g)	Pore Volume (cm^3/g)
Modernite (SiO_2/ Al_2O_3=20)	418 (457)	0.133 (0.152)
Y-zeolites (SiO_2/ Al_2O_3=80)	717 (809)	0.196 (0.253)
ZSM-5 (SiO_2/ Al_2O_3=23)	299 (529)	0.096 (0.145)
ZSM-5 (SiO_2/ Al_2O_3=30)	377 (494)	0.114 (0.119)
ZSM-5 (SiO_2/ Al_2O_3=80)	407 (487)	0.076 (0.178)
ZSM-5 (SiO_2/ Al_2O_3=280)	390 (461)	0.098 (0.140)

Different surface area and micropore volumes were found compared to the start material (number in the parentheses). BET indicates that cobalt incorporation decreases the surface area and the micropore volume of the zeolites.

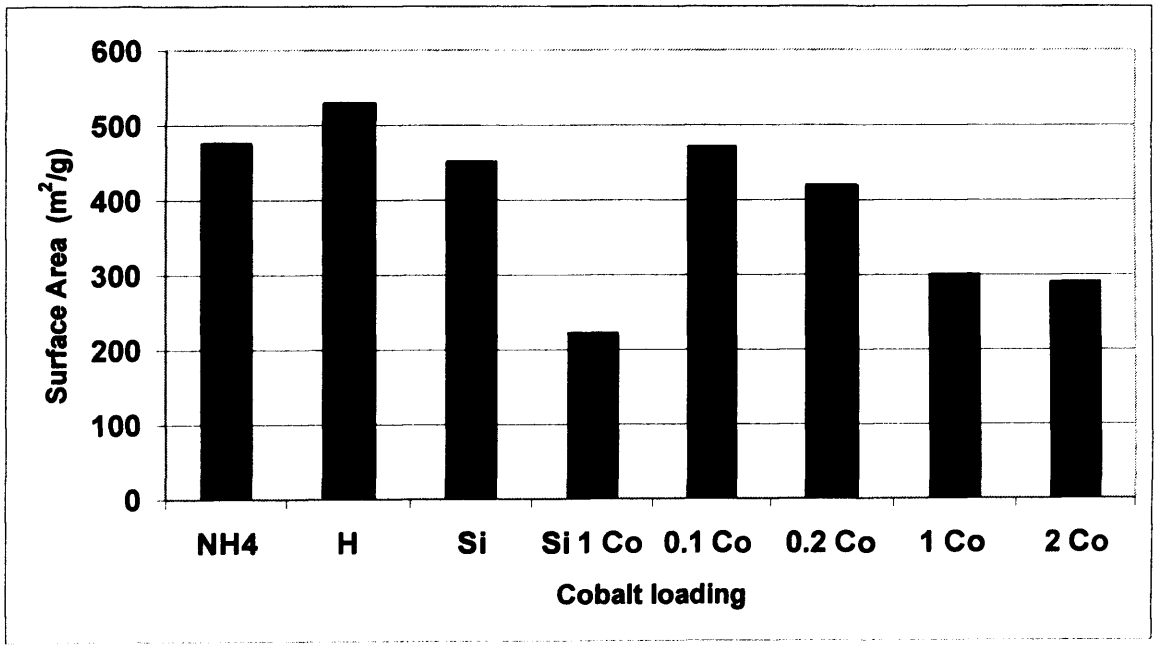

Figure 5.13 Surface area for ZSM-5 (SiO_2/ Al_2O_3=23).

The more cobalt that is loaded into the zeolites, the more the surface area decreases and silanation of the sample followed by solid state ion exchange with 1 Co/Al means the surface area is less than half that of the starting material.

Examining the XRD percentage crystallinity, the BET surface area measurement and the micropore volume, the silanation followed by solid state ion exchange with 1-Co/Al appears to block the pores. Increasing the number of sites exchanged with cobalt leads to a decrease in the micropore volume, indicating cobalt can go inside the pores with the solid state ion exchange method.

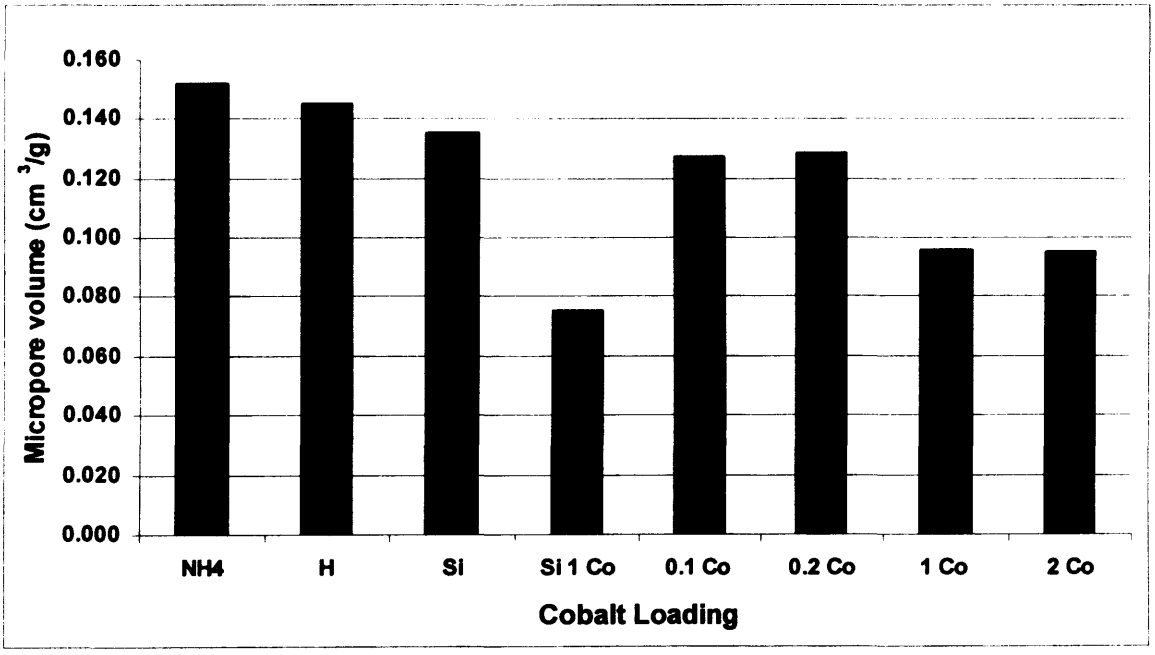

Figure 5.14 Micropore volume for ZSM-5 (SiO_2/ Al_2O_3= 23).

The BET and micropore volumes for the ZSM-5 (silica/alumina = 30) are presented in **Figure 5.15.**

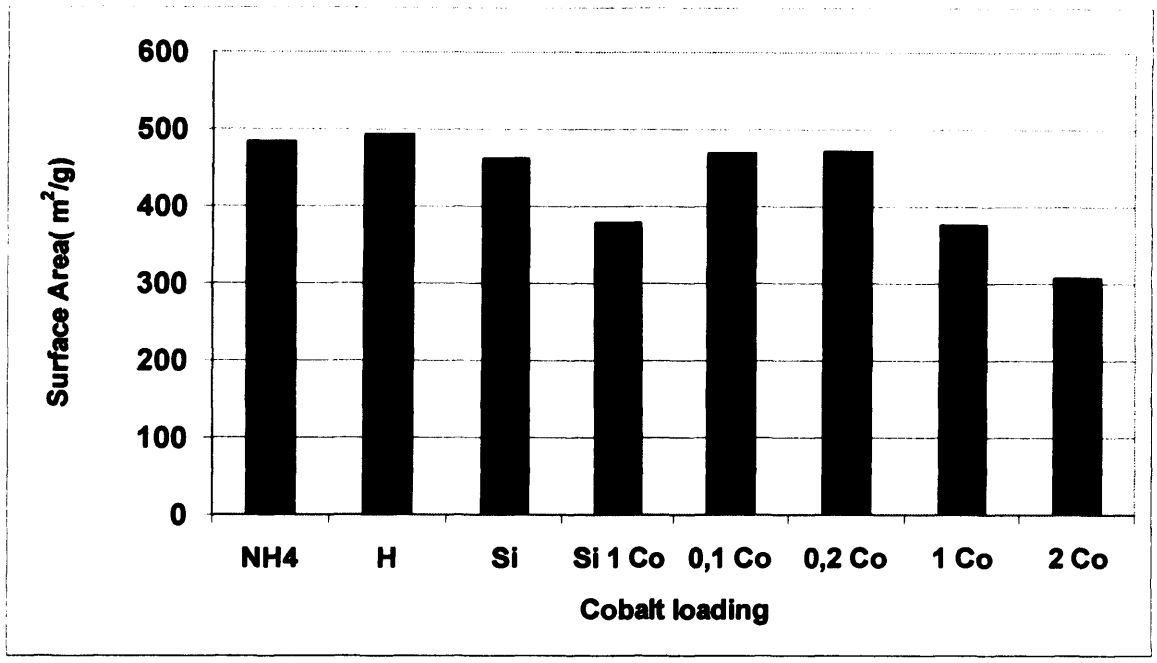

Figure 5.15 BET for ZSM-5 (SiO_2/ Al_2O_3=30).

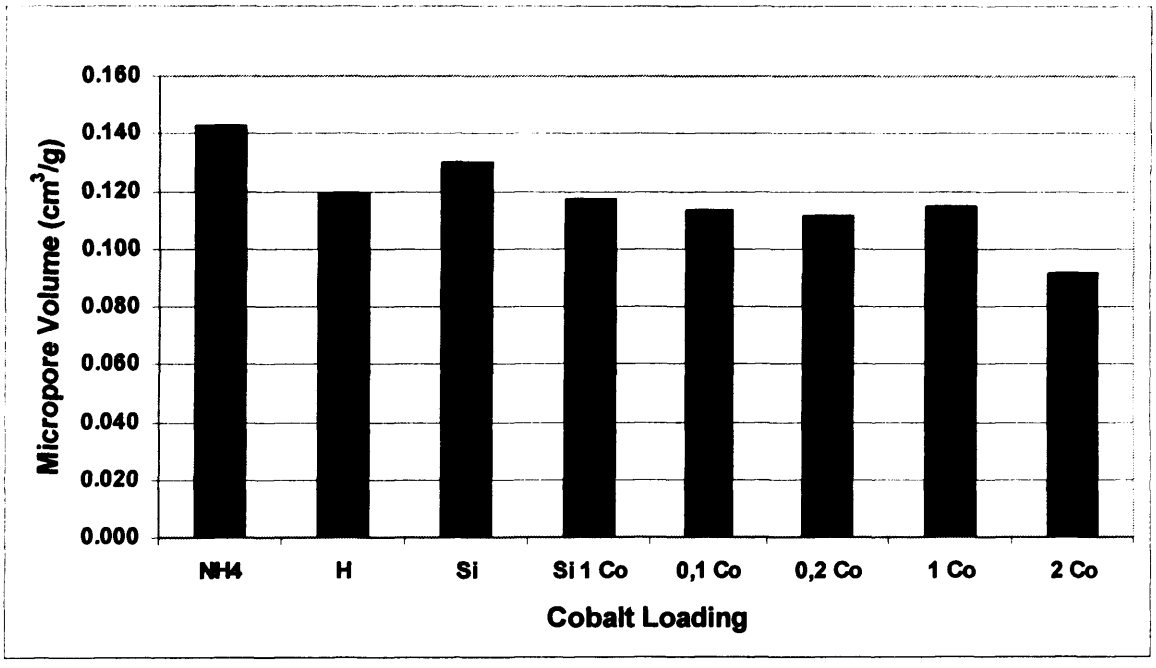

Figure 5.16 Micropore volume (cm^3/g) for ZSM-5 (SiO_2/ Al_2O_3=30).

The lower the SiO_2/ Al_2O_3 mole ratio the more alumina is in the zeolite composition which allows a higher cobalt loading. It can be seen that for the same sample of ZSM-5 a lower BET and micropore volume when more cobalt is loaded. A sample with 0.1 Co/Al with a SiO_2/ Al_2O_3 ratio of 23 will contain more cobalt than a sample with 0.1-Co-Al for a SiO_2/ Al_2O_3 of

30. Some pore blocking might have occurred due to cobalt species either dispersed in the channel or deposited at the outer surface of the zeolite, leading to the observed surface area and porous volume decrease [19].

5.3.4. Inductively coupled plasma mass spectrometry (ICPMS).

It is important to know the real cobalt loading of the zeolites, to know the amount of cobalt that is unreacted or the loss of cobalt during the washing steps of the solid state ion exchange. The data are reported in **Table 5.9** and **Table 5.10**

Table 5.9 ICP-MS of Co-zeolites.

Catalyst	Theoretical Co/ Al ratio Starting physical mixture	ICP-MS result Co/Al ratio
Modernite (SiO_2/ Al_2O_3= 20)	1	0.60
Y-zeolites (SiO_2/ Al_2O_3=80)	1	0.64
ZSM-5 (SiO_2/ Al_2O_3=280)	1	0.70
ZSM-5 (SiO_2/ Al_2O_3=80)	1	0.79
ZSM-5 (SiO_2/ Al_2O_3=30)	0.1	0.06
ZSM-5 (SiO_2/ Al_2O_3=30)	0.2	0.11
ZSM-5 (SiO_2/ Al_2O_3=30)	1	0.72
ZSM-5 (SiO_2/ Al_2O_3=30)	2	0.81
ZSM-5 (SiO_2/ Al_2O_3=23)	0.1	0.04
ZSM-5 (SiO_2/ Al_2O_3=23)	0.2	0.08
ZSM-5 (SiO_2/ Al_2O_3=23)	1	0.65
ZSM-5 (SiO_2/ Al_2O_3=23)	2	0.75

Table 5.10 ICP-MS of silanated zeolites.

Zeolites	Cobalt loading for 1 Al After silanation Starting physical mixture	ICP-MS result Co/Al ratio
ZSM-5 (SiO_2/ Al_2O_3=23)	1	0.42
ZSM-5 (SiO_2/ Al_2O_3=30)	1	0.30
ZSM-5 (SiO_2/ Al_2O_3=80)	1	0.25

The results of ICP-MS show that the loading was smaller that the physical mixture used at the beginning of the solid state ion exchange. It can be concluded that solid state ion exchange following by a long washing procedure does lead to a stoichiometric exchange. The silanation decreases the overall amount of cobalt present in the zeolites.

5.3.5. X-Ray photoelectron spectroscopy (XPS).

XPS was used to identify the amount of cobalt on the surface after a long washing procedure. It was also used to compare the amount of cobalt on the surface between silanated and unsilanated.

Table 5.11 XPS results for a 0.1-Co-ZSM-5 (SiO_2/ Al_2O_3=30) and 2-Co-ZSM-5 (SiO_2/ Al_2O_3=30).

Sample	Theoretical Co/Al	ICP-MS Co/Al	XPS Co/Al
0.1-Co-ZSM-5 (SiO_2/ Al_2O_3=30)	0.1	0.06	0
2-Co-ZSM-5 (SiO_2/ Al_2O_3=30)	2	0.81	0.9

No cobalt on the surface was detected with a 0.1-Co/Al ratio. ICP-MS for this catalyst showed the presence of cobalt for this loading, so cobalt can be incorporated in the zeolite channel and can not be detected by XPS. An experimental reason can also be responsible for this result. ICP-MS was made with 0.5g of catalyst and XPS is performed with material covering a double sided sticky tape disc of approximately 6 mm in diameter with powder. So the amount of sample analysed by XPS is very low compared to the amount of sample

analysed by ICP-MS. So if cobalt is well dispersed in the sample it is more difficult to detect it on the surface however when sample with high loading of Co/Al are analysed by XPS, a large amount of cobalt on the surface of the zeolites is detected.

Table 5.12 XPS results for a 1-Co-ZSM-5 (SiO_2/ Al_2O_3=23) and 1-Co-silanated-ZSM-5 (SiO_2/ Al_2O_3=23).

Sample	Theoretical Co/Al	ICP-MS Co/Al	XPS Co/Al
1-Co-ZSM-5 (SiO_2/ Al_2O_3=23)	1	0.65	1
1-Co-silanated-ZSM-5 (SiO_2/ Al_2O_3=23)	1	0.42	0.3

A large amount of cobalt has been detected on the surface of the zeolites. Silanation decreased the amount of cobalt on the surface.

Table 5.13 XPS results for a 1-Co-ZSM-5 (SiO_2/ Al_2O_3=23) and 1-Co-silanated-ZSM-5 (SiO_2/ Al_2O_3=23).

Sample	Therotical Al/Si	XPS Al/Si
1-Co- ZSM-5 (SiO_2/ Al_2O_3=23)	11.5	14.9
1-Co-silanated-ZSM-5 (SiO_2/ Al_2O_3=23)	-	22.9

The XPS results show an increase of Al/Si ratio after silanation meaning the silanation has occurred.

5.4. Catalysts testing.

5.4.1. Testing of acid zeolites.

The protons which balance the negative charge of a zeolite framework (**Figure 5.17**) are not strongly bound to the framework and are able to move and to react with molecules [20].

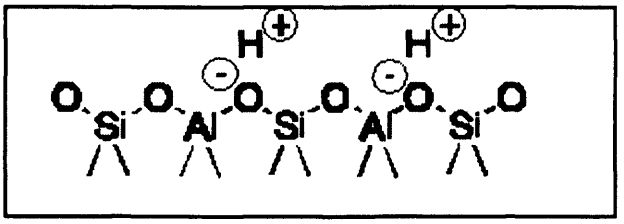

Figure 5.17 Zeolites's Brönsted acidity [20].

A protonated zeolite thus can act as a Brönsted acid. Firstly, proton zeolites without cobalt were investigated for the oxidation of *n*-decane in liquid phase. The proton forms of the zeolites are well known to be heterogeneous acid catalysts [21-22]. Silanated zeolites were also tested.

Table 5.14 Conversion for proton and silanated zeolites.

Catalyst	Conversion (%)
None	0.18
ZSM-5 (SiO_2/ Al_2O_3=23)	0
Si-ZSM-5 (SiO_2/ Al_2O_3=23)	0
ZSM-5 (SiO_2/ Al_2O_3=30)	0
Si-ZSM-5 (SiO_2/ Al_2O_3=30)	0
ZSM-5 (SiO_2/ Al_2O_3=80)	0
Si-ZSM-5 (SiO_2/ Al_2O_3=80)	0
ZSM-5 (SiO_2/ Al_2O_3=280)	0
Y- zeolites (SiO_2/ Al_2O_3=80)	0
Mordenite (SiO_2/ Al_2O_3=20)	0

Reactions conditions: 100°C, stirring speed 600 rpm, 15 bar O_2, decane (10g), H-zeolites (0.05g), 24 hours.

The liquid phase reaction using H-zeolites with accessible protons switches off the autoxidation. The silanation of external sites in H-ZSM-5 using large organosilane molecules decreases the density of such sites at the external surfaces [10] but enough protons are still accessible to scavenge the autoxidation. So the acid zeolites prevent the propagation of the

autoxidation, which is a major problem of this reaction because autoxidation is an unselective radical mechanism, which gives very low terminal selectivity.

5.4.2. Testing of cobalt zeolites.

5.4.2.1. Low loading of cobalt with 24 hours runtime.

Different loadings of cobalt have been prepared with different types of zeolites. Firstly, the results for low loading of cobalt (0.1-Co/Al and 0.2-Co/Al) will be presented for a runtime of 24 hours.

Table 5.15 Conversion for low cobalt loading.

Catalyst	Loading of cobalt for 1 Al	Conv. (%)
No catalyst	-	0.4
ZSM-5 (SiO_2/ Al_2O_3=23)	0.1-Co	0
ZSM-5 (SiO_2/ Al_2O_3=23)	0.2-Co	0
ZSM-5 (SiO_2/ Al_2O_3=30)	0.1-Co	0
ZSM-5 (SiO_2/ Al_2O_3=30)	0.2-Co	0

Reactions conditions: 100°C, stirring speed 600 rpm, 15 bar O_2, decane (10g), catalyst (50 mg) and runtime (24 hours).

The best result of Iglesia [23] for the oxidation of *n*-hexane in liquid phase is with a ZSM-5 with a theoretical loading 0.1-Mn/Al (0.088-Mn/Al by ICPM-MS). For the oxidation of *n*-decane, low cobalt loading did not promote the conversion after 24 h reaction. No conversion has been observed, meaning the presence of protons available in the zeolites after solid state ion exchange with 0.1cobalt or 0.2cobalt can switch off the autoxidation. After these results, it was decided to increase the amount of cobalt in the zeolites.

5.4.2.2. Higher loading of cobalt with a run time of 8 hours.

Different ratios of SiO_2/ Al_2O_3 ZSM-5, which allow different loading of cobalt were tested for a run of 8 hours. The lower the SiO_2/ Al_2O_3 ratio the greater the loading of cobalt. **Table 5.18** shows the conversion of *n*-decane related to the amount of cobalt present in the catalyst.

Table 5.16 Conversion and amount of cobalt for different SiO_2/Al_2O_3 ratio of ZSM-5 exchanged with 1-Co/Al for a run of 8 hours.

Catalyst	Amount of cobalt in the catalyst (mg)	Conv. (%)
SiO_2/Al_2O_3 =23	1.17	0.06
SiO_2/Al_2O_3 =30	1.00	0.05
SiO_2/Al_2O_3 =80	0.43	0
SiO_2/Al_2O_3 =280	0.11	0
Blank	0	0

Reactions conditions: 100°C, stirring speed 600 rpm, 15 bar O_2, decane (10g), catalyst (50 mg) and runtime (24 hours).

Table 5.17 shows the product distribution related to the conversion for each Co-ZSM-5.

Table 5.17 Conversion and product profile for different SiO_2/Al_2O_3 mole ratio of ZSM-5 exchanged with 1 Co/Al for a run of 8 hours

Cat.	Conv. (%)	5/4 one	3 one	2 one	5/4 ol	3 ol	2 ol	1 ol	C_5 acid	C_6 acid	C_7 acid	C_8 acid	C_9 acid	C_{10} acid
Blank	0	-	-	-	-	-	-	-	-	-	-	-	-	-
SiO_2/ Al_2O_3= 23	0.06	25	17	10	14	16	13	0	5	0	0	0	0	0
SiO_2/ Al_2O_3= 30	0.05	27	15	10	13	17	11	0	7	0	0	0	0	0
SiO_2/ Al_2O_3= 80	0	-	-	-	-	-	-	-	-	-	-	-	-	-
SiO_2/ Al_2O_3= 280	0	-	-	-	-	-	-	-	-	-	-	-	-	-

Reactions conditions: 100°C, stirring speed 600 rpm, 15 bar O_2, decane (10g), catalyst (50mg) and runtime (8 hours).

The high SiO_2/Al_2O_3 ratio did not show any activity. However low SiO_2/Al_2O_3 ratio which contains more cobalt showed a small conversion of *n*-decane after 8 hours. During the ion exchange process, cobalt replaces the proton, so there is less proton available (stop the autoxidation) than the starting material and more cobalt available, which can do the homolytic decomposition of ROOH and propagate the reaction. The conversion is higher than the blank reaction, so it is due to more cobalt. The product profile at low conversion did not show terminal products.

The previous results have shown that the amount of cobalt is very relevant to the catalytic performance of the catalyst. To try to increase the amount of cobalt present in the catalyst, a preparation of catalyst with a physical mixture of 2-Co/Al was made with ZSM-5 with SiO_2/Al_2O_3 =23 and SiO_2/Al_2O_3 =30. The ICP-MS result has showed a Co/Al ratio of 0.75 and 0.81. The ICP-MS result is higher than a catalyst prepared with a physical mixture of 1-Co/Al (0.65). The long washing procedure may avoid the overexchange. The results for 2-Co/Al ZSM-5 with SiO_2/Al_2O_3 =23 and SiO_2/Al_2O_3 =30 are listed in **Table 5.20**.

Table 5.18 Conversion and product profile for different SiO_2/ Al_2O_3 ratio of ZSM-5 exchanged with 2-Co/Al for a run of 8 hours.

Cat.	Co (mg)	Conv. (%)	5/4 one	3 one	2 one	5/4 ol	3 ol	2 ol	1 ol	C_5 acid	C_6 acid	C_7 acid	C_8 acid	C_9 acid	C_{10} acid
Blank	0	0	-	-	-	-	-	-	-	-	-	-	-	-	-
SiO_2/ Al_2O_3=23	1.3	0.14	29	14	12	11	11	9	1	7	3	2	0	1	0
SiO_2/ Al_2O_3=30	1.1	0.12	22	16	14	15	6	6	1	9	4	4	2	0	1

Reactions conditions: 100°C, stirring speed 600 rpm, 15 bar O_2, decane (10g), catalyst (50 mg) and runtime (8 hours).

Increasing the amount of cobalt in the zeolites will increase the conversion. However the product profile looks similar to both autoxidation and VMgO catalyst with a poor terminal selectivity and a high selectivity to internal oxygenated products.

Different zeolites with different shape of channels and different pore diameter than ZSM-5 (**Table 5.1**) were also tested to see if there is any change in the product distribution. Co-Y and Co-mordenite were also tested for a run of 8 hours.

Table 5.19 Conversion and product profile for Y-zeolites and mordenite exchanged with 1-Co/Al for a run of 8 hours

Catalyst	Co (mg)	Conv. (%)	5/4 one	3 one	2 one	5/4 ol	3 ol	2 ol	1 ol	C_5 acid	C_6 acid	C_7 acid	C_8 acid	C_9 acid	C_{10} acid
Blank	0	0	-	-	-	-	-	-	-	-	-	-	-	-	-
1-Co-Y	0.35	0.01	27	13	12	13	11	11	0	7	3	0	3	0	0
1-Co-mordenite	1.2	0.07	19	15	12	13	17	12	0	7	2	2	0	1	0

Reactions conditions: 100°C, stirring speed 600 rpm, 15 bar O_2, decane (10g), catalyst (50 mg) and runtime (8 hours).

No major difference is observed in the product profile after 8 hours for a very low conversion. The change in the size of the pore (5 Å for ZSM-5, 7 Å for modernite and 8 Å for Y-zeolites) did not influence the product distribution. Only increasing the amount of cobalt increased the conversion.

The activity of cobalt exchanged silanated ZSM-5 was also investigated for a short runtime of 8 hours. The aim of the silanation was to prevent the cobalt from anchoring on the external surface of the zeolites during the solid state ion exchange, which would give an unselective reaction (no spatial constraints). Firstly, the different ZSM-5 samples were silanated and then ion exchanged with a physical mixture of 1-Co/Al.

Table 5.20 Conversion of 1-Co-silanated-ZSM-5.

1-Co-ZSM-5	Conv. (%)
Blank	0
SiO_2/ Al_2O_3=23	0
SiO_2/ Al_2O_3=30	0
SiO_2/ Al_2O_3=80	0

Reactions conditions: 100°C, stirring speed 600 rpm, 15 bar O_2, decane (10g), catalyst (50 mg) and runtime (8 hours).

Cobalt silanated zeolites did not show conversion after 8 hours of run, which means Brönsted acidity is still available to inhibit the autoxidation.

5.4.2.3. Higher loading of cobalt with a run time of 16 hours.

The same catalysts were used for a longer runtime (16 hours)

Table 5.21 Amount of colbat versus conversion for different ZSM-5

Catalyst	Amount of cobalt in the catalyst (mg)	Conv. (%)
SiO_2/Al_2O_3 =23	1.17	0.40
SiO_2/Al_2O_3 =30	1.00	0.32
SiO_2/Al_2O_3 =80	0.43	0.35
SiO_2/Al_2O_3 =280	0.11	0.14
Blank	0	0.04

Table 5.22 Product distribution of different 1-Co-ZSM-5 for a run of 16 hours

Cat.	Conv. (%)	5/4 one	3 one	2 one	5/4 ol	3 ol	2 ol	1 ol	C_5 acid	C_6 acid	C_7 acid	C_8 acid	C_9 acid	C_{10} Acid
Blank	0.04	45	13	17	14	9	0	0	0	0	0	0	0	0
SiO_2/ Al_2O_3=23	0.40	20	14	15	9	6	9	1	9	5	8	1	1	2
SiO_2/ Al_2O_3=30	0.32	22	20	19	10	8	2	1	4	4	3	5	0	2
SiO_2/ Al_2O_3=80	0.35	27	12	15	12	12	3	1	6	1	5	5	0	1
SiO_2/ Al_2O_3=280	0.14	18	15	12	13	17	12	1	7	2	2	0	1	0

Reactions conditions: 100°C, stirring speed 600 rpm, 15 bar O_2, decane (10g), catalyst (50 mg) and runtime (16 hours).

Table 5.23 Activity of 2-Co-ZSM-5.

Catalyst	Co (mg)	Conv. (%)	5/4 one	3 one	2 one	5/4 ol	3 ol	2 ol	1 ol	C_5 acid	C_6 acid	C_7 acid	C_8 acid	C_9 acid	C_{10} acid
Blank	0	0.04	45.2	13.3	17.2	14.1	9.8	0	0	0	0	0	0	0	0
SiO_2/ Al_2O_3=23	1.35	1.12	21.2	14.5	16.6	10.2	7.5	10.4	1.4	7.4	6.3	5.2	1.2	1.2	1.1
SiO_2/ Al_2O_3=30	1.13	0.80	27.2	12.2	14.7	12.3	11.4	5.1	1.3	6.5	1.8	5.2	5.2	0	1.1

Reactions conditions: 100°C, stirring speed 600 rpm, 15 bar O_2, decane (10g), catalyst (50 mg) and runtime (16 hours).

As observed for a run of 8 hours, more cobalt in the zeolites will give higher conversion. For example ZSM-5 (SiO_2/ Al_2O_3=23) gives a conversion of 1.12% whereas ZSM-5 (SiO_2/ Al_2O_3=280) gives a conversion of 0.14 % for the same runtime. Increasing the conversion increases the amount of cracked acids formed.

Table 5.24 Activity of 1-Co-Y and 1-Co-mordenite.

Catalyst	Co (mg)	Conv. (%)	5/4 one	3 one	2 one	5/4 ol	3 ol	2 ol	1 ol	C_5 acid	C_6 Acid	C_7 acid	C_8 acid	C_9 acid	C_{10} acid
Blank	0	0.04	45.5	13.7	17.3	14.6	9.2	0	0	0	0	0	0	0	0
1-Co-Y	0.35	0.18	28.5	12.6	7.3	17.6	11.3	14.2	1.7	6.8	0	2.2	1.3	1.1	0
1-Co-mordenite	1.2	1.20	29.8	15.3	11.3	15.4	8.2	6.4	1.2	7.4	3.3	1.8	3.6	0	1.5

Reactions conditions: 100°C, stirring speed 600 rpm, 15 bar O_2, decane (10g), catalyst (50 mg) and runtime (16 hours).

Replacing ZSM-5 zeolites by Y-zeolites or modernite did not improve the terminal selectivity. Mordenite which has a low SiO_2/Al_2O_3 ratio, which allows a high loading of cobalt shows the best conversion after 16 hours run.

Table 5.25 Silanated 1-Co-ZSM-5.

1 Co-ZSM-5	Co (mg)	Conv. (%)	5/4 one	3 one	2 one	5/4 ol	3 ol	2 ol	1 ol	C_5 acid	C_6 acid	C_7 acid	C_8 acid	C_9 acid	C_{10} acid
Blank	0	0.04	45.2	13.1	17.2	14.3	9.4	0	0	0	0	0	0	0	0
SiO_2/Al_2O_3=23	0.75	0.22	24.3	16.1	10.3	14.1	11.1	14.2	1.1	6.2	0	2.4	1.1	1.2	0
SiO_2/Al_2O_3=30	0.42	0.20	22.9	13.7	7.7	18.6	11.3	16.5	1.7	8.6	0	2.2	1.4	1.1	0
SiO_2/Al_2O_3=80	0.14	0.07	26.3	17.3	18.4	10.5	9.6	9.7	0	8.3	1.3	1.6	1.6	0	0

Reactions conditions: 100°C, stirring speed 600 rpm, 15 bar O_2, decane (10g), catalyst (50 mg) and runtime (16 hours).

Cobalt silanated zeolites gave lower conversion than the non silanated cobalt zeolites.

No improvement of the terminal selectivity is observed, only a decrease in the conversion.

5.4.2.4. Higher loading of cobalt with a run time of 24 hours.

After 8 hours and 16 hours the terminal selectivity obtained was very low. So it was decided to increase the runtime to 24 hours, to increase the conversion and possibly increase the terminal selectivity.

Table 5.26 Relation between cobalt loading and conversion.

catalyst	Amount of cobalt in the catalyst (mg)	Conv. (%)
SiO_2/Al_2O_3 =23	1.17	1.12
SiO_2/Al_2O_3 =30	1.00	1.08
SiO_2/Al_2O_3 =80	0.43	0.87
SiO_2/Al_2O_3 =280	0.11	0.42
Blank	0	0.39

Table 5.27 Activity of 1-Co-ZSM-5

1-Co-ZSM-5	Conv. (%)	5/4 one	3 one	2 one	5/4 ol	3 ol	2 ol	1 ol	C_5 acid	C_6 acid	C_7 acid	C_8 acid	C_9 acid	C_{10} acid
Blank	0.39	32.4	20.8	21.9	1.6	3.0	2.0	1.0	3.9	3.8	2.5	5.1	0	1.9
SiO_2/Al_2O_3=23	1.12	21.3	14.3	15.4	11.7	6.4	10.3	1.1	8.5	5.6	6.6	1.4.	1.7	1.9
SiO_2/Al_2O_3=30	1.08	19.2	14.3	17.2	14.3	10.4	10.8	1.8	5.3	1.4	6.5	1.7	1.4	0.9
SiO_2/Al_2O_3=80	0.87	20.6	16.0	15.1	15.3	9.4	6.5	0.7	9.4	2.4	1.5	3.3	1.2	2.1
SiO_2/Al_2O_3=280	0.42	20.1	18.2	12.1	17.2	15.3	8.7	1.5	6.3	2.3	1.1	0	0	0

Reactions conditions: 100°C, stirring speed 600 rpm, 15 bar O_2, decane (10g), catalyst (50 mg) and runtime (24 hours).

Table 5.28 Activity of 2-Co- ZSM-5.

2-Co-ZSM-5	Co (mg)	Conv. (%)	5/4 one	3 one	2 one	5/4 ol	3 ol	2 ol	1 ol	C_5 acid	C_6 acid	C_7 acid	C_8 acid	C_9 acid	C_{10} Acid
Blank	0	0.39	32.2	21.2	22.7	2.7	3.8	2.3	1.6	4.2	4.5	3.7	5.8	0	1.7
SiO_2/ Al_2O_3=23	1.35	2.20	21.4	13.4	14.3	7.8	5.7	9.5	1.3	13.6	4.4	6.5	5.4	1.4	1.8
SiO_2/ Al_2O_3=30	1.13	1.60	25.4	14.2	15.2	8	5.5	8.7	1.4	10.8	6.3	5.3	2.3	0	1.5

Reactions conditions: 100°C, stirring speed 600 rpm, 15 bar O_2, decane (10g), catalyst (50mg) and runtime (24 hours).

Table 5.29 Activity of 1-Co-Y and 1-Co-mordenite.

Catalyst	Co (mg)	Conv. (%)	5/4 one	3 one	2 one	5/4 ol	3 ol	2 ol	1 ol	C_5 acid	C_6 acid	C_7 acid	C_8 acid	C_9 acid	C_{1} aci
Blank	0	0.39	32.2	21.2	22.7	2.7	3.8	2.3	1.6	4.2	4.5	3.7	5.8	0	1.7
1-Co-Y	0.35	0.73	20.4	16.4	14.6	15.4	14.5	8.2	1.2	8.2	2.2	1.2	0.2	0.2	1.2
1-Co-mordenite	1.2	1.56	19.1	13.2	15.4	14.3	10.5	8.3	1.7	7.5	2.6	2.6	7.8	1.4	1.5

Reactions conditions: 100°C, stirring speed 600 rpm, 15 bar O_2, decane (10g), catalyst (50 mg) and runtime (24 hours).

Table 5.30 Activity silanated 1-Co-ZSM-5.

Catalyst	Co (mg)	Conv. (%)	5/4 one	3 one	2 one	5/4 ol	3 ol	2 ol	1 ol	C_5 acid	C_6 acid	C_7 acid	C_8 acid	C_9 acid	C_{10} acid
Blank	0	0.39	32.2	21.3	22.2	2.6	3.7	2.1	1.1	4.1	4.4	3.4	5.3	0	1.9
SiO_2/ Al_2O_3=23	0.75	0.35	27.2	20.3	15.1	15.4	5.7	6.3	1.4	7.1	1.3	2.2	0	0	1.2
SiO_2/ Al_2O_3=30	0.42	0.45	23.2	15.9	11.1	12.4	9.3	8.4	1.2	8.3	6.3	2.6	3.8	1.2	1.2
SiO_2/ Al_2O_3=80	0.14	0.137	35.3	15.3	4.5	2.7	9.3	10.2	1.2	5.6	0	0	7.3	2.3	0.8

Reactions conditions: 100°C, stirring speed 600 rpm, 15 bar O_2, decane (10g), catalyst (50 mg) and runtime (24 hours).

The silanation of ZSM-5 reduces the activity of the catalyst, to the level of the blank and no more terminal product is observed. This suggests that the reaction is mainly occurring on the external surface of the zeolites, because once the surface sites are removed, conversion is

considerably decreased. Spatial constraints around the catalytic sites did not lead to a preference for terminal oxidation after 24 hours.

Co-zeolites are active catalyst at 100°C without radical initiator for the oxidation of *n*-decane. The rate of *n*-decane reaction with O_2 increased with the loading of cobalt in the zeolites. Cobalt mordenite has the lowest silica alumina ratio (SiO_2/Al_2O_3=20), so has the highest amount of cobalt (1-Co/Al has been used for the solid state ion exchange), and shows the highest conversion for a run of 24 hours. The best example of the improved conversion with higher Co loading is given by the two ZSM-5 catalysts where the zeolite structure is the same but with a SiO_2/Al_2O_3ratio of 80, a conversion of 0.87 % is reached after 24 hours, while with a ratio of 280, it is only half this at 0.42 %.

5.4.2.5. Relationship between amount of cobalt and conversion.

Table 5.32 relates the performance of different Co-zeolites with the amount of cobalt detected by ICP-MS to the conversion for a run of 24 h.

Table 5.32 Relation between conversion and cobalt loading.

Zeolites	SiO_2/ Al_2O_3	Amount of cobalt (mg)	Conv (%)
None	-	0	0.39
1-Co-Mordenite	20	1.20	1.56
1-Co-ZSM-5	23	1.17	1.12
2-Co-ZSM-5	23	1.35	2.20
1-Co-ZSM-5	30	1.00	1.08
2-Co-ZSM-5	30	1.13	1.60
1-Co-ZSM-5	80	0.43	0.87
1-Co-Y	80	0.35	0.73
1-Co-ZSM-5	280	0.11	0.42

From the **Table 5.32,** it is easy to conclude that the amount of cobalt is relevant for the performance of the catalyst. More cobalt loaded gives a higher conversion for the same runtime.

5.4.3. Increase the mass of catalyst.

The work by Iglesia [23] for *n*-hexane showed a difference in selectivity when a large amount of Mn-ZSM-5 (1g) is loaded for a short period of time at low conversions. As a check of the autoxidation mechanism versus heterogeneous catalytic mechanisms, reactions were carried out in a similar way using the 1-Co-ZSM-5 with *n*-decane. Different amount of catalysts (0.05g, 0.5g and 1g) were tested. During the ion exchanged process, cobalt can go on the surface of the zeolites or inside the channels. **Chapter 3** has shows that *n*-decane and oxygen can react together via autoxidation which give a low terminal selectivity. Cobalt on the

surface of the catalyst can catalyse the decomposition of the ROOH species from the autoxidation, which results in a poor terminal selectivity. These two mechanisms, autoxidation and decomposition of ROOH by cobalt on the surface of the catalyst can hide or dilute a third mechanism, which is the activity of the cobalt inside the channel, which should be regioselective. Increasing the mass of catalyst increased the numbers of channels available and may help to perform the third mechanism inside the pores which would be expected to increase the terminal selectivity .

Table 5.33 Conversion and product profile with different masses of 1-Co-ZSM-5.

1-Co-ZSM-5	Conv. (%)	5/4 one	3 one	2 one	5/4 ol	3 ol	2 ol	1 ol	C_5 acid	C_6 acid	C_7 acid	C_8 acid	C_9 acid	C_{10} Acid
Blank	0.39	32.2	21.3	22.2	2.6	3.7	2.1	1.1	4.1	4.4	3.4	5.3	0	1.9
1g	2.56	21.8	14.4	15.3	10.4	6.4	8.9	1.5	7.2	5.2	4.2	2.3	2.7	1.4
0.5g	1.36	19.3	16.3	15.3	8.6	6.6	9.6	1.4	7.3	4.3	8.3	1.3	1.5	1.5
0.05g	1.1	21.3	13.3	15.1	9.6	6.5	9.5	1.3	6.3	5.5	8.5	1.3	1.4	2.4

Reactions conditions: 1-Co-ZSM-5 (SiO_2/ Al_2O_3=23) 24h, 100°C, 600 rpm, 15 bar O_2, *n*-decane (10g).

Different masses of catalyst (1-Co-ZSM-5(SiO_2/ Al_2O_3=23)) have been investigated. The selectivity of 1-decanol did not change. Increasing the amount of catalyst by a factor of 20 increased the conversion from 1.1 % to 2.56 %.

5.4.4. Use of PS-Tempo as radical scavenger with catalyst.

Acid zeolites promote an ionic decomposition of the ROOH which prevents the generation of radicals and avoid the autoxidation mechanism. The use of a different radical scavenger such as PS-tempo allows the determination of whether the reaction with Co-zeolites proceeds via a radical mechanism. If there is no conversion with the use of a radical scavenger the

mechanism of the reaction is a radical mechanism with Co-zeolites [24]. The target of this test is to scavenge the autoxidation, which as has already be demonstrated in **Chapter 3** proceeds via a radical mechanism and also to scavenge the radical reaction performed by the cobalt on the surface of the zeolites. So only the reaction inside the channels of the zeolites will be detected and may show a higher terminal selectivity.

Table 5.34 Activity of 1-Co-ZSM-5 (SiO_2/Al_2O_3=23) with radical scavenger.

Temperature	Mass used of PS-Tempo (mg)	Conversion (%)
100°C	50	0
110°C	50	0
120°C	50	0
130°C	50	0

Reactions conditions: Radical scavenger (0.50mg), 1-Co-ZSM-5 (0.05g), 100°C, 600 rpm, 15 bar O_2, decane (10g), 24 hours.

The addition of a radical scavenger inhibits the reaction which indicates that the reaction proceeds via a radical mechanism. The size PS-tempo is large (described in Chapter 3) meaning it is unable to penetrate the pores of the zeolites. This must mean the reaction being scavenged, either occurs on the external sites of the zeolite, or in the liquid phase.

5.4.5. Use of both zeolites as catalyst.

The target of this reaction is to use an acid zeolites H-ZSM-5 (SiO_2/ Al_2O_3=23) to inhibit the autoxidation in the liquid phase and to promote the activity of 1-Co-ZSM-5 as a heterogeneous catalyst to see if there is any difference in the product distribution profile.

Table 5.35 Activity of the combination of H-ZSM-5 with 1-Co-ZSM-5.

Mass H-ZSM-5	Conv. (%)	5/4 one	3 one	2 one	5/4 ol	3 ol	2 ol	1 ol	C_5 acid	C_6 acid	C_7 acid	C_8 acid	C_9 acid	C_{10} Acid
0	1.12	21.2	13.2	15.6	10.7	6.2	9.1	1.3	6.2	5.2	8.3	1.3	1.2	2.1
0.05g	0.12	31.6	22.3	17.5	8.3	6.1	8.5	0	12.1	6.2	0	0	0	0
0.1g	0	-	-	-	-	-	-	-	-	-	-	-	-	-

Reactions conditions: 24h, 100°C, 600 rpm, 15 bar O_2, decane (10g), 1-Co-ZSM-5 (0.05g) and different mass of H-ZSM-5 (SiO_2/ Al_2O_3=80) were added at the beginning of the experiment.

Overall conversion is decreased from 1.12 % to 0.125% when H-ZSM-5 (0.05g) is added and terminal selectivity is not increased. Increasing the mass of proton zeolites to 0.1g stops the reaction.

5.4.6. Leaching test.

15 minutes was enough to observe the leaching for VMgO catalyst (see chapter 4). A leaching test has been carried out with 1-Co-mordenite (SiO_2/Al_2O_3=20). The removal of the catalyst was by hot filtration [25] after 15 min of reaction at 100°C, then the filtrate is put back the mixture for 23h45.

Table 5.36 Leaching test with 1-Co-mordenite (SiO_2/Al_2O_3=20).

1-Co-mordenite	Conv. (%)	5/4 one	3 one	2 one	5/4 Ol	3 ol	2 ol	1 ol	C_5 acid	C_6 acid	C_7 acid	C_8 acid	C_9 acid	C_{10} acid
Blank (24h)	0.39	32.2	21.3	22.2	2.6	3.7	2.1	1.1	4.1	4.4	3.4	5.3	0	1.9
Run 24 h	1.56	19.3	13.1	15.1	14.2	10.2	8.4	1.3	7.2	2.3	2.4	7.3	1.3	1.2
15 min Filtration	0	-	-	-	-	-	-	-	-	-	-	-	-	-
23h45 Filtrate	0.27	31.2	21.1	15.3	6.3	3.3	5.6	1.7	8.7	3.3	3.2	1.2	-	-

Reactions conditions: 100°C, 600 rpm, 15 bar O_2, decane (10g)

The conversion after the filtration is 0.27%, which is below the conversion of the autoxidation (blank), which has a conversion of 0.39%. Co-zeolites prepared by solid state solid ion exchange with long washing at the end of the preparation prevents the leaching of cobalt from the catalyst when exposed to the solution for 15 minutes. 15 minutes is perhaps too short for cobalt to leach into the solution, so another test has been performed after 8 hours of reactions using the same procedure with another catalyst (1-Co-ZSM-5 SiO_2/ Al_2O_3(=23)).

Table 5.37 leaching test with 1-Co-ZSM-5 (SiO_2/Al_2O_3=23).

Co-ZSM-5	Conv. (%)	5/4 one	3 one	2 one	5/4 Ol	3 ol	2 ol	1 ol	C_5 acid	C_6 acid	C_7 acid	C_8 acid	C_9 acid	C_{10} Acid
Blank (24h)	0.39	32.2	21.3	22.2	2.6	3.7	2.1	1.1	4.1	4.4	3.4	5.3	0	1.9
Run 24h	1.12	21.2	14.1	15.2	11.4	6.4	10.2	1.1	8.2	5.9	6.4	1.4	1.3	1.3
8h Filtration	0.08	35.5	14.5	12.6	14.4	12.2	8.3	0	5.3	0	0	0	0	0
16h Filtrate	0.12	23.3	19.2	24.2	12.5	8.6	6.1	1.1	6.8	0	0	0	0	0

Reactions conditions: 100°C, 600 rpm, 15 bar O_2, *n*-decane (10g)

When the 1-Co-ZSM-5 catalyst is removed from the autoclave after 8 hours, the conversion of the filtrate after 16 hours is still below the maximum conversion (0.39%) observed for the autoxidation using these conditions. So it can be concluded that Co from 1-Co-ZSM-5 does not leach into the solution. Both tests after 15 minutes and 8 hours have showed that the catalysts do not leach in the solution.

5.5. Discussion.

Catalysts have been characterised by XRD, BET, TGA, ICP-MS and XPS. Firstly, the XRD of the different catalysts have showed only reflections of the framework of the zeolites. No additional reflections, no shifting of the reflections and no cobalt cluster has been observed for the different loading. Only a decrease of the intensity of the reflections is observed when

cobalt is loaded or passivation of the external surface is performed. Different reasons can induce the lowering of the XRD reflections.

- The presence of cobalt inside the pores induces a local distortion of the zeolites surface [26].
- Cobalt on the zeolites surface.
- The evolution of HCl during the preparation can also affect the structure. [6]

The distortion of the lattice when cobalt is loaded in the pores can be responsible for the decrease in crystallinity and can explain the results in **Figure 5.8 and 5.11**. When the amount of cobalt loaded is increased, the crystallinity decreases for the different zeolites. More cobalt in the pores and more distortion of the lattice means a decrease in crystallinity. After passivation, a larger amount of cobalt is loaded inside the channel and can explain the difference of crystallinity between silanated (% crystallinity =60%) and unsilanated (% crystallinity=80%) for the same 1-Co/Al ratio. Passivation of the external surface of the zeolites produces an amorphous silica layer, which can also be responsible for the decrease in the crystallinity measured by XRD.

Cobalt on the zeolite surface can also decrease the intensity of reflections. Cobalt has been detected in high amounts (1-Co/Al detected) on the surface by XPS analysis. Passivation of the external surface prevents the cobalt from anchoring on the zeolites surface but XPS has showed that a small amount of cobalt is present after silanation. The amount of cobalt detected by XPS is lower for a silanated zeolite (Co/Al=0.3) than an unsilanated (Co/Al=1) zeolite for the same amount of Co/Al loaded.

The evolution of HCl during the preparation can lead to the alteration of the zeolites' structure and lead to a lower crystallinity. The more $CoCl_2.6H_20$ is loaded the more HCl is generated

during the calcination step, which lead to more dealumination and can also explain the loss of crystallinity when cobalt loading is increased. Lowering the heating ramp, which slows down the evolution of HCl gas, which can then be flushed away more easily by the flow of nitrogen used during the calcination steps did not improve the crystallinity of the sample.

The BET and micropore volume analyses showed that the surface area of the catalyst and the micropore volume are dependent on the amount of cobalt loaded in the zeolites. The more cobalt that is loaded, the more the pore volume is decreased gradually. Some pore blocking has occurred due to cobalt species either dispersed in the channel or deposited at the outer surface of the zeolite, leading to the observed surface area and porous volume decrease [27]. It can be concluded that the distribution of cobalt in the zeolites is on the surface of the zeolites (XPS results) and inside the channels of the zeolites (decrease of the pore volume). The most important secondary effect of passivation of the external surface of zeolites is to promote the shape-selective reactions is narrowing or blocking entrances of the pores [28-31] and can explain the decrease of pore volume after silanation.

The data from XPS analysis showed that cobalt was not detected and may due to a very high dispersion for the low Co/Al loading however the cobalt was detected by ICP-MS meaning that the cobalt goes inside the channel. Higher Co/Al ratios show a large amount of cobalt on the surface. XPS also demonstrated that silanation does not prevent the cobalt from anchoring on the surface.

Thomas [4] has reported very high terminal selectivity with Co-AlPO-18 and Mn- AlPO-18 but one of the major disadvantages of these catalysts is the leaching of the metal by polar products. The different leach tests have showed that the leaching of the metal from the

zeolites is not responsible for the conversion, which is an interesting point for a catalyst in liquid phase.

Different mechanisms can occur during the reaction, which make the study very difficult. The first one is the autoxidation, which is the reaction between *n*-decane and oxygen without catalyst [32] (see **Chapter 3**).

Initiation: $I \rightarrow R^*$

Propagation: $R^* + O_2 \rightarrow RO_2^*$

$RO_2^* + HR \rightarrow ROOH + R^*$

The first products made from this mechanism are the hydroperoxide species (ROOH), which can take part in different mechanisms.

The first possible mechanism is the reaction of the acid sites of the zeolites with hydroperoxide. Acid sites will cause an ionic decomposition of the ROOH [33]. This mechanism avoids the propagation of the radical in the solution, which is responsible for the conversion.

Acid decomposition $ROOH \rightarrow RO^+ + OH^-$

The autoxidation is an undesired radical reaction with poor terminal selectivity, so proton zeolites can scavenge this reaction, which is an advantage. Silanated zeolites decrease the number of acid sites, but still enough acid sites can scavenge the autoxidation reaction after silanation.

Metalic ions can have a dual function. Metal can promote the hydroperoxide decomposition or can initiate the autoxidation. Cobalt catalysts have been proposed to act via Haber-Weiss

mechanisms in liquid phase [34 -35]. This mechanism involves a free radical mechanism for the hydroperoxide decomposition.

Initiation:

$$Co^{2+} + ROOH \rightarrow Co^{3+} + RO^{*} + OH^{-}$$

$$Co^{3+} + ROOH \rightarrow Co^{2+} + ROO^{*} + H^{+}$$

Propagation :

$$RO^{*} + RH \rightarrow ROH + R^{*}$$

$$R^{*} + O_2 \rightarrow ROO^{*}$$

$$ROO^{*} + RH \rightarrow ROOH + R^{*}$$

This mechanism can be applied to the cobalt on the surface of the zeolites (no spatial constraint on zeolites surface). In this mechanism above there is no direct docking of the alkane with the oxidation centre. Cobalt induces an unselective radical mechanism by homolytic decomposition of the hydroperoxide. Homolytic decomposition gives radicals, which can react further on the alkane chain and can explain the difference of conversion for the different loadings of cobalt. The use a radical scavenger can stop this radical mechanism. In the absence of steric constraint it will be easier to remove a proton from a CH_2 than CH_3 and explain the low terminal selectivity of this mechanism. External sites are easily accessed by reactants and are not protected against undesired side reactions by the shape-selective environment within zeolite channels [36-38]. This mechanism, which is independent of the different shape and size zeolites channels, can explain the different results obtained for 8 h, 16 h and 24 h runs for the different Co-zeolites. The more cobalt on the surface, the higher is the conversion of *n*-decane for the same runtime. This mechanism increases the rate of ROOH decomposition compared to the autoxidation and explains the higher conversion with the

same runtime. The silanation decreases the amount of cobalt on the surface (XPS results) and a lower conversion is observed than the unsilanated sample for the same runtime, which confirm the activity of cobalt on the surface of the catalyst. With zeolites wich have a low loading of cobalt, there is no conversion. ICP-MS results have showed that cobalt is present in the catalyst and XPS results have showed that no cobalt is present in the surface of the catalyst. That can be explained by the protons available on the surface which scavenge the formation of radicals and so no reaction occurs inside the channel with cobalt.

Metal can also react directly with alkane to form radical species [38].

$$RH + M^{(n+1)+} \rightarrow M^{n+} + R^{\bullet} + H^{+}$$

This step will be followed by oxygen insertion to give ROOH species (see mechanism in **Chapter 3**). In the third case, ROOH formation on the external Co-zeolite channels (reaction 6) lead to nonselective oxygen insertion along the alkane chain. This mechanism can be responsible for the initiation of the autoxidation by cobalt on the zeolite surface, which is an unselective mechanism. The metal on the surface of the zeolites is only involved in the initiation and can explain the results in table 5.19 where the initiation period is shorter with Co-zeolites than the autoxidation.

Another mechanism is proposed by Iglesia [3] for the decomposition of ROOH in the zeolite channels. In this mechanism, an oxidation centre inside the channels can induce terminal selectivity. The key point of this mechanism described below is the direct bonding of the linear alkanes to the metal (step II, **Figure 5.18**), which can induce terminal selectivity.

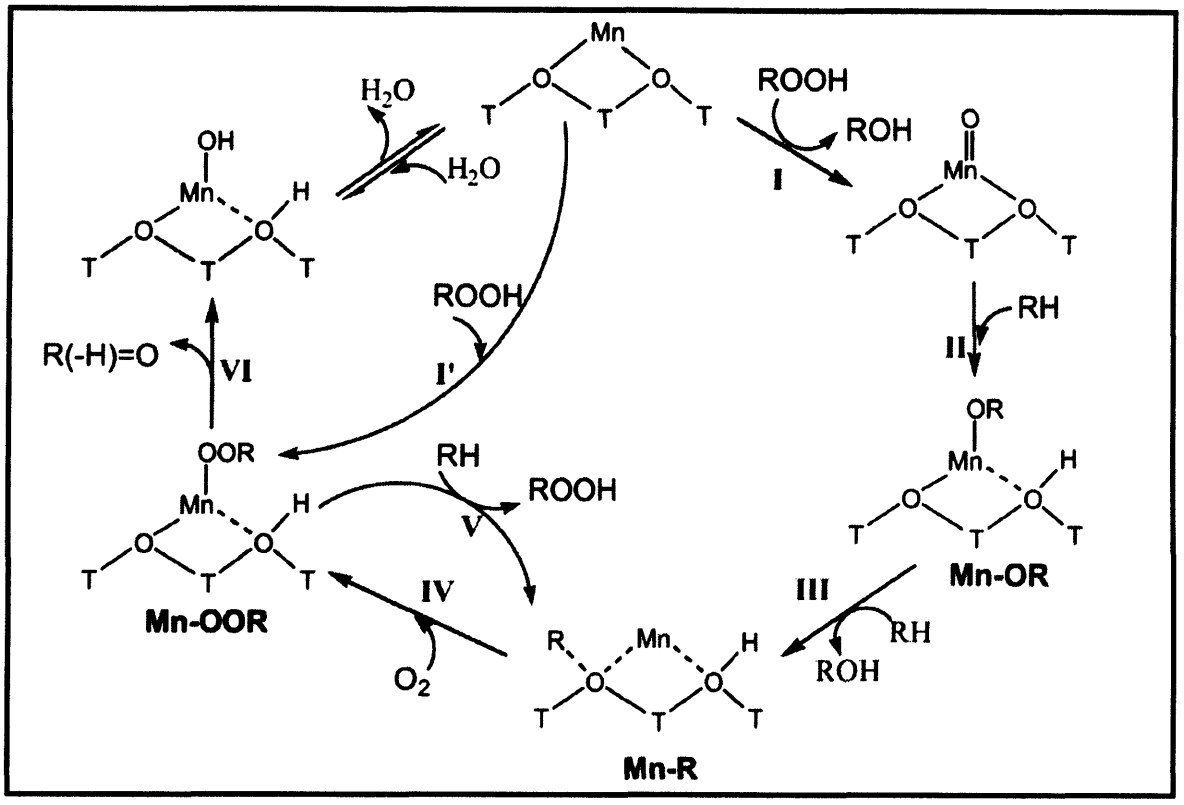

Figure 5.18 Proposed mechanism for ROOH decomposition mechanism on zeolites-confined Mn sites [3].

In Figure **5.19**, ROOH is the hydroperoxide, ROH is hexanol, R-(-H)=O is hexanone or hexanal and Mn-OOR, Mn-OR and Mn-R are Mn-bound reactive intermediates. In this mechanism, oxygen insertion can be influenced by spatial constraints that orient alkanes via step II, III, and V. This mechanism explains the high terminal selectivity found by Iglesia [3].

The experiments with PS-tempo were carried out to try and promote this mechanism. PS-tempo is a bulky radical scavenger which can stop the autoxidation and can also stop the radical mechanism of cobalt on the surface of the zeolites and just allow the reaction inside the channel. This reaction gave no conversion which suggests that no heterogeneous reaction occurs in the pores of the Co-zeolites and explains the lack of regioselectivity in the product profile. Increasing the mass of catalyst to prevent the dilution of any prevalent effects of spatial constraints on regioselectivity did not show better terminal selectivity. Spatial

constraints did not lead to any preference for terminal oxidation with *n*-decane with all the different zeolites tested with different loading of cobalt.

5.6. Conclusion.

Based on the results described above, the following main conclusions can be drawn. During the preparation, cobalt can be anchored randomly onto the surface sites or in the pores. The low loading of cobalt does not have enough cobalt to promote the reaction with ROOH species and a lot of acid sites are still available in the zeolites to scavenge the autoxidation and explain the lack of conversion. However, higher cobalt loadings have enough cobalt to catalyse the reaction. Passivation does not completely prevent cobalt from anchoring on the surface of the zeolites and also narrowing the pore size. The attempt to come in the spatial constraint of zeolites with an oxidation centre did not help to improve the terminal selectivity of the reaction. Different loading of oxidation centre and silanation of the zeolites did show a difference of terminal selectivity for the oxidation of *n*-decane in liquid phase. A similar product distribution is observed for the autoxidation (**Chapter 3**) and VMgO (**Chapter 4**). Conversion was proportional to amount of cobalt loaded in the zeolites, suggesting that the relevant step involves decomposition of hydroperoxides on cobalt redox sites on the zeolites surface.

5.7. References.

[1] A. Corma, Chemical Reviews, 95, (1995), 559.

[2] R. Szostak, Molecular Sieves: Principles of Synthesis and Identification, Van Nostrand Reinhold, New York, (1989).

[3] B. Zhan, B. Modén, J. Dakka, J.G. Santiesteban, E. Iglesia, Journal of Catalysis 245, (2007), 316.

[4] J.M.Thomas, R. Raja, G. Sankar, R.G. Bell, Nature, (1999), 227.

[5] Handbook of Zeolites Sciences and Technology, S.M. Auerbach, K.A. Carrado, P.K. Dutta, New York, (2003).

[6] H.G. Karge, Studies in Surface Science and Catalysis, 5, (1997), 1901.

[7] F.M. Bobonich, Theoretical and Experimental Chemistry 36, (2000), 117.

[8] P. Sazama , J. Dedecek , V. Gábová, B. Wichterlová, G. Spotob, S. Bordiga, Journal of Catalysis 254, (2008), 180.

[9] H.S. Lacheen, E. Iglesia, Journal Physical Chemistry B, 110, (2006), 5462.

[10] W. Ding, G.D. Meitzner, E. Iglesia, Journal of Catalysis 206, (2002), 14.

[11] D.J. Kim, H.S. Chung, Applied Clay Science 24, (2003), 69.

[12] T.A.J. Hardenberg, L. Mertens, P. Mesman, H.C. Muller, C.P. Nicolaides, Zeolites, 12, (1992), 685.

[13] S.E. Axon, J. Klinowski, Applied Catalysis 56, (1989), L9.

[14] E.L. Wu, S.L. Lawton, D.H. Olson, A.C. Rohrman, G.T. Kokotailo, Journal of Physical Chemistry, 83 , (1979), 2777.

[15] X. Wang, H. Chen, W.M.H. Sachtler, Applied Catalysis B: Environmental 26, (2000), 227.

[16] H.K. beyer, H.G. Karge, G. Boebely, Zeolites 8, (1998), 79.

[17] I.W.C.E. Arends, R.A. Sheldon, M. Wallau, U. Schuchardt, Angewandte Chemie International Edition, 36, (1997), 1114.

[18] Handbook of Zeolites Sciences and Technology, S.M. Auerbach, K A. Carrado, Prabir K. Dutta, (2003).

[19] M. Mhamdi, S. Khaddar-Zine, A. Ghorbel, Reaction Kinetics and Catalysis Letters, 88, (2006), 149.

[20] W. Schmidt, Max-Planck-Institut für Kohlenforschung, (2008).

[21] S. Wuyts, K. De Temmerman, D.E. De Vos, P.A. Jacobs, Chemical European Journal 11, (2005), 386.

[22] N. Katada, M. Niwa, Catalysis Surveys from Asia 8, (2004), 161.

[23] B. Zhan, B. Modén , J. Dakka , J.G. Santiesteban, E. Iglesia, Journal of Catalysis 245, (2007), 316.

[24] A.L.J. Beckwith, V. W. Bowry, K.U. Ingold, Journal of American Chemistry Society 1, 114, (1992), 4983.

[25] R.A. Sheldon, M. Wallau, I.C.E. Arends, U. Schuchardt, Accounts of Chemical Research, 31, (1998), 485.

[26] K. Pierloot, A. Delabie, and C. Ribbing Journal of Physical Chemistry B, 102, (1998), 1789.

[27] M. Mhamdi, S. Khaddar-Zine, A. Ghorbel, Reaction Kinetics and Catalysis Letters 88, (2006), 149.

[28] C.T. O'Connor, K.P. Möller and H. Manstein, KONA 25, (2007), 230.

[29] F. Bauer , W.H. Chenb, E. Bilz , A. Freyer , V. Sauerlandc, S.B. Liub,Journal of Catalysis 251, (2007), 258.

[30] C.T. O'Connor, K.P. Möller, H. Manstein, Journal of Molecular Catalysis A: Chemical, 181, (2002), 15.

[31] E. Klemm, M. Seitz, H. Scheidat, G. Emig, Journal Catalysis, 173, (1998), 177.

[32] N. Kuprowicz, J. S. Ervin, S. Zabarnick, Fuel 83, (2004), 1795.

[33] C.E. Frank, Chemical Review 46, (1950), 155.

[34] R.A. Sheldon, J.K. Kochi, Metal-Catalyzed Oxidations of Organic Compounds, Academic Press, New York, 1981.

[35] C.L. Hill, Activation and Functionalization of Alkanes, Wiley, NewYork, 1989.

[36] Y.S. Bhat, J. Das, K.V. Rao, A.B. Halgeri, Journal of Catalysis 159, (1996), 368.

[37] T. Kunieda, J.H. Kim, M. Niwa, Journal of Catalysis 188, (1999), 431.

[38] K.U. Ingold, Inhibition of the Autoxidation of Organic Substances in the Liquid Phase, Chemical Reviews, 61, (1961), 563.

Chapter Six

n-hexane oxidation

6.1. Introduction.

n-hexane (C_6H_{14}) with a boiling point of 69°C is the second linear alkane liquid at room temperature after *n*-pentane (boiling point 39°C). *n*-hexane is a shorter alkane than *n*-decane and it is easier to see the effect on the terminal selectivity of a catalyst with shorter chain (**Table 6.1**).

Table 6.1 Comparison between *n*-decane and *n*-hexane.

Alkanes	Number of CH_2	Number of CH_3	Ratio CH_3 / CH_2
n-hexane	4	2	1/2
n-decane	8	2	1/4

The use of *n*-hexane will also allow the comparison to the best heterogeneous catalysts reported in the literature [1, 2] for oxidation of *n*-hexane in liquid phase.

6.2. Data of the best results in the literature.

Thomas [2-5] has reported the best results in the literature for the terminal oxidation of *n*-hexane in the liquid phase. Iglesia [6] tried to reproduce Thomas`s data with the same catalyst for the oxidation of *n*-hexane. The comparison of the results from these two studies are reported in **Table 6.2**.

Table 6.2 Thomas's and Iglesia's results with AlPO catalyst.

Author	Temperature (°C)	Catalyst	Conversion (%)	Total Terminal Selectivity (%)
Thomas	100	Co-AlPO-5	2.4	8.6
		Co-AlPO-18	7.2	61.3
		Mn-AlPO-18	8.7	65.5
Iglesia	100	Mn-AlPO-5 & Mn-AlPO-18	0.02-0.05	7
Iglesia	130	Mn-AlPO-5	0.5	4.1
		Mn-AlPO-18	1.4	3.76

n-Hexane conversions (0.02-0.05% at 100°C) measured by Iglesia [6] on MnAlPO-5 and MnAlPO-18 were 100 times smaller than reported previously on MnAlPO-18 (7.2%) by Thomas [2]. The terminal selectivity measured by Iglesia [6] is 10 times smaller than the terminal selectivity measured by Thomas. Increasing the temperature to 130°C increased a little bit the conversion but decreases the terminal selectivity from 7% to 4.1% or 3.76 %.

The next best results for the terminal oxidation of *n*-hexane in liquid phase has been reported by Iglesia [1].

Table 6.3 Details of Iglesia conversion and selectivity.

Time (hours)	Conversion (%)	Terminal selectivity (%) with Mn-ZSM-5	Terminal selectivity (%) Autoxidation
0.5	0.005-0.007	24	7
2.5	0.013	18.5	8
4	0.047	15	8
7	0.1	10	7

Table 6.3 demonstrates a clear difference in terminal selectivity when a catalyst (>20 %) is present in contrast with the autoxidation reaction (8 %) at similar conversions. In the case of a catalyst being present, the terminal selectivity is initially high, but this declines as the conversion increases (~10% terminal selectivity when conversion is 0.1 %).

6.3. Experimental conditions for each study.

Before moving on to compare these results to those obtained at Cardiff, **Table 6.4** it is helpful to explain the different reactors used, the different experimental conditions and the different methods of analysis used for each team.

Table 6.4 Comparison for the experimental conditions for each team.

Team	Thomas [2]	Iglesia [1]		Cardiff
Catalyst tested	AlPO-18	AlPO-18	ZSM-5	ZSM-5 & AlPO-18
Autoclave	high pressure stainless-steel catalytic reactor	high pressure glass reactor	high pressure glass reactor	high pressure stainless-steel catalytic reactor
Monitor the reaction	Small aliquots of the sample were removed	extracting a sample periodically (0.50 ml)	extracting a sample periodically (0.50 ml)	each point on the plot is one reaction
Pressure	Dry air was fed under pressure into the reaction vessel 15 bar ambient temperature	constant bar by adding O_2 periodically 5.5 bar ambient temperature	constant 5 bar by adding O_2 periodically 3 bar ambient temperature	Reactor pressurised with O_2 5 bar ambient temperature
Temperature (°C)	100-130°C	100-130°C	130°C	130°C
n-hexane	50 g (76 ml)	25 ml	25 ml	10 g (15 ml)
Stirring	400 rpm	-	-	600 rpm
Catalyst	0.5g	0.2g	1g	0.6g Zeolites 0.12g AlPO
GC column	BPX5 capillary column (25m, 0,32mm)	DB-wax column (60 m, 0.32 mm , 0.5 μm) Hewlett-Packard 5890)	DBWAX capillary column (60 m,0.25 mm,0.5 μm) Agilent J&W Scientific)	CP Wax 52CB, (25m, 0.53 mm, 2.0 μm) Chrompack
Liner	lined with poly ether ketone.	Glass reactor	Glass reactor	None or Glass liner
Internal standard	4.8 g dichlorobenzene	0.2 ml dichlorobenzene	0.20 ml Dichlorobenzene	0.150 ml trichlorobenzene

For Iglesia, The ratio of *n*-hexane (ml) over AlPO (g) is 125 and the ratio of *n*-hexane (ml) over ZSM-5 (g) is 25. Cardiff has kept the same volume ratio of *n*-hexane (ml)/ catalyst (mg) for the testing of the AlPO and zeolites. The second point to note is the way the hexanal selectivity is calculated by Iglesia [1]. Shown below (**Figure 6.1**), is a typical GC trace provided in the supplementary information [1]. As can be seen there are two overlapping peaks, these are 2-hexanone with a retention time of 42.32 and hexanal with a retention time of 42.45. The calculation for the production of hexanal is made by separating the peak tailing of the 2-hexanone as shown by the red lines (**Figure 6.1**, lines added by authors).

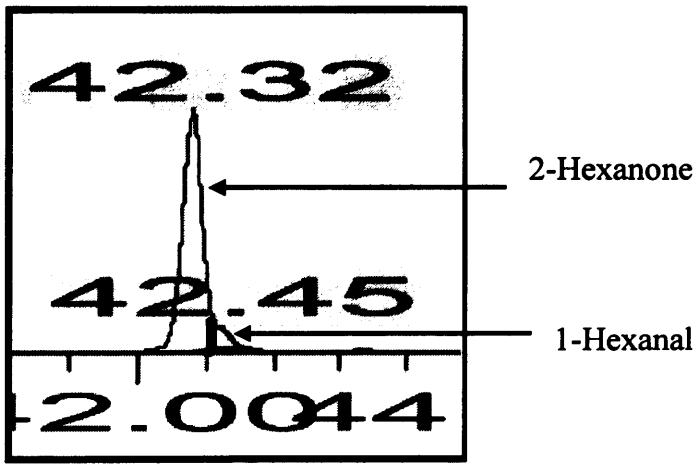

Figure 6.1 [1] Separation between 2-hexanone and hexanal on Iglesia GC trace

Only one peak is present in GC traces obtained at Cardiff for 2-hexanone and hexanal. Therefore, for the literature results the terminal selectivity refers to hexanal, hexanol and hexanoic acid, while at Cardiff terminal selectivity will be reported only for 1-hexanol and hexanoic acid. Importantly, when discussing his results Iglesia only reports terminal selectivity and does not give details about the contribution of 1-hexanal in his calculation. From the GC trace available, it was estimated at 10%.

6.4. Catalysts.

6.4.1 Introduction.

Kinetic diameter of *n*-hexane is 4.3 Å [7] and the spatial constraints imposed by AlPO and ZSM-5 catalysts were examined in **Figure 6.2**.

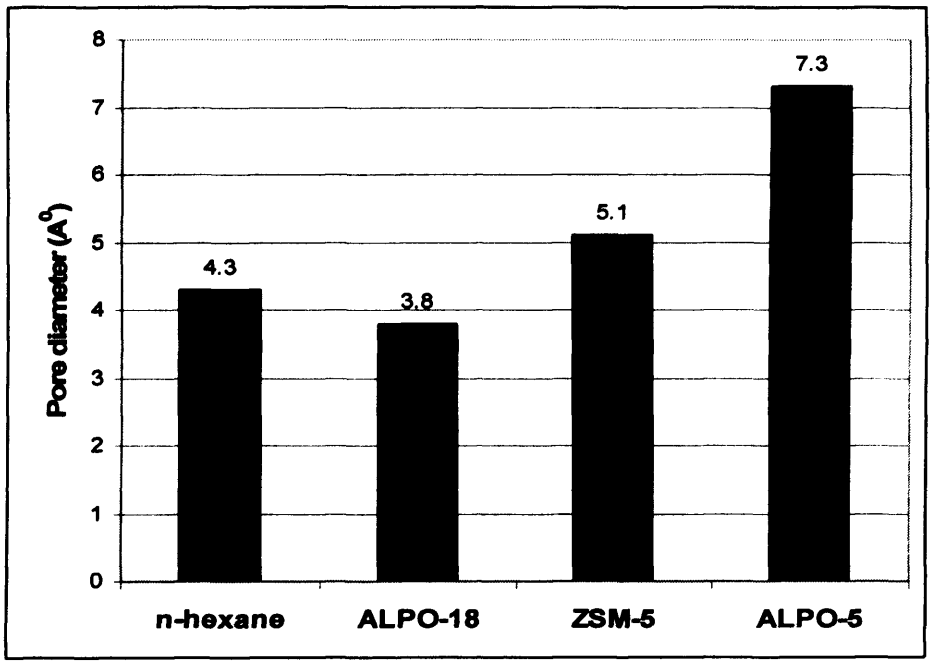

Figure 6.2 Comparison of the pore diameter of the catalyst to the diameter *n*-hexane.

Thomas [2] reports his best results for the oxidation of *n*-hexane in liquid phase with an AlPO-18, which has a pore size of 3.8 Å. Iglesia [6] referenced to Breck [7] showed that the kinetic diameter of *n*-hexane is 4.3 Å, *i.e.* larger than the pores within AlPO-18 window, which suggests than *n*-hexane can not enter the pore and suggests that steric control of *n*-hexane oxidation by AlPO-18 is not credible, however ZSM-5 and AlPO-5 are large enough to admit *n*-hexane inside their channels.

6.4.2. ZSM-5 catalysts.

6.4.2.1 Solid state ion exchanged

Three different loadings of cobalt have been incorporated in ZSM-5 (SiO_2/ Al_2O_3 mole ratio 23). Two low theoritical loadings of 0.1 Co/Al (ICP-MS 0.06 Co/Al) and 0.2 Co/Al (ICP-MS 0.11 Co/Al) similar to the Iglesia Theoritical loading 0.1 Mn/Al (ICP-MS 0.088) in ZSM-5 (SiO_2/ Al_2O_3 mole ratio 24). Higher theoritical loading with 1 Co/Al (ICP-MS 0.65) were also prepared and tested. These catalysts were already characterised and tested for the oxidation of *n*-decane in Chapter 5.

6.4.3. AlPO catalysts.

Co-AlPO-18, Mn-AlPO-18 and Co-AlPO-5 were synthesised by Michelle Gilhespy at Johnson Matthey [8], who was informed of the methodology by Gopinathan Sankar , an author on the Thomas publication [2]. These materials were also tested in Cardiff for the oxidation of *n*-hexane.

6.5. Autoxidation.

Before the catalysts were tested, it was decided to investigate the conversion and the terminal selectivity of autoxidation, which will be the baseline to compare the activity of the tested catalysts.

6.5.1. Results.

Thomas reported the performance of two aluminophosphates containing cobalt or manganese substituted into the framework, as regioselective catalysts for the oxidation of *n*-hexane, but did not report the results for the autoxidation in his paper [2]. For Iglesia [1], the autoxidation has a steady terminal selectivity of around 8 % throughout the conversion range tested.

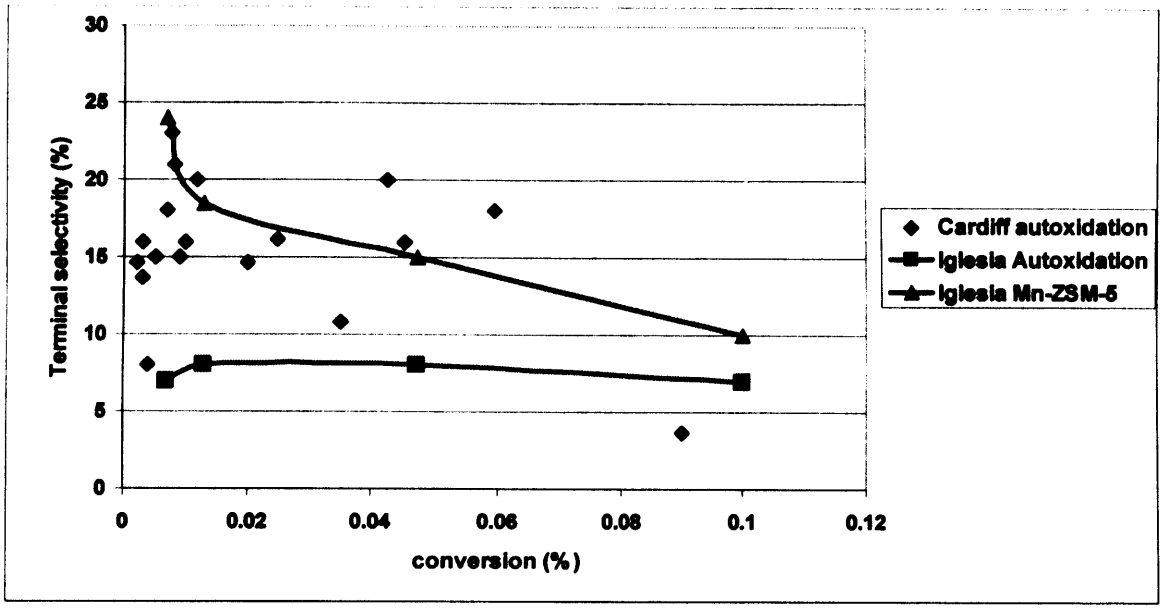

Figure 6.3 Comparison of Cardiff's autoxidation results with Iglesia results.

A higher terminal selectivity has been found for the autoxidation results at Cardiff compared to those presented by Iglesia [1]. Some of the points obtained in Cardiff autoxidation overlap with Iglesia's results with a catalyst. Some control experiments have been performed to examine possible effects of impurities by adding branched alkanes to *n*-hexane during autoxidation reactions. Basic calculations have been carried out to find out the amount of impurities present at the start of the reaction when 25 ml of *n*-hexane (the volume used by Iglesia) is used. This amount of impurity was compared to the amount of terminal products formed when a conversion of 0.007% is reached with a selectivity of 25 % (best results obtained by Iglesia for the oxidation of *n*-hexane).

n-Hexane purity (99%) from Fluka.

Volume used by Iglesia =25 ml, purity (%)= 99%

Density=0.6548 g/ml

Mass=0.6548g/ml*25ml=16.37g

Mass of impurity at the start= 16.37g* 0.01 = **164 mg of impurities at the beginning.**

Conversion 0.007 % & selectivity (25%) = **0.37 mg of Terminal products made**

From these simple calculations it is easy to see that terminal products made may come from the impurities present at the beginning of the reaction. Additions of further quantities of the impurities were added at the start of the reaction to see if the amount of terminal product detected could be increased. The same purity of *n*-hexane (99%) from the same supplier (Fluka) is being used in Cardiff as was used by Iglesia [1]. It should be noted that in his paper Iglesia makes no reference to extra purification. Fluka were emailed with regards to the 1% of impurities present, with the three major impurities present in the batch used by Cardiff being.

- 2-metyhylpentane (0.005%)

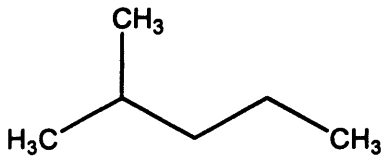

- 3-methylpentane (0.253%)

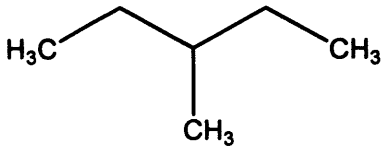

- Methylcyclopentane (0.294%)

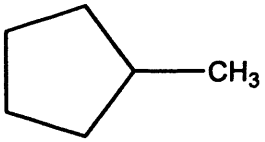

The total percentage of the impurity disclosed by Fluka is equal to 0.552 %, while the quoted total level of impurities is ≤1 %. Two other impurities, 1-hexene and 2-hexene, were also investigated as promotors for the autoxidation of *n*-hexane.

The first impurity tested was 3-methylpentane (**Figure 6.4**). Different masses were added at the beginning of the reaction to see the effect of this impurity on the terminal selectivity at low conversion (0.003 to 0.007). In each case the results are compared at 2 blank reactions (without impurity) performed with *n*-hexane from the same bottle.

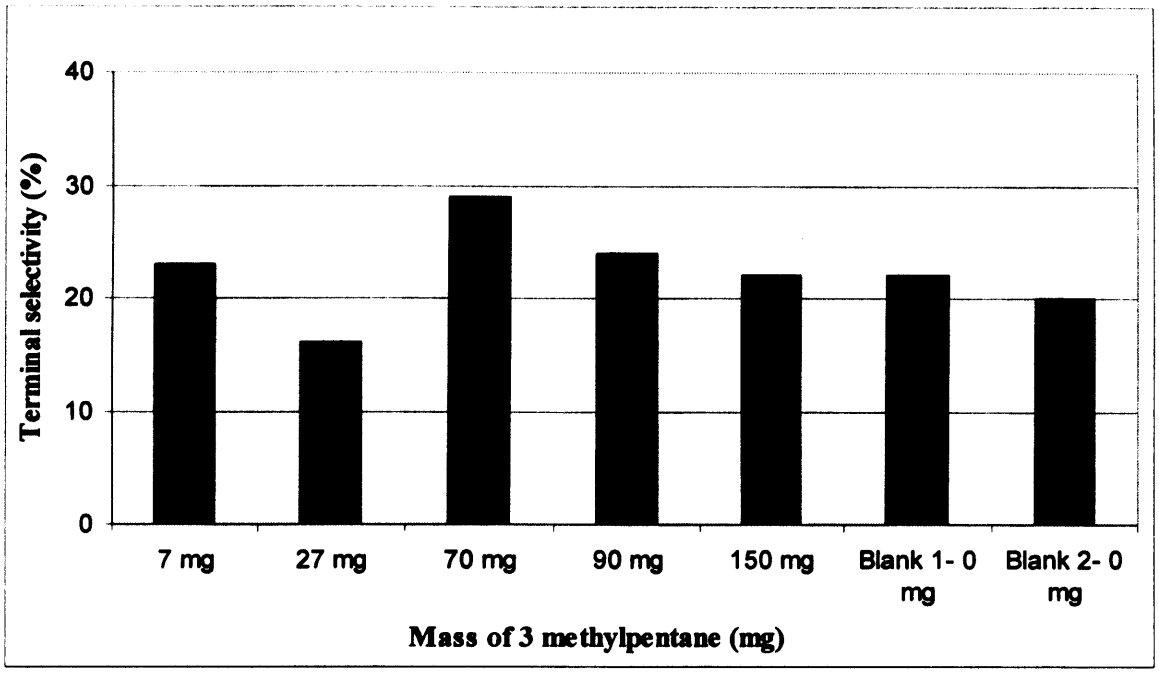

Figure 6.4 Terminal selectivity with different masses of 3-methylpentane.

Adding different masses of 3-methylpentane at the beginning of the reaction does not improve terminal selectivity. Very high terminal selectivity is still observed for the short runs with low conversion.

The same test has been carried out with methylcyclopentane (**Figure 6.5**) as impurity added at the beginning of the reaction.

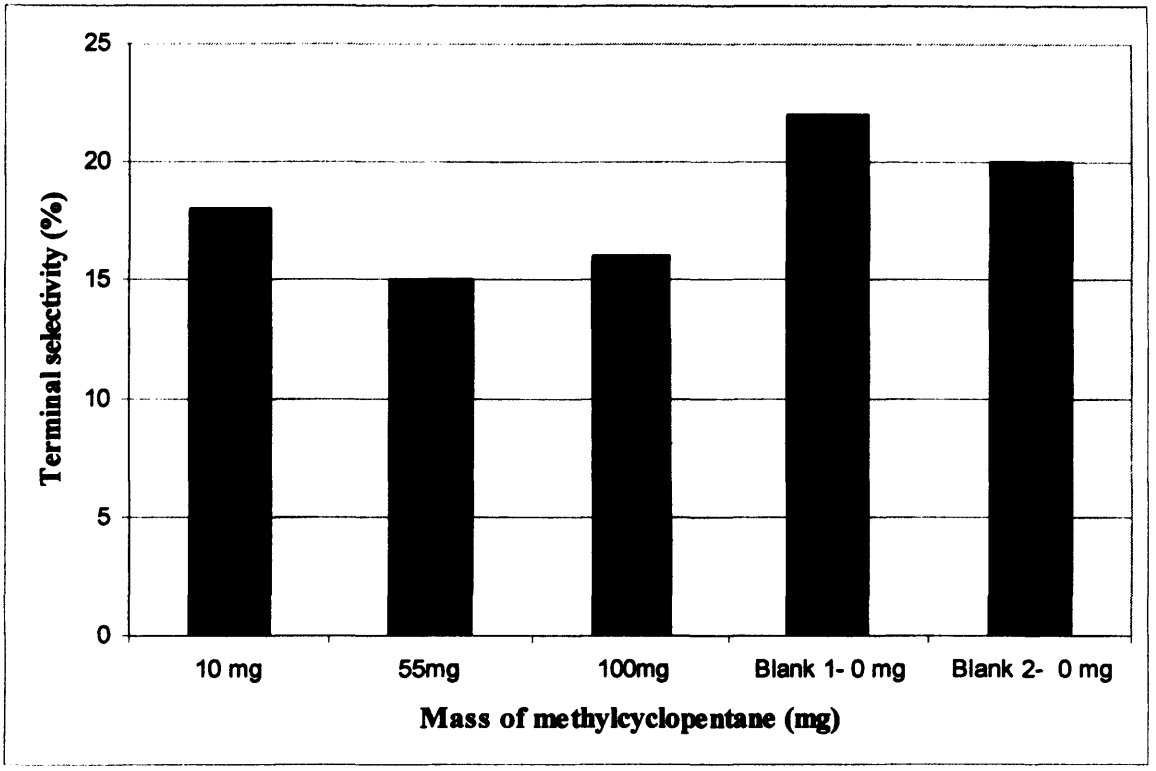

Figure 6.5 Terminal selectivity with different masses of methylcyclopentane.

Adding methylcyclopentane at the start of the reaction gives results very close to the blank reaction, with the terminal selectivity remaining very high at the short run times with low conversion (0.003 to 0.007).

2-methylcyclopentane as impurity was also added at the beginning of the reaction to investigate its effect on the terminal selectivity (**Figure 6.6**).

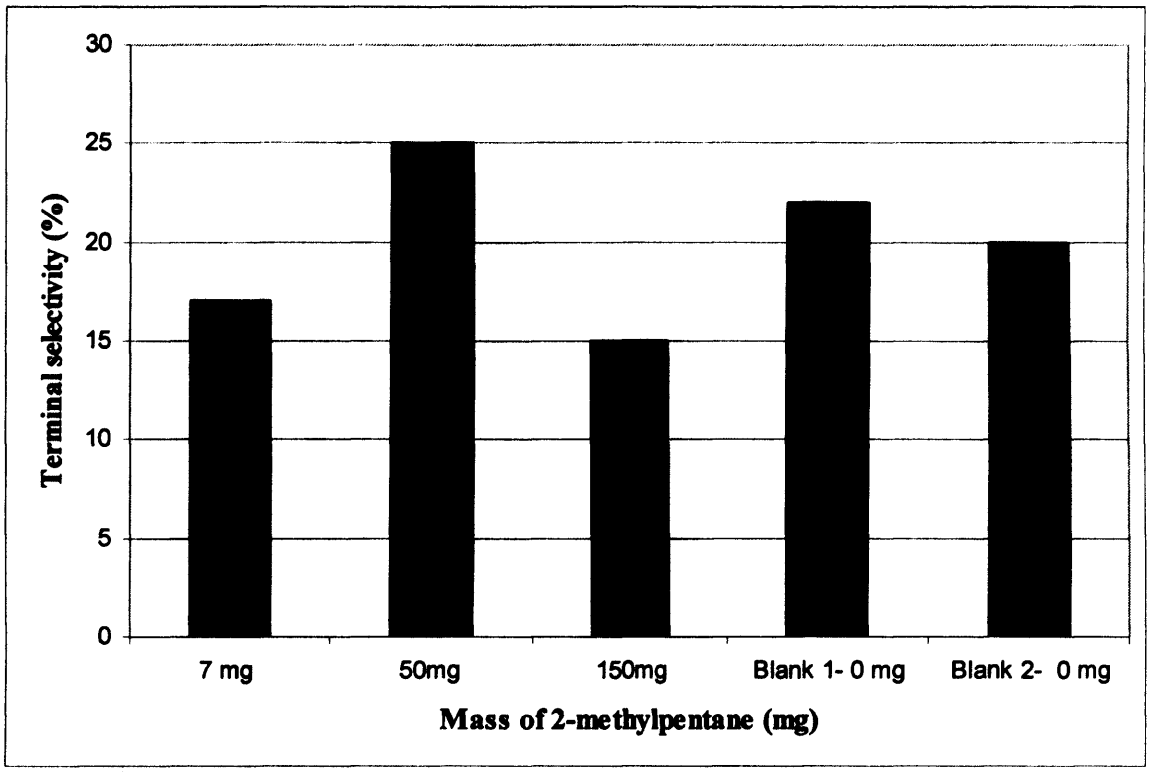

Figure 6.6 Terminal selectivity with different masses of 2-methylcyclopentane.

Addition of 2-methylpentane has no effect on the product distribution in a short reaction with low conversion

1-hexene and 2-hexene as impurities were also investigated (**Figure 6.7 and Figure 6.8**).

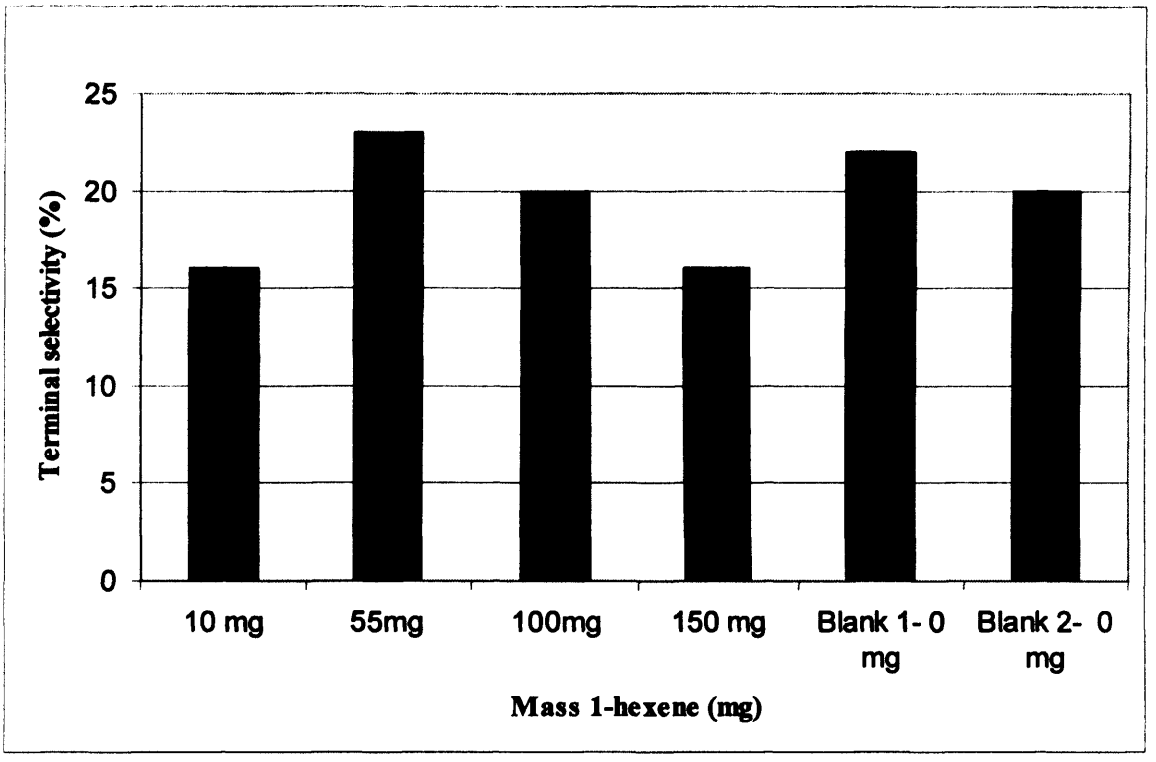

Figure 6.7 Terminal selectivity with different masses of 1-hexene.

Figure 6.8 Terminal selectivity with different masses of 2-hexene.

Adding an alkene does not improve the terminal selectivity.

Other tests have been carried out with a fresh bottle of *n*-hexane under a nitrogen atmosphere. The aim of this was to check if the terminal selectivity changes with the age of the reactants. Air and *n*-hexane may react together slowly to form impurities that have an effect on the autooxidation reaction.

Table 6.5 Terminal selectivity with fresh feed at low conversion.

Conversion (%)	Terminal selectivity (%)
0.005	21
0.007	21
0.005	17

High terminal selectivity is found with fresh feed. The evolution of the terminal selectivity after two of three months was not tested with this fresh bottle (end of my PhD).

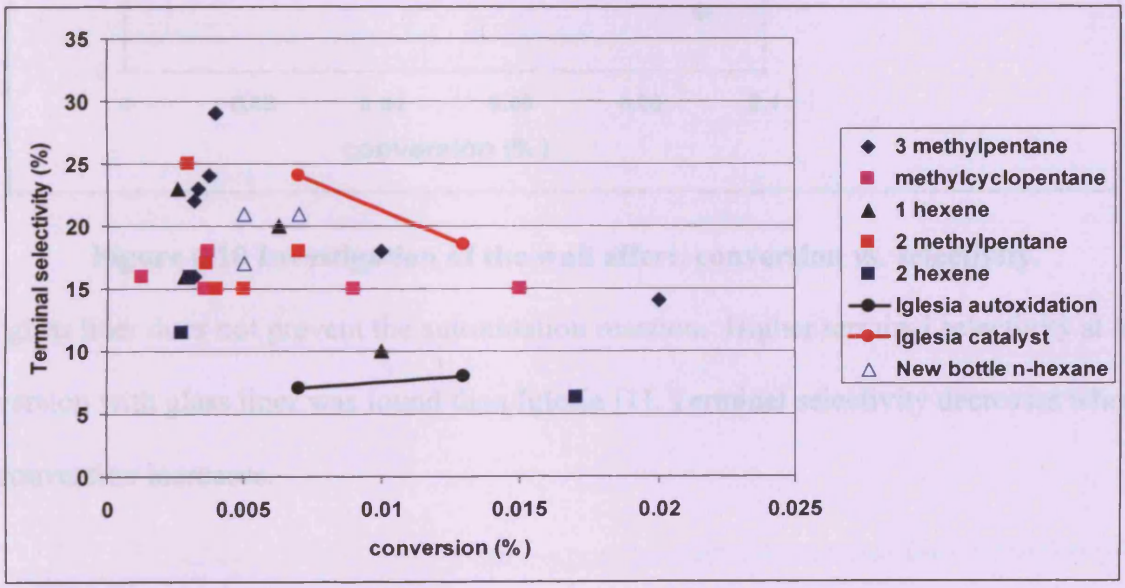

Figure 6.9 Summary of the results.

Adding an impurity at the beginning of the reaction does not improve significantly the terminal selectivity at low conversion. Terminal selectivity found at Cardiff is higher than the terminal selectivity found by Iglesia [1] for autoxidation. With an opened bottle, *n*-hexane and air can react together at room temperature and may give peroxide or other products, which may be responsible for the high terminal selectivity but high terminal selectivity was found

with a new bottle of n-hexane under nitrogen atmosphere meaning high terminal selectivity is not due to a slow reaction occurring between hexane and air over time.

The catalytic effect of the autoclave stainless steel walls were investigated by executing the same reaction with a glass liner.

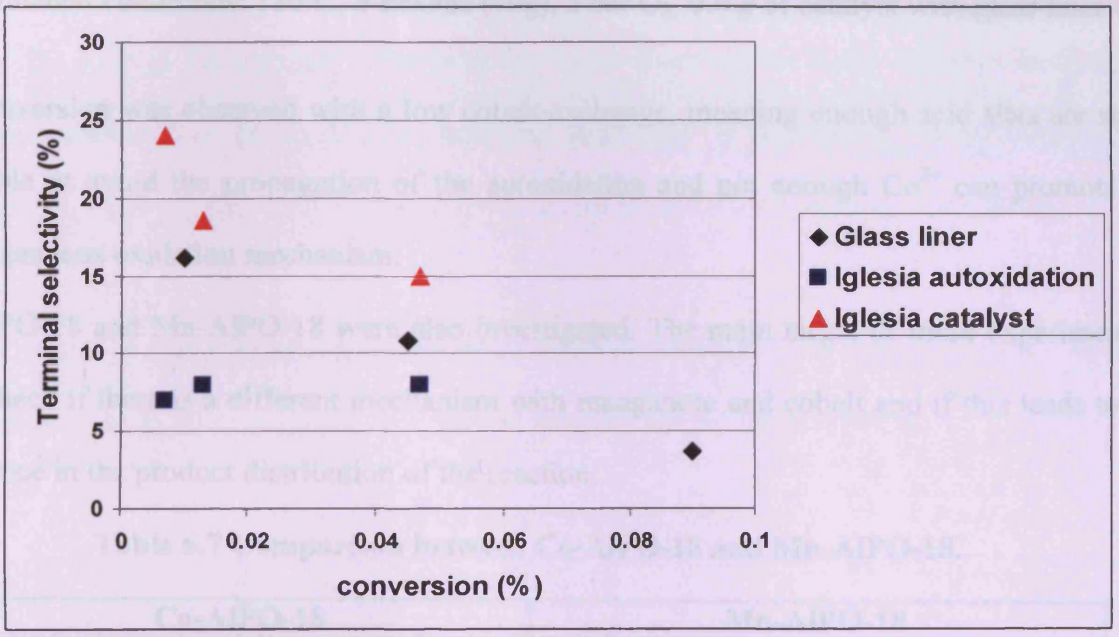

Figure 6.10 Investigation of the wall effect, conversion *vs.* selectivity.

The glass liner does not prevent the autoxidation reaction. Higher terminal selectivity at low conversion with glass liner was found than Iglesia [1]. Terminal selectivity decreases when the conversion increases.

6.6. Catalyst testing.

The ZSM-5 used by Iglesia [1] had a SiO_2/Al_2O_3 mole ratio of 24. The ZSM-5 used at Cardiff has SiO_2/ Al_2O_3 mole ratio of 23. Iglesia [1] shows his best results with a low theoretical loading of manganese (0.1 Mn/Al). Similar loading were prepared by solid state ion exchange with cobalt and tested.

Table 6.6 Conversion versus time for the low loading (Co-ZSM-5).

Co/Al	Time	Conversion (%)
0.1	1h	0
0.1	2h	0
0.1	3h	0
0.2	1h	0
0.2	2h	0
0.2	3h	0

Experimental conditions: 130°C, *n*-hexane (10g), 5 bar O_2, 0.6 g of catalyst with glass liner.

No conversion was observed with a low cobalt exchange, meaning enough acid sites are still available to avoid the propagation of the autoxidation and not enough Co^{2+} can promote a heterogeneous oxidation mechanism.

Co-AlPO-18 and Mn-AlPO-18 were also investigated. The main target of these experiments is to check if there is a different mechanism with manganese and cobalt and if this leads to a difference in the product distribution of the reaction.

Table 6.7 Comparison between Co-AlPO-18 and Mn-AlPO-18.

Co-AlPO-18		**Mn-AlPO-18**	
Conversion (%)	Terminal selectivity (%)	Conversion (%)	Terminal selectivity (%)
0.017	20	0.019	17
0.099	10	0.109	10
1.54	4	1.54	4

Similar terminal selectivity and total yields for the same runtime were observed for these catalysts. No difference between the chemistry of cobalt and manganese even at low conversion. Increasing the conversion decreases the terminal selectivity in both cases.

The target of these reactions was to investigate the influence of different porous supports were also investigated (Co-AlPO-5, Co-AlPO-18 and Co-ZSM-5) on the product distribution with the same redox cation (cobalt).

Table 6.8 Comparison between 1-Co-AlPO-5, Co-AlPO-18 and Co-ZSM-5.

Co-AlPO-5		Co-AlPO-18		1-Co-ZSM-5	
Total Yield (%)	Terminal selectivity (%)	Total Yield (%)	Terminal selectivity (%)	Total Yield (%)	Total Yield (%)
0.021	18	0.017	20	0.014	16
0.079	11	0.099	10	0.1	8
1.34	4.1	1.54	4	1.8	6

No difference in the terminal selectivity has been observed for these different catalysts for similar conversions. In each case, terminal selectivity is decreasing when conversion is increasing. The product distribution is not affected by spatial constraints of the pores.

All the data for autoxidation and activity of different catalysts have been plotted on the graph (**Figure 6.11**) to allow a simple comparison between the different systems.

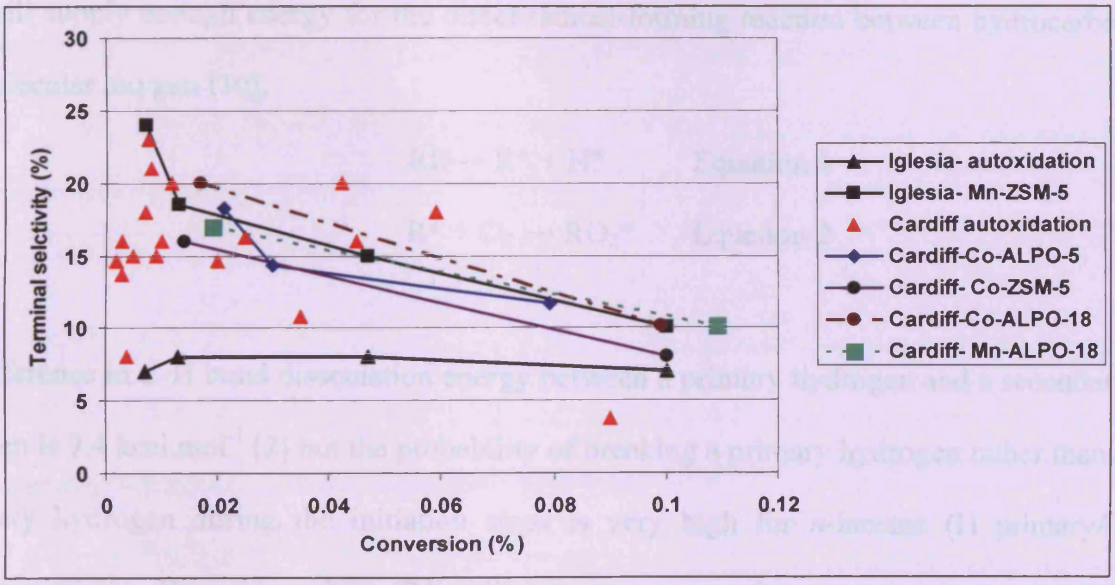

Figure 6.11 Conversion versus. Selectivity for a number of systems used in *n*-hexane oxidation

No improvement in the terminal selectivity was found for the oxidation of *n*-hexane with a catalyst over Cardiff autoxidation. The plot for Mn-zeolites, different AlPO and Cardiff

autoxidation are very similar for the terminal selectivity obtained. Iglesia autoxidation results are lower than the results obtained at Cardiff for the autoxidation reaction.

6.7. Discussion.

The chain length of *n*-hexane is shorter than *n*-decane. In *n*-hexane, 6 hydrogen atoms are primary and 8 are secondary compared to *n*-decane which also has 6 primary hydrogens but 16 secondary hydrogens. For *n*-hexane, the ratio primary/secondary hydrogen is 0.75 compared to *n*-decane, which is 0.37.

The initiation of liquid phase autoxidation of hydrocarbons proceeds via a free radical chain mechanism described in equation 1. The two main possible activating agents of the autoxidation are heat and impurities in the feed, which decompose to give radical species [9]. Heat will supply enough energy for the direct radical-forming reaction between hydrocarbon and molecular oxygen [10].

$$RH \rightarrow R^* + H^* \qquad \text{Equation 1}$$

$$R^* + O_2 \rightarrow RO_2^* \qquad \text{Equation 2}$$

The difference in C-H bond dissociation energy between a primary hydrogen and a secondary hydrogen is 9.4 kcal.mol^{-1} [2] but the probability of breaking a primary hydrogen rather than a secondary hydrogen during the initiation steps is very high for *n*-hexane (H primary/H secondary =0.75). Then this radical (R*) will insert oxygen to form primary hydroperoxide (ROOH) in a case of C-H primary bond is broken or a secondary hydroperoxide (ROOH) is formed in a case of C-H secondary bond is broken (more easily). Our results (**Figure 6.3**) for the autoxidation are related to the C-H bond energy dissociations with 75 % internal oxidation products (secondary carbon) and 25% terminal selectivity (primary carbon) at low conversion.

The test with the different masses of impurities and the glass liner did not influence the terminal selectivity at low conversion compared to the spread of results obtained at Cardiff for the autoxidation reaction.

The general sequences for the autoxidation reaction are initiation propagation and termination [9]

Initiation $RH \rightarrow R^* + H^*$

Propagation $R^* + O_2 \rightarrow RO_2^*$

$RO_2^* + RH \rightarrow RO_2H + R^*$

Termination $R^* + R^* \rightarrow RH + R(-H)$

$RO_2^* + OH^* \rightarrow ROH + O_2$

$R^* + R^* \rightarrow R\text{-}R$

From the mechanism above, it can be observed that the first stable products made from the autoxidation are the alcohols. Primary RO_2^*or ROOH will decompose to the primary alcohols. The second phase of the reaction is the hydroperoxide decomposition. Hydroperoxides can break down by thermal scission to give free radicals [9].

$$ROOH \rightarrow RO^* + {}^*OH$$

The thermal decomposition of hydroperoxide promotes the generation of radicals which will initiate further attack on the hydrocarbon. In the same time over oxidation will occur on the first oxygenated products formed. All these reactions occur in the same time and give a difficult product distribution when conversion increases. The further oxidation reactions will be described below.

The results with a catalyst at low conversion can be separated into two sections. Firstly, zeolites with low loading of cobalt (**Table 6.6**) are acid catalysts (high H^+ content) with only a small amount oxidation centre (Co^{2+}). Acid zeolites have already been shown to inhibit the

autoxidation by preventing the propagation ROOH species [1]. Acid catalysts are promoting an ionic decomposition of the ROOH which prevents the generation of radicals or metal catalysed decomposition of ROOH which supply radical species by homolytic hydroperoxide decomposition.

$$\text{Acid decomposition} \quad ROOH \rightarrow RO^{+} + OH^{-}$$

No conversion is observed with the low loading of cobalt meaning the oxidation centre does not participate in the initiation step and there is no direct docking by the alkane to oxidation centre.

Secondly, catalysts with a higher loading of cobalt or AlPO with cobalt or manganese (**Table 6.7 and Table 6.8**) show a conversion because the acidic proton has been replaced by Co^{2+}. No acid sites, means there is no ionic decomposition of the ROOH. No differences have been observed for the zeolites and AlPO with different sizes of pores (**Table 6.8**) meaning that the steric constraints do not influence the oxygen insertion and shows that the catalyst is doing a decomposition of the ROOH but does not participate in its formation.

Cobalt and manganese containing compounds are known to be highly efficient catalysts for the liquid-phase decomposition of ROOH via free radicals [11]. Intermediates along this reaction path are alkoxy and alkylperoxy radicals:

$$ROOH + Me^{II} \rightarrow RO^{*} + Me^{III}OH$$

$$ROOH + Me^{III}OH \rightarrow ROO^{*} + Me^{II} + H_2O$$

$$RO^{*} + RH \rightarrow R^{*} + ROH$$

The main role of the metal ions is to catalyze the homolytic decomposition of the intermediate hydroperoxide (ROOH) according to equations above. As a result of this decomposition,

metal ions generate chain initiating radicals, which form alcohols as oxidation first products according to last equation.

The alcohols and ketones formed as the primary products of alkane oxidations can be oxidised further to carboxylic acids by cleavage of C-C bonds, as shown in the simplified reaction sequence below [12].

$$R_1\text{-}CH_2\text{-}CH_2\text{-}R_2 \rightarrow R_1\text{-}CH_2\text{-}CH\text{-}(OH)\text{-}R_2 \rightarrow R_1\text{-}CH_2\text{-}C(=O)\text{-}R_2 \rightarrow R_1\text{-}CO_2H + R_2\text{-}CO_2H$$

So at low conversion, the first products formed are alcohols. The numbers of cracked products increase with the conversion, so the terminal selectivity (C_6) must decrease because the number products as cracked products increase, so terminal selectivity (C_6) can not be stable versus conversion, in contradiction with Iglesia, where the terminal selectivity is stable (8%) versus conversion for the autoxidation (meaning the autoxidation is very selective to terminal C_6 products because the number of products increase with conversion) and decrease when a catalyst is used. This increase of the number of cracked products will dilute the initial terminal selectivity. It has to be also considered that *n*-hexane can be functionalise in more than one position and cleave to more than 2 products. The other contradiction is the same conversion for the same time with and without catalyst but the metal is doing the catalytic decomposition of the ROOH, so there is an increase in the rate of the reaction. So for the same runtime, the conversion must be higher than the autoxidation.

6.8. Conclusion.

The Cardiff results show that autoxidation is responsible for high terminal selectivity at low conversion for the oxidation of *n*-hexane in liquid phase. These results have been repeated many times at Cardiff. The use of a glass liner to mimic Iglesia's glass reactor does not change the high terminal selectivity. The test with the different impurities added at the beginning of the reaction did not decrease or increase significantly the terminal selectivity of the autoxidation. The same purity of *n*-hexane was used for the work at Cardiff and by Iglesia. The Cardiff autoxidation results are similar to Iglesia terminal selectivity with a catalyst. No results are presented by Thomas for the autoxidation. Cardiff catalysts do not improve the terminal selectivity and similar results for the terminal selectivity are obtained to the autoxidation. No difference for the product distribution has been observed between the different sizes of pores used or the different oxidation centre (Mn or Co). The results show that catalyst is only participating to decompose the ROOH. Iglesia can not reproduce Thomas data with AlPO and Cardiff can not reproduce Thomas and Iglesia's autoxidation data for the liquid phase oxidation of *n*-hexane.

6.9. References.

[1] B. Zhan, B. Modén, J. Dakka, J.G. Santiesteban, E. Iglesia, Journal of Catalysis 245, (2007), 316.

[2] J.M.Thomas, R. Raja, G. Sankar, R.G. Bell, Nature, (1999), 227.

[4] R. Raja, J.M. Thomas, Chemical Communications, (1998), 1841.

[5] R. Raja, G. Sankar, J.M. Thomas, Journal of the American Chemical Society, 121, (1999), 119.

[6] B. Modén, B. Zhan, J. Dakka, J.G. Santiesteban and E. Iglesia, Journal Physical Chemistry C, 111, (2007), 1402.

[7] D.W. Breck, Zeolite Molecular Sieves; Wiley: New York, (1974).

[8] M. Gilhespy, Johnson Matthey, Billingham.

[9] C.E. Frank, Chemical Reviews 46, (1950), 155.

[10] K.U. Ingold, Inhibition of the autoxidation of organic substances in the liquid phase, (1961), 563.

[11] M. Hartmann, S. Ernst, Angewandte Chemie International Edition, 5, 39, (2000), 888.

[12] R.A. Sheldon and J.A. Kochi, Metal Catalyzed Oxidations of Organic Compounds, Academic Press, New York, (1981).

Chapter Seven

Conclusion and Future Research

This thesis describes the preparation, characterization and catalytic evaluation of VMgO and cobalt ion exchanged zeolites for the liquid phase oxidation of alkanes. The reaction studied was terminal oxidation of long chain linear alkanes using the selective oxidation of *n*-decane to 1-decanol as a model reaction. Based on the work carried out to date, the main conclusions that can be drawn are as follows.

Firstly the present work attempts to summarize the status of liquid phase autoxidation and to point out the difficult problem of controlled hydrocarbon autoxidation. The initiation step or activation of the autoxidation is mainly accomplished by heat, which can supply enough energy for the direct radical-forming reaction between hydrocarbon and molecular oxygen or by impurities, which decompose to give free radicals under reactions conditions. Direct reaction of radicals with oxygen result in the formation of hydroperoxide (ROOH). The hydroperoxide is unstable and breaks down by thermal scission to form radical fragments for further oxidative attack on the hydrocarbon. This fact complicates enormously the study of the autoxidation. The radical species can be stabilised by the use of a radical scavenger and prevent the autoxidation reaction. The product distribution of the autoxidation has a poor terminal selectivity. Increasing the temperature leads to higher conversion but results in more cracked products and less selectivity for oxygenated C_{10} products.

Catalysts did not show considerable activity for this reaction with low conversion and very poor terminal selectivity. The use of a mixed metal oxide catalyst (VMgO) improved the conversion compared to the autoxidation for the same runtime with the same conditions. Unfortunately, this activity is due to the leaching of the catalyst after 15 min of reaction, which can be use in homogeneous catalysis (detailed below).

The steric constraints around the oxidation centre with zeolites did not change the position of insertion of oxygen in the alkane chain resulting by a similar terminal selectivity compared to the autoxidation results. By catalysing the decomposition of the hydroperoxide, the catalyst promotes the generation of radicals which will initiate further attack on the hydrocarbon. The result of this hydroperoxide decomposition by catalysts is an increase in the conversion compared to the autoxidation for the same runtime with the same experimental conditions. Cobalt leaching was not responsible for the activity, which is an interesting point for a heterogeneous catalyst in the liquid phase.

Finally, the contradiction should be noted in the autoxidation data between Cardiff and the best results available in the literature published by Iglesia [1] and Thomas [2] for the oxidation of *n*-hexane in liquid phase. No data on the autoxidation is available from Thomas. For Iglesia the terminal selectivity is stable versus conversion in contradiction with the use of catalyst (terminal selectivity decrease versus time). Cardiff results for the autoxidation of *n*-hexane at low conversion gave the same terminal selectivity as observed by Iglesia. These results cast doubt on heterogeneous mechanism proposed by Iglesia to justify the heterogeneous activity of Mn-ZSM-5 in the liquid phase. The common agreement between both teams is to work at very low conversion to examine the activity of a catalyst for oxidation of a linear alkane in liquid phase. The results found at Cardiff during this thesis and

by Iglesia confirm that the results published by Thomas are extremely high and can not be reproduced. All the catalyst tested in this study for *n*-hexane and *n*-decane did not influence the product distribution of the reaction. Only conversion was affected by the use of a catalyst.

The first suggestion for the future work in the liquid phase is to carefully study the ability of catalyst to initiate autoxidation because it is during this step the oxygen is inserted into the alkane chain to give a hydroperoxide. It can be done by working at very low conversion, but isolating and working with these unstable products (radicals and ROOH) will be another challenge, then following by a study of hydroperoxide decomposition by various catalysts. Hydroperoxide are the first products made by the alkane oxidation in the liquid phase with and without catalyst, and the fragments formed by the decomposition of the peroxide serve as initiators for further oxidative attack on the hydrocarbon and complicates enormously the study of the oxidation process giving a large product distribution, so the importance of working at very low conversion to avoid these further reactions is clear. It should be kept in mind that decomposition of the peroxy radical (ROO*) may occur before the formation of the hydroperoxide (ROOH). Promoting selective hydroperoxide formation and decomposition with a catalyst will allow a better control over oxidative process, so a better control of the product profile of the reaction.

Zeolites have shown a dual function during this study. Zeolites can act as radical scavengers and kill the autoxidation, which is an advantage and can also by the incorporation of metal in the framework promote the first step of the autoxidation (removal of hydrogen from the alkane) to form the radical species or promote the decomposition of the ROOH species. It would be interesting to find a way to protect the external surface of the zeolites to prevent the in a metal anchor during ion exchange and at the same time leave enough acid sites to stop

the autoxidation. To investigate different loadings of metal with different sizes of channels will also be an interesting research topic. Another thing to be done is the use of an excess of catalyst and to extract the product from the channels to check if more terminal products are present but trapped within the pores of the zeolites.

It has been shown that many parameters can be manipulated to control the reaction. A deeper investigation of temperature, pressure, stirring speed on the product profile of reaction would be interesting. Repeat reactions with glass reactor to compare to Iglesia results have also to be done. It will be also interesting to change the kind of reactor and use a fixed bed in liquid phase with porous catalyst will may give better terminal selectivity than a batch reactor. Another parameter which can be varied is the oxidant. For example, the use of N_2O for the oxidation of linear alkanes in liquid phase has not been reported. A mild oxidant may make the autoxidation reaction more difficult and will improve the activity of the catalyst.

A new design of a new catalyst can be envisaged. A few ppm of homogeneous vanadium has showed to be very active for the oxidation of *n*-decane with oxygen without solvent. Ligands around vanadium may provide a good homogeneous catalyst and a selective route to access to the oxidation centre and form 1-decanol. For a heterogeneous catalyst, different aspects have to be considered. The first one is some inhibiting sites to prevent the autoxidation and the second one is the spacial constraint with a very oxidative metal to induce terminal selectivity. Tea bag technology or carbon nanotubes with active metal could provide this dual function and have never been reported in the literature for the oxidation of long linear alkanes in liquid phase.

Another suggestion for future work is an indirect method presented in the introduction with two steps for selective terminal oxidation of long linear alkane. It is a gas phase process with heterogeneous catalysts. A multi step process can be a disadvantage as it will be more

expensive but if the two step process can be more regioselective than the direct oxidation, a higher yield can be obtained offsetting the cost of the process. The suggestion is ammoxidation followed by an oxidation of the nitrile group. Ammoxidation is particularly attractive and as it leads to a terminal functionalisation of the alkane with guaranteed C≡N functionality. Once the terminal functionalisation has been achieved the nitrile group can be oxidised to give the primary alcohol. As an example, it has been shown that *n*-hexane can be converted to hexanenitirle (monosubstitution) with a selectivity of 30 % and to adiponitile (disubstitution) with the selectivity of (40%) [3]. The conversion of this vapour phase ammoxidation is 15%. This is not necessarily a disadvantage to have dinitrile substitution because the terminally activated products are of high value. Takahashi et al. [4] have shown a heterogeneous catalytic method for the oxidation of the nitrile to the corresponding alcohol in one step. The oxidation over hydrous zirconium oxide can be carried out heterogeneously and the products are easily isolated. The reduction of aliphatic nitriles proceeds efficiently to give the corresponding alcohols.

It will be interesting to investigate this method with long linear alkanes and may study the feasibility to carry out the terminal functionalisation of linear alkanes reaction in one step by passing the feed over the two different catalysts.

References.

[1] B. Zhan, B. Modén, J. Dakka, J. G. Santiesteban, E. Iglesia, Journal of Catalysis 245, (2007), 316.

[2] J. M.Thomas, R. Raja, G. Sankar, R.G. Bell, Nature, (1999), 227.

[3] B.M. Reddy, B. Manohar, Journal of Chemical Society, (1993), 330.

[4] K. Takahashi, M. Shibagaki, H. Matsushita, Chemical Letters, 1, (1990), 311.